

VARIATION OF SULPHATE SOURCE REGIONS AFFECTING SULPHATE  
CONCENTRATIONS IN THE EASTERN MEDITERRANEAN ATMOSPHERE

A THESIS SUBMITTED TO  
THE GRADUATE SCHOOL OF NATURAL AND APPLIED SCIENCES  
OF  
MIDDLE EAST TECHNICAL UNIVERSITY

BY

ZEYNEP MALKAZ

IN PARTIAL FULFILLMENT OF THE REQUIREMENTS  
FOR  
THE DEGREE OF MASTER OF SCIENCE  
IN  
ENVIRONMENTAL ENGINEERING

FEBRUARY 2014



Approval of the thesis:

**VARIATION OF SULPHATE SOURCE REGIONS AFFECTING SULPHATE  
CONCENTRATIONS IN THE EASTERN MEDITERRANEAN  
ATMOSPHERE**

submitted by **ZEYNEP MALKAZ** in partial fulfillment of the requirements for the degree of **Master of Science in Environmental Engineering Department, Middle East Technical University** by,

Prof. Dr. Canan Özgen \_\_\_\_\_  
Dean, Graduate School of **Natural and Applied Sciences**

Prof. Dr. Faika Dilek Sanin \_\_\_\_\_  
Head of Department, **Environmental Engineering**

Prof. Dr. Gürdal Tuncel \_\_\_\_\_  
Supervisor, **Environmental Engineering Dept., METU**

Assist. Prof. Dr. Seda Aslan Kılavuz \_\_\_\_\_  
Co-Supervisor, **Environmental Eng. Dept., Kocaeli University**

**Examining Committee Members:**

Prof. Dr. Göksel Demirer \_\_\_\_\_  
Environmental Engineering Dept., METU

Prof. Dr. Gürdal Tuncel \_\_\_\_\_  
Environmental Engineering Dept., METU

Assoc. Prof. Dr. Ayşegül Aksoy \_\_\_\_\_  
Environmental Engineering Dept., METU

Assoc. Prof. Dr. Emre Alp \_\_\_\_\_  
Environmental Engineering Dept., METU

Assist. Prof. Dr. Seda Aslan Kılavuz \_\_\_\_\_  
Environmental Engineering Dept., Kocaeli University

**Date:** February 6, 2014

**I hereby declare that all information in this document has been obtained and presented in accordance with academic rules and ethical conduct. I also declare that, as required by these rules and conduct, I have fully cited and referenced all the material and results that are not original to this work.**

Name, Last name: Zeynep Malkaz

Signature:

## **ABSTRACT**

# **VARIATION OF SULPHATE SOURCE REGIONS AFFECTING SULPHATE CONCENTRATIONS IN THE EASTERN MEDITERRANEAN ATMOSPHERE**

Malkaz, Zeynep

M.Sc., Department of Environmental Engineering

Supervisor: Prof. Dr. Gürdal Tuncel

Co-Supervisor: Assist. Prof. Dr. Seda Aslan Kılavuz

February 2014, 164 pages

Mediterranean atmosphere, particularly Eastern Mediterranean is one of the most complex air bodies around the world. The region is under strong influence of natural sources located at North Africa and Middle East, and anthropogenic sources located at the north of the basin. Sulphate anomaly is one of the peculiarities of the Eastern Mediterranean atmosphere.  $\text{SO}_4^{2-}$  concentrations in aerosol and rain water is among the highest recorded in the Europe and North America. Sulphate concentrations measured by various researchers in the Eastern Mediterranean atmosphere varies between 5 and 12  $\mu\text{g}/\text{m}^3$ . Although very high  $\text{SO}_4^{2-}$  concentrations in the Eastern Mediterranean is well documented in literature, the reason for such high levels is not clear. In this study variation of  $\text{SO}_4^{2-}$  source regions affecting  $\text{SO}_4^{2-}$  concentrations in the Eastern Mediterranean atmosphere between 1990 and 2006 was investigated

using source and receptor oriented trajectory statistics approaches. Back trajectories were calculated for every day for Antalya and Çubuk, which are two locations in Turkey where long-term  $\text{SO}_4^{2-}$  data are available. The source regions affecting these locations were determined using Potential Source Contribution Function (PSCF). Because of PSCF depends on measurement data and can be applied for the periods where  $\text{SO}_4^{2-}$  measurement results are available. A different method which bases on distribution of  $\text{SO}_2$  emission in Europe and transport of pollutants and called Region of Influence, RoI was also used. RoI is applied at locations where measurement results are not available. Weighing of RoI results based on height of trajectory segment were attempted.

Keywords: Eastern Mediterranean Atmosphere, Back trajectory, Potential Source Contribution Function (PSCF), Sulphate ( $\text{SO}_4^{2-}$ )

## ÖZ

### DOĞU AKDENİZ ATMOSFERİNDEKİ SÜLFAT KONSANTRASYONUNU ETKİLEYEN SÜLFAT KAYNAK BÖLGELERİNİN DEĞİŞİMİ

Malkaz, Zeynep

Yüksek Lisans, Çevre Mühendisliği Bölümü

Tez Yöneticisi: Prof. Dr. Gürdal Tuncel

Ortak Tez Yöneticisi: Yrd. Doç. Dr. Seda Aslan Kılavuz

Şubat 2014, 164 sayfa

Akdeniz atmosferi, özellikle de Doğu Akdeniz atmosferi dünyadaki en karmaşık hava kütlelerinden biridir. Doğu Akdeniz bölgesi; Kuzey Afrika ve Orta Doğu daki doğal kaynakların ve havzanın kuzeyindeki antropojenik kaynakların kuvvetli etkileri altındadır. Sülfat anomalisi, Doğu Akdeniz bölgesinde atmosferin önemli özelliklerinden birisidir. Ülkemizde içinde bulunduğu bu bölgede ölçülen  $SO_4^{2-}$  konsantrasyonları, Avrupa ve Kuzey Amerika daki değerlerin çok üzerindedir. Çeşitli araştırmacılar tarafından Doğu Akdeniz de ölçülen sülfat konsantrasyonunun  $5 \mu g/m^3$  ve  $12 \mu g/m^3$  arasında değiştiği görülmektedir.  $SO_4^{2-}$  konsantrasyonunun Doğu Akdeniz bölgesinde neden bu kadar yüksek olduğu bilinmemektedir. Bu çalışmada 1990 ve 2006 yılları arasında Doğu Akdeniz atmosferindeki  $SO_4^{2-}$  konsantrasyonunu etkileyen kaynak bölgelerinin değişimi, kaynak ve alıcı odaklı yörünge istatistiği yaklaşımları kullanılarak araştırılmıştır. Uzun süreli  $SO_4^{2-}$  verilerinin bulunduğu Türkiye'deki iki istasyon olan Antalya ve Çubuk'da 1990 ve 2006 yılları arasındaki

hergün için, geri yörüngeler hesaplanmıştır. Bu istasyonları etkileyen kaynak bölgeler kaynak odaklı yörünge istatistik metodu, yani potansiyel kaynak katkı fonksiyonu (PSCF) ile tanımlanır. PSCF belirli zaman aralıklarında uygulanmıştır. PSCF, ölçülen  $SO_4^{2-}$  konsantrasyonlarına bağlıdır ve sadece ölçüm sonuçlarının bulunduğu zaman dilimlerinde uygulanır. Avrupa'daki  $SO_2$  emisyonu dağılımına ve kirleticilerin taşınımına bağlı ilgi bölgeleri (RoI) olarak tanımlanan farklı bir method daha kullanılmıştır. Bu yaklaşımın avantajı, ölçüm sonuçlarının bulunmadığı noktalar ve zaman dilimleri için uygulanabilmesidir. Yörünge segmentinin yüksekliği RoI yaklaşımına entegre edilmesiyle methodun daha gerçekçi sonuçlar vermesine çalışılmıştır.

Anahtar Kelimeler: Doğu Akdeniz Atmosferi, Geri yörünge, Potansiyel Kaynak Katkı Fonksiyonu, Sülfat ( $SO_4^{2-}$ )

To My Beloved Family



## ACKNOWLEDGEMENTS

I would like to express my sincere gratitude to the following people for their tremendous help and support. Without their encouragement and guidance, I would never have been able to realize this work.

First and foremost, I would like to express my greatest appreciation to my thesis supervisor Prof. Dr. Gürdal Tuncel for his patience, unlimited support, enthusiasm, and valuable comments. I would like to show gratitude to my co-supervisor Assist. Prof. Dr. Seda Aslan Kılavuz for her guidance, comments and support. I feel motivated and encouraged whenever I talk to her.

I would also like to thank to my committee members Prof. Dr. Göksel Demirer, Assoc. Prof. Dr. Ayşegül Aksoy and Assoc. Prof. Dr. Emre Alp for their encouragement, insightful comments and valuable suggestions.

I would like to thank Dr. Güray Doğan for introducing me to the MapInfo as well for their precious assistance in the preparation and completion of this study. I would also like to thank Dr. Deniz Genç Tokgöz and Sema Yurdakul for encouragement and support throughout the research.

I would like to express my sincere gratitude to the people who give a magic touch to my life. Elif Küçük, Mayıs Kurt, Şule Özkal, Pınar Özsoy, Beste Şimşek, Başak Utku, I am very grateful for your eternal friendship, moral support, and great contributions.

I am truly and deeply indebted to Gül Ayaklı, Sena Uzunpınar, Selcen Ak, İlker Balcılar, Ebru Koçak, Nilüfer Ülgüdür for helping me in getting through tough times. I would like to thank to my roommates and all of our group members for their friendship and support. I am so lucky to have met you.

Last but not the least, I send heartfelt thanks to my parents, my brother, my grandmother, my aunt and her husband. They put faith in me all through my life and without their support and encouragement nothing would be possible. I am so glad that I have you.

## TABLE OF CONTENTS

ABSTRACT .....	v
ÖZ .....	vii
ACKNOWLEDGEMENTS .....	xi
TABLE OF CONTENTS .....	xiii
LIST OF TABLES .....	xvi
LIST OF FIGURES .....	xvii
LIST OF ABBREVIATIONS .....	xx
CHAPTERS	
1. INTRODUCTION .....	1
2. LITERATURE REVIEW .....	5
2.1 Eastern Mediterranean Atmosphere .....	5
2.2 Trajectories .....	11
2.3 Trajectory Statistics .....	17
2.3.1 Flow Climatology .....	18
2.3.2. Potential Source Contribution Function .....	19
2.4 Sources and Transport of Sulphur Compounds .....	22
3. METHODOLOGY .....	25
3.1 Study Area .....	25
3.1.1. Stations Selected for PSCF Calculations .....	25
3.1.1.1 Southern Anatolia Station (Antalya).....	26

3.1.1.2. Central Anatolia Station (Çubuk, Ankara) .....	27
3.1.2. Stations Selected for RoI Calculations .....	27
3.1.2.1. Western Mediterranean Station (Corsica, France) .....	28
3.1.2.2. Eastern Mediterranean Station (Ashdod, Israel) .....	28
3.2. Description of Study Domain .....	28
3.3. Data Preparation .....	30
3.3.1. Pollutant Data .....	31
3.3.2. Back Trajectory Data .....	35
3.4. Potential Source Contribution Function (PSCF) .....	39
3.5. Regions of Influence (RoI) Approach.....	43
4. RESULTS AND DISCUSSIONS .....	45
4.1. Investigation of Weighting Trajectory Segments, Based on Their Altitude ...	45
4.2. Variation in SO <sub>4</sub> <sup>2-</sup> Source Regions as Determined by PSCF Approach, Between 1993 and 2006.....	54
4.2.1. Antalya Station.....	57
4.2.2. Çubuk Station .....	63
4.2.3. Relation between PSCF Values and SO <sub>2</sub> Emissions.....	69
4.2.4. Comparison of PSCF Results Obtained for Çubuk and Antalya Stations	75
4.3. Region of Influence (RoI) Approach .....	79
4.3.1. Variation in SO <sub>4</sub> <sup>2-</sup> Source Regions as Determined by RoI Approach Between 1980 and 2010 in Four Stations at Eastern and Western Mediterranean.....	81
4.3.1.1. At Antalya Station .....	81
4.3.1.2 At Çubuk Station.....	94
4.3.1.3. At Middle East (Ashdod, Israel) Station.....	107
4.3.1.4. At Western Mediterranean (Corsica, France) Station .....	119
4.4. Comparison of the Results Obtained by PSCF and RoI Approaches .....	130

5. CONCLUSION.....	139
6. RECOMMENDATIONS FOR FUTURE RESEARCH.....	147
REFERENCES .....	149

## LIST OF TABLES

Table 3. 1 Summary table for getting emission data from EMEP .....	33
Table 3. 2 Example for SO <sub>x</sub> emission data format, EMEP .....	34
Table 3. 3 Example of back trajectory data format, TrajStat.....	38
Table 3. 4 Height weightings used in calculations.....	40
Table 4. 1 Number of total trajectory segments without altitude weighting and with three different altitude weightings for countries in grid system used at PSCF calculation.....	50
Table 5. 1 Variation of average PSCF results of regions during the study period...	140
Table 5. 2 Variation of average RoI results of regions during the study period.....	142

## LIST OF FIGURES

Figure 2. 1 Eastern Mediterranean Region.....	11
Figure 2. 2 Schematic pictures of (a) a Lagrangian model and (b) Eulerian model...	13
Figure 2. 3 Example of back trajectory.....	15
Figure 3. 1 Locations of sampling stations.....	26
Figure 3. 2 Antalya Station, Hi-Vol sampler.....	27
Figure 3. 3 Second grid system (gridded domain of $1^{\circ} \times 1^{\circ}$ ) .....	30
Figure 3. 4 Distribution of SO <sub>2</sub> data at EMEP grid system .....	34
Figure 3. 5 Example of trajectory monthly calculation window of TrajStat.....	37
Figure 4. 1 Top and side view of trajectory groups associated with highest 20% of pollution and marine factor scores in PMF study performed on Antalya aerosol data.....	47
Figure 4. 2 Effect of three different altitude weighting preferences to distribution of PSCF values at Çubuk station for the combined years 1993 and 1994 .....	49
Figure 4. 3 Distribution of PSCF values for a Çubuk Station for 1993+1994 using altitude weighting type 3 with legend 1, legend 2 and legend 3. ....	54
Figure 4. 4 Distribution of PSCF values for Antalya Station with two year intervals between 1993 and 2000.....	58
Figure 4. 5 Grid-based percent differences between biyearly PSCF distributions. Differences were calculated between different years and 1993+1994. ....	60
Figure 4. 6 Country Average of two years period PSCF results using altitude weighting type 3 for Antalya Station between 1993 and 2000 .....	62
Figure 4. 7 Two years period of PSCF results using altitude weighting type 3 for Çubuk Station between 1993 and 2006.....	64
Figure 4. 8 Distribution of differences of PSCF values between each of the 2-yr-long intervals and (1993+1994) period.....	66

Figure 4. 9 Country Average of two years period PSCF results using altitude weighting type 3 for Çubuk Station between 1993 and 2006 .....	68
Figure 4. 10 Variation of SO <sub>2</sub> emissions in Europe, between 1980 and 2010 .....	70
Figure 4. 11 Variation in SO <sub>2</sub> emissions in selected Western and Eastern European countries .....	72
Figure 4. 12 Location of significant SO <sub>2</sub> point sources in some of the countries around Turkey. ....	75
Figure 4. 13 Distribution of PSCF values at Çubuk and Antalya Stations between 1993 and 2000 .....	76
Figure 4. 14 Percent difference between PSCF values at each grid calculated for Antalya and Cubuk stations. ....	78
Figure 4. 15 Yearly Change of RoI distribution between 1980 and 2010 calculated for Antalya Station .....	82
Figure 4. 16 Direction of back trajectories computed at an earlier work at Antalya station.....	85
Figure 4. 17 Percent variation of Antalya RoI values at each grid, relative to 1980 RoI's, between 1985 and 2010.....	87
Figure 4. 18 Variation of average RoI value at each country, between 1980 and 2010, for Antalya station .....	91
Figure 4. 19 Variation of potential source regions affecting Çubuk station between 1980 and 2010.....	95
Figure 4. 20 Percent variation of Çubuk RoI values at each grid, relative to 1980 RoI's, between 1985 and 2010.....	99
Figure 4. 21 Difference between RoI values at each grid calculated for Antalya and Cubuk Stations. ....	102
Figure 4. 22 Variation of average RoI value at each country, between 1980 and 2010, for Çubuk Station .....	104
Figure 4. 23 Yearly Change of RoI distribution between 1980 and 2010 calculated for Ashdod Station.....	108
Figure 4. 24 Percent variation of RoI values calculated for Ashdod, Israel at each grid, relative to 1980 RoI's, between 1985 and 2010.....	112

Figure 4. 25 Variation of average RoI value at each country, between 1980 and 2010, for Ashdod, Israel .....	116
Figure 4. 26 Yearly Change of RoI distribution between 1980 and 2010 calculated for Corsica Station .....	120
Figure 4. 27 Percent variation of Corsica RoI values at each grid, relative to 1980 RoI's, between 1985 and 2010 .....	124
Figure 4. 28 Variation of average RoI value at each country, between 1980 and 2010, for Corsica Station .....	127
Figure 4. 29 Comparison of PSCF and RoI results as a two years period from 1993 to 2000 at Antalya Station.....	131
Figure 4. 30 Comparison of PSCF and RoI results as a two years period from 1993 to 2006 at Çubuk Station.....	132

## LIST OF ABBREVIATIONS

ARL	Air Resources Laboratory, United States
CEIPS	Centre on Emission Inventories and Projections
CMB	Chemical Mass Balance
CWT	Concentration Weighted Trajectory
DMS	Dimethylsulphide
ECE	Economic Commission for Europe
EMEP	Co-operative Programme for Monitoring and Evaluation of the Long-range Transmission of Air Pollutants in Europe
FTP	File Transfer Protocol
GIS	Geographical Information System
HYSPLIT	Hybrid Single Particle Lagrangian Integrated Trajectory Model
METU	Middle East Technical University
NCAR	National Center for Atmospheric Research, United States
NCEP	National Centers for Environmental Prediction, United States
NOAA	National Oceanic and Atmospheric Administration, United States
PMF	Positive Matrix Factorization
PSCF	Potential Source Contribution Function
RoI	Regions of Influence
SO <sub>x</sub>	Sulfur Oxides

## CHAPTER 1

### INTRODUCTION

Air pollution has been a major issue in all over the world because it directly affects the human life, acidification of water and soil, natural ecosystem and agriculture. Mainly, negative effects of industrialization and characteristics of air bodies identify the properties of atmosphere. Especially, Mediterranean atmosphere, particularly the Eastern Mediterranean atmosphere, is one the most complex air bodies around the world because of strong polarity of sources affecting chemical composition of the Mediterranean atmosphere and different economic levels of countries at the source regions affecting the Eastern Mediterranean. When the chemical composition of Eastern Mediterranean atmosphere is investigated, the high sulphate concentrations are outstanding and the reasons of such high values are not obviously stated. Therefore, it is aimed that variation of  $\text{SO}_4^{2-}$  source regions affecting  $\text{SO}_4^{2-}$  concentrations in the Eastern Mediterranean atmosphere between 1980 and 2010 was investigated using source and receptor oriented trajectory statistics approaches.

The related studies shows that high levels of  $\text{SO}_2$  and particulate matter caused air pollution before 1970's, but regional and global air pollution became important after 70's. Transport of particles and gases via the atmosphere is the most important mechanism for dispersion of pollutants in the regional and global scales. Because of the absence of boundaries within the earth's atmosphere, gases and particles produced from one point source can be transported around the globe. To analyze the long range transport of pollutants, the European Monitoring and Evaluation Program

(EMEP) and many national and international monitoring stations were established around the world.

Natural sources of sulfate are the oxidation of SO<sub>2</sub> emitted from volcanoes and dimethylsulphide (DMS) produced by biogenic processes in the marine environment. On the other hand, main anthropogenic sources are combustion of fossil fuels, especially coal combustion. Also, industrial activities are typical sources of SO<sub>2</sub> not only in urban and industrial areas, but also in the regional scale.

When the international actions to control long range transport of sulphur emission is studied, it is seen that the first meeting related to the long range transport of pollutants was organized by United Nations Conference on the Human Environment in Stockholm in 1972. Increasing problems of acid rain in Europe was priority issue at the conference. The basics of the Co-operative Programme for Monitoring and Evaluation of the Long-range Transmission of Air Pollutants in Europe (EMEP) were established in 1978. Twenty four of Economic Commission for Europe (ECE) countries and the European Community participated to the program. In 1985, the first sulfur protocol was discussed and signed in Convention on Long-range Transboundary Air Pollution meeting. With the reduction of sulphur emissions between 30 and 60% by 1993, direct decrease in sulfur concentration of European atmosphere was seen. Furthermore, in atmosphere of Western Europe, more than 70% decrease in SO<sub>4</sub><sup>2-</sup> concentrations was reported.

In addition, in 1998 Oslo Protocol was developed for further reduction of sulfur emission. Main methods which were suggested in this protocol were effects-based approach, the critical load concept, best available technology, energy savings and the application of economic instruments. When the protocol relating to Abate Acidification, Eutrophication and Ground-level Ozone formation entered into force, sulphur emissions in Europe decreased at least 63%. Before the protocol, critical load studies showed that 93 x 10<sup>6</sup> ha land area in Europe exceeds critical acid loads. With the application of protocol, the critical acid loaded area decreased to 15 x 10<sup>6</sup> ha.

Instead of these protocols, regional agreements such as Mediterranean basin and Black Sea region agreements to improve environmental conditions at specific regions were conducted. For Mediterranean basin, Barcelona Convention including management of the resources in the Mediterranean Basin, monitoring of information, assessment of the states of pollution, the enforcement measures for the framework convention and related protocols were approved in 1975. In order to control the pollution in the Mediterranean region, monitoring of the Mediterranean Sea itself and atmospheric component were started in 1988.

The purpose of this study is to investigate the variation of  $\text{SO}_4^{2-}$  source regions affecting the Mediterranean atmosphere in last 30 years. The main objectives of the work are summarized below:

1. To investigate the weighting trajectory segments, based on their altitude at their location in trajectory statistic,
2. Variation in source regions of  $\text{SO}_4^{2-}$  as determined by altitude weighted potential source contribution function (PSCF) approach, between 1993 and 2006,
3. Variation of sulphate source regions calculated by altitude weighted regions of influence (RoI) approach between 1980 and 2010,
4. To compare the results obtained by PSCF and RoI methods.



## **CHAPTER 2**

### **LITERATURE REVIEW**

#### **2.1 Eastern Mediterranean Atmosphere**

Different types of aerosol sources, sea water with high relative humidity and solar irradiance that drives photochemical processes make the Mediterranean basin special for atmospheric aerosol research (Haywood and Boucher, 2000). Some studies show that the highest aerosol radiative forcing in the world is detected at this region during summer. For the Eastern Mediterranean area, in summer time, huge amounts of particulate pollutants originate from Europe and mineral dust particles are formed and transported by long range transport process from arid areas of Northern Africa such as Sahara desert (Lelieveld et al., 2002, Mihalopoulos et al., 1997, Kalivitis et al., 2007).

In atmosphere, ammonium, sulfate and organic matter are the primary scattering particles. Therefore the components have an important role in Eastern Mediterranean atmosphere. Study conducted by Kalivitis et al. (2011) at research station of the University of Crete by continuous measurement of aerosol particles reveals the chemical composition of the Eastern Mediterranean atmosphere. The effect of dust particles from Northern Africa toward Mediterranean can easily be seen in levels of absorption.

Various pollutant sources resulting from long range transport and pollutants emitted from Eastern and Western part of Europe directly affect the Mediterranean

atmosphere (Lelieveld et al., 2002). Moreover, arid belts which cover from the North Africa to the Eastern Mediterranean surround the southern and eastern shores of the Mediterranean. The studies related to the aerosol chemical composition (Kubilay and Saydam, 1995; Querol et al., 2004), effect of dust events (Kubilay et al., 2000; Viana et al., 2002) and mineral dust source regions (Rodriguez et al., 2001; Escudero et al., 2006) define the aerosol chemical composition in the Mediterranean atmosphere. The research of Kubilay et al. (2000) implies that long range transport of dust from North Africa to Eastern Mediterranean happen especially in spring time, also dust sources in the Middle East generally transport to the Eastern Mediterranean in autumn. On the other hand, Rodriguez et al. (2001) and Escudero et al. (2006) define that the transportation from North Africa to the Western and Central Mediterranean takes place especially in summer (Moulin et al., 1998; Escudero et al., 2006).

In order to explore the chemical and physical characteristics of aerosols, the Mediterranean is the only important natural air laboratory. The effects of Saharan and Middle East ,which are dust source areas, should be evaluated when investigating the Eastern Mediterranean atmosphere in terms of aerosol composition (Koçak et al., 2012).

Researches which are conducted in the Eastern Mediterranean show that natural and anthropogenic sources directly impact the qualities of aerosol load. Due to the deposition from the atmosphere, Mediterranean region is susceptible to pollutants (Chester et al., 1993). The studies show that there are high pollutant concentrations in Eastern Mediterranean atmosphere and the sources of this high values are not sightful. In this context, Doğan et al. (2008) focuses on source and receptor oriented techniques to identify sources which affect chemical composition of the Eastern Mediterranean aerosol. Based on this technique, it is deduced that in terms of long range transport factor, Aegean coast, Northwest Turkey, Balkan countries, Ukraine and regions located in the northern part of Ukraine are the main source areas. In order to define the chemical characterization of aerosols in the Mediterranean atmosphere, very effective researches have been performed from the beginning of 1970s (Migon et al., 1990; Mateu et al., 1996a; Tov et al., 1997). These researches

indicate that anthropogenic and crustal components are the main properties of the atmosphere over the Mediterranean Sea. The contribution of these components is directly based on distance between sources and receptor sites. In order to develop some control system for air pollutants, the locations of pollution sources should be determined (Chester et al., 1993).

Generally, studies related to the aerosol composition have been carried out in the western part of the Mediterranean region. However, in recent years, topics associated with concentration of elements and their episodic/seasonal variability and factors affecting these variations have been researched in eastern part of the basin. (Kubilay and Saydam, 1995; Güllü et al., 1998; Herut, 2001; Bardouki et al., 2003; Sciare et al., 2003; Koçak et al., 2004a, b).

Mainly, three general source types directly affect the Mediterranean atmosphere. These can be classified as anthropogenic sources which are placed at the north and northwest of this region, strong crustal source sited in North Africa and marine source which comes from Mediterranean Sea. When these source types are evaluated in terms of pollution transport to the Eastern Mediterranean, it is seen that anthropogenic sources are the most significant ones (Güllü et al., 2005).

There are many studies which have been completed in specific period of years, especially during summer, though several studies on physicochemical characterization of aerosols have been carried out in the Eastern Mediterranean (Ichoku et al., 1999; Kouvarakis et al., 2002b; Andreae et al., 2002; Bryant et al., 2006). Hydrological cycle and climate of the Mediterranean may change depending on the atmospheric transport and deposition of aerosols (Lelieveld et al., 2002). The physical, chemical, and optical properties of aerosols and the limited knowledge on the processes affect the distributions. The magnitude of the impacts of aerosols on ocean productivity, hydrological cycle, and climate of the Mediterranean are not sufficiently comprehended.

It is known that both anthropogenic and natural sources influence the composition of aerosol burden in Eastern Mediterranean. Sulfate and carbonaceous particles that have undergone long range transport from Europe and Asia are the main anthropogenic components. On the other hand, natural aerosol components consist of sea salts, mineral dust particles and biogenically produced sulfur aerosols. (Mihalopoulos et al., 1997; Özsoy et al., 2000; Formenti et al., 2001; Andreae et al., 2002).

When the concentrations of ions such as  $\text{SO}_4^{2-}$  and  $\text{NO}_3$  are examined, lower concentrations, compared to those detected during the summer, are observed in winter season. Due to the lower rate of particle removal by wet deposition in summer, the accumulation of particles in the atmosphere is observed. Also, the activation of photochemical formation in summer improves the concentrations of  $\text{nss-SO}_4^{2-}$  and  $\text{NO}_3$  (Koçak et al., 2004a).

The research of Koçak et al. (2004a) concludes that the concentrations and the seasonal variation of  $\text{nss-SO}_4^{2-}$  are compatible with previous studies which are carried out in the Eastern Mediterranean (Luria et al., 1996; Güllü et al., 1998; Kouvarakis et al., 2002a). The study performed at Erdemli proves that very high sulfate concentrations are observed over the Mediterranean. The levels are comparably higher than those over continental Europe (URL 1).

In the atmosphere over Israel and the Eastern Mediterranean sea, unusually high sulfate levels, especially in summer, have been presented. The long range transport of sulphates emanating from industrial areas of eastern and central Europe may explain this occurrence. In addition to this, marine biogenic production of sulphate from the oxidation of dimethylsulphide may cause the high sulfate levels. The results of the study of Ganor et al. (2000) shows that biogenic generation of sulphate from the Mediterranean sea increases the sulphate content of the aerosol over Israel during the summer season. Also,  $\text{SO}_4^{2-}$  levels found in Israel and Syria mainly varies between 6.7 and 15  $\mu\text{g m}^{-3}$ . Higher sulfate level in air over Eastern Mediterranean and Israel has been measured. The highest sulphate values are found in summer and

an annual average sulphate concentration of  $10 \pm 1.5 \mu\text{g m}^{-3}$  have clearly expresses by Luria et al. (1996).

Main effect of atmospheric sulphate on the environment is that it plays a role as cloud condensation nuclei on rain formation in the Eastern Mediterranean region. Approximately 90% of the particles at Lake Kinneret (northern Israel) contain sulphur. Local pollution, long range transport from distance sources, transport of crustal mineral matter from desert regions surrounding Israel and biogenic sources, i.e. oxidation of dimethylsulphide (DMS) from marine biological sources to sulphate can be classified as potential sources of these high atmospheric sulfate grades (Ganor et al., 2000).

Mixtures of anthropogenic and crustal components of the sources are the main elements of the atmosphere over the Mediterranean Sea (Chester et al., 1993). Short and long term episodic variations are observed for concentrations of most of the elements and ions. Transport of crustal material from North Africa during the transient period and storm activity over the eastern Mediterranean Sea during the winter season assign short-term variations in concentrations of lithophilic and sea salt related species (Güllü et al., 1998; Koçak et al., 2004a).

Although strong natural and anthropogenic sources surround the Turkey, there is no homogenous distribution around the country. In Eastern Mediterranean region, huge quantities of crustal particles arising from desert areas at the North Africa and Middle East are one of the crucial natural sources (Kubilay et al., 2000; Rodriguez et al., 2001). The other one is the sea salt particles emitted from Mediterranean Sea (Kuloğlu and Tuncel, 2005). While the natural sources are stated at southern part of Turkey, anthropogenic sources of particles which are industrial emissions are located in the north, especially northwest of Turkey (Koulouri et al., 2008).

Considering such high sulfate concentrations in Eastern Mediterranean atmosphere, identification of source regions affecting the aerosol concentrations in the Mediterranean region becomes important. By using source or receptor modeling,

source region apportionment is applied. In this purpose, the study of Doğan et al. (2010) focuses on PSCF for  $\text{SO}_4^{2-}$  and  $\text{NO}_3$  in the Black sea and Mediterranean coasts of Turkey.

The region of lands around the Mediterranean Sea is defined as Mediterranean Basin or Mediterranean in biogeography. In this region, Mediterranean climate is observed and main characteristics of this climate are mild, rainy winters and hot, dry summers. Therefore, Mediterranean forests, woodlands and scrub vegetation are promoted. Some parts of the Europe, Asia and Africa constitute the Mediterranean basin (Krijgsman et al., 2001).

Mediterranean Sea is enclosed by the Europe and Anatolia on the north, North Africa on the south and Levant (countries of eastern Mediterranean) on the east. Also, the Mediterranean Sea is stated as a portion of the Atlantic Ocean. The name of Mediterranean comes from Latin; mediterraneus means inland or in the middle of the land (URL 2).

Eastern Mediterranean or Levant refers to the countries which are located in the east of the Mediterranean Sea. As shown in Figure 2.1, Cyprus, State of Palestine, Lebanon, Syria, Jordan and Israel are the countries of the Eastern Mediterranean (URL 3).

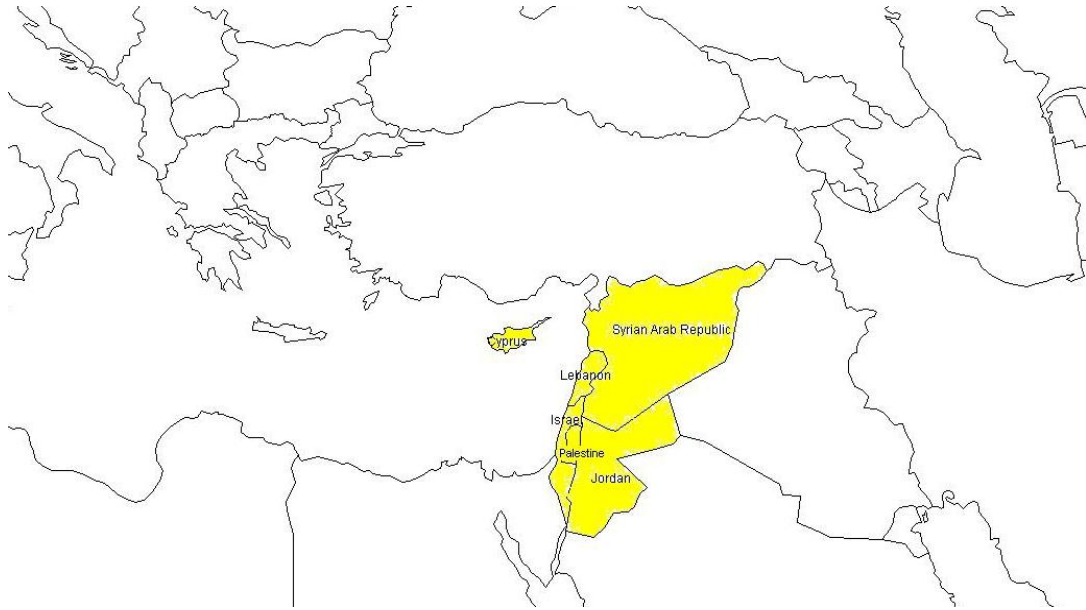


**Figure 2. 1 Eastern Mediterranean Region**

The area of Mediterranean basin is approximately  $2.3 \times 10^3 \text{ km}^2$ . The basin consists of more than 20 nations. Due to the geographic location of the Mediterranean basin, where it is at the junction of the three continents, biodiversity has an important role in this region. When the historical progress of Mediterranean geology is investigated, dynamic changes on plate tectonics, mountain uplift and active volcanism have a significant role (URL 4).

## **2.2 Trajectories**

The general definition of trajectory is the time integration of the position of an air parcel due to transportation by the wind. Trajectory is basically identified as the path along which an air mass has traveled. For instance, a fluid particle, ‘signed’ at a certain point in space at a given time is traced forward or backward in time along its trajectory (Stohl et al., 2002). Based on the dynamic processes in the atmosphere, there are many different applications of trajectories. Evaluating the airborne pollen dispersion (Sauliene, 2006), identifying the route of water vapor transport (D’Abreton and Tyson, 1996), correlating the source-receptor relation of air pollutants (Miller, 1987; Stohl, 1996) and examining the air mass flow around mountains (Steinacker, 1984), identification of the characteristics of an air mass for a

specific site (Lee and Leifer, 1993), investigation of the sources of moisture in the atmosphere during snowfall events (URL 5) are some of the examples for the application of trajectories.

In order to identify the long-range transport of air pollutants in the atmosphere, in first sight, trajectories are used (Pack et al., 1978). Forward and backward trajectories of an air mass are very useful components in order to interpret an air quality event. For the determination of the sources of pollutants measured at a point in space and time, back trajectories are used in studies of air pollution. In other words, for ascertaining the origins and sources of pollutants, mainly back trajectory analysis is used. On the other hand, for determining the dispersion of pollutants, forward trajectory analysis is a helpful and effective technique (URL 6).

A wide variety of atmospheric models have been used to calculate the trajectories. Mainly two approaches, which are Eulerian and Lagrangian, become important to understand air motions. While Lagrangian models simulate variations in the chemical composition of a specific air parcel as it is advected in the atmosphere, Eulerian models define the concentrations of settled calculated cells (Seinfeld and Pandis, 2006).

The theoretical account of Lagrangian modeling moves with the local wind. Therefore, mass exchange between the air parcel and its surrounding, and species emissions allowed to enter the parcel through its base are excluded and not observed. A specific air parcel which moves through time and space is taken into consideration in Lagrangian modeling (Byers, 1974; Dutton, 1986).

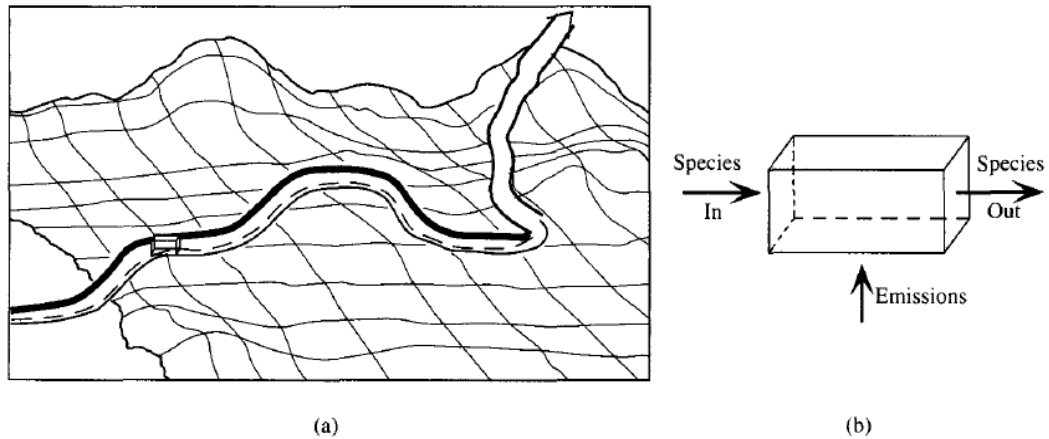


**Figure 2. 2 Schematic pictures of (a) a Lagrangian model and (b) Eulerian model (Seinfeld and Pandis, 2006)**

As shown in Figure 2.2 which focuses on the schematic pictures of Lagrangian and Eulerian models, concentrations at different locations at different times are simulated as continuous movement of air parcel by the Lagrangian models. Whereas, modeling of the species concentrations at all locations as a function of time are calculated by the Eulerian models which stays fixed in space (Seinfeld and Pandis, 2006).

When the Eulerian and Lagrangian models are compared, it is pointed out that Eulerian model is easy to apply. Although assuming a homogeneous air shed in Eulerian model makes everything simpler, Lagrangian model supplies more information. However, due to neglecting of horizontal dispersion, it might calculate higher concentrations (Seinfeld and Pandis, 2006).

The below differential trajectory computation explains the particular small air parcel's trajectory;

$$\frac{dS}{dt} = u [S(t)] \tag{2.1}$$

where t : time,

S: position vector,

u: wind velocity vector.

The route of the position vector can be calculated when we know the initial position of  $S_0$  of the parcel at time  $t_0$  as stated through Equation 2.2:

$$S(t) = S(S_0, t) \quad (2.2)$$

and inverse transformation is identified through Equation 2.3,

$$S_0(t = t_0) = S_0(S, t) \quad (2.3)$$

Equation 2.3 gives an information about the initial coordinates of the parcel (S,t).  $S_0$  at time  $t_0$  is the initial coordinate and it is named as Lagrangian coordinates (Dutton, 1986).

Because of the inhomogeneities of wind fields, turbulent and convection motions, and precipitation processes, a single trajectory is not sufficient to describe the path of an air box. Therefore the computed trajectory can represent only a limited period of the route of an air parcel.

$$S(t) = S_0 - \int_t^{t_0} u(\tau) d\tau \quad (2.4)$$

Assuming that at time  $t_0$  the trajectory ends at the location  $S_0$ , the straightforward integration of Equation 2.4 can calculate the location of the air parcel  $S(t)$  at time  $t$  on this backward trajectory (Seinfeld and Pandis, 2006). For instance, calculated air parcel trajectory arriving at Antalya during May 21, 2010 is shown in Figure 11. Based on the 5 days back trajectory computation, the air parcel started over the Spain, traversed the Middle European Countries air basin picking up emissions from the various sources along their way, and finally trajectory segments end up at the receptor (Antalya). Heights of three different starting points which are implied by green- 1500m, blue- 500m and red- 100m are shown in Figure 2.3.

NOAA HYSPLIT MODEL  
 Backward trajectories ending at 1400 UTC 21 May 10  
 CDC1 Meteorological Data

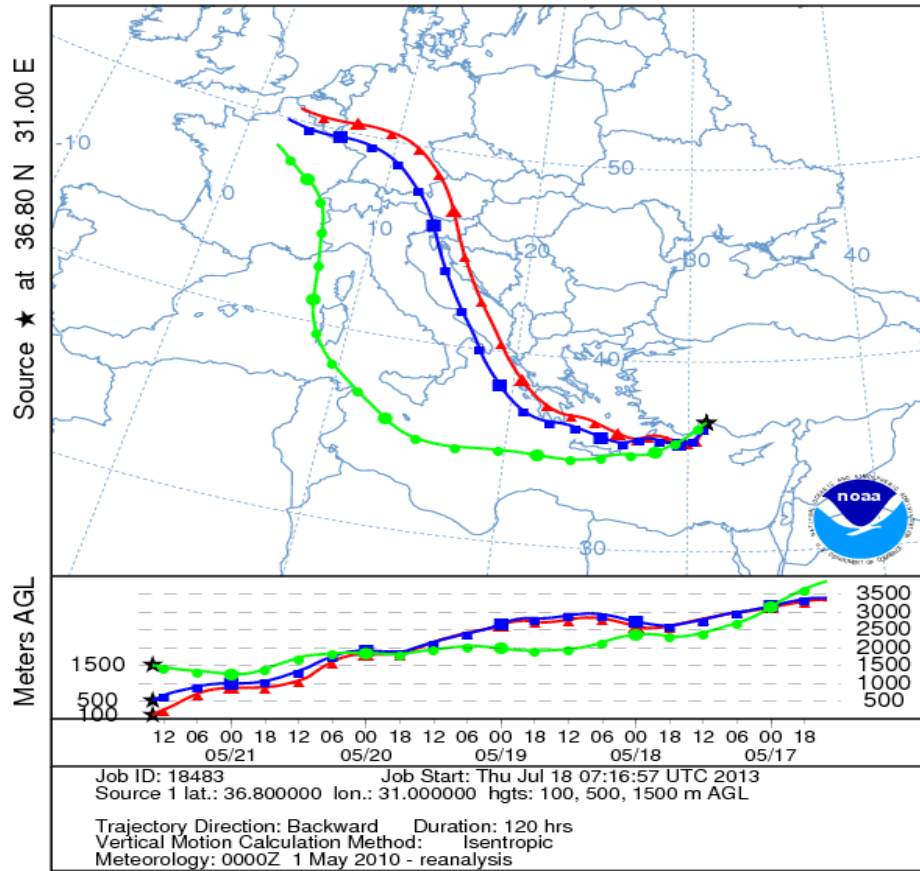


**Figure 2. 3 Example of back trajectory**

For the solution of the trajectory equation, the differential trajectory equation expands  $S(t)$  in a Taylor series about  $t = t_0$ , evaluates at  $t_1 = t_0 + \Delta t$  and finally, with the first approximation of the equation, Equation 2.5 is obtained;

$$S(t_1) \approx S(t_0) + (\Delta t) u(t_0) \tag{2.5}$$

By the iteration, the final Equation 2.6 forms;

$$S^i(t_1) \approx S(t_0) + \frac{1}{2} (\Delta t) [u(t_0) + u^{i-1}(t_1)] \tag{2.6}$$

where the superscript  $(i)$  : number of iteration,

$u^i(t_1)$  : the position vector at position  $S^i(t_1)$ .

Equation 2.6 is a kinematic solution and only wind information is applied to this calculation. Not only the wind information but also the velocity and mass information are taken into consideration at dynamic solutions (Danielsen, 1961). The

research of Merrill (1986) compares the three isentropic Lagrangian trajectory techniques, one is kinematic (using only wind information) and two are dynamic (using both mass and velocity fields). As a result of this research it is found that 12-h data interval is useful for dynamic technique due to routine aerological observations (twice daily data available) whereas significant discrepancies were found for kinematic technique.

During the computation of trajectories, errors because of truncation of the finite difference equations should be estimated. Incorrect treatment of the map-scale factor, wind data interpolation error, and magnitude of position errors are the points which should be remarked. Especially, interpolation error of wind data originates from horizontal interpolation of the wind velocity component (Walmsley and Mailhot, 1983). Moreover, due to the absence of routine observation of vertical winds, many different assumptions are carried out and this situation causes many errors. Therefore, the vertical winds are less correct (Stohl, 2002).

At the theoretical estimates of error in position, each error of individual time step is added to each other. However, in the real atmosphere, the errors may be cancelled out some of the time. Therefore, the theoretical error is at maximum level and upper estimates of the errors in a trajectory model have occurred (Walmsley and Mailhot, 1983).

Mainly, trajectory model is done using mean horizontal and vertical winds from a meteorological model by integrating the trajectory equation. Forward trajectories focus on where a particle will go. On the other hand, backward trajectories identifies where the particle came from (Walmsley and Mailhot, 1983).

Trajectories are used to get geographical information in order to find possible location of the release if the location of release is not known. The researchers can determine the horizontal advection component of trajectory by the use of observed or analyzed winds. For the computation of the vertical component of trajectory, trajectories are assumed as isobaric (following a constant pressure), isentropic

(following a constant potential temperature) and kinematic (moving with the vertical velocity wind fields generated by a diagnostic or prognostic meteorological model) (Munzur, 2008).

Although the isobaric trajectory models were widespread in the past, the important vertical motions were ignored in this model (Harris and Kahl, 1994). Presently, isentropic trajectory models are very practical because the trajectory calculation can be done without vertical motion data. Moving along sloping isentropic surfaces forms the vertical motion (Fuelberg et al., 1996). The seasonal variation in atmospheric transport patterns to Summit, Greenland was investigated at Kahl's study (Kahl et al., 1997) by using the isobaric back trajectories. Geostrophic wind relationship was used to identify horizontal wind fields whose components are calculated at each trajectory time step.

### **2.3 Trajectory Statistics**

In the field of air pollution control, the pioneer researches on air motion trajectories were conducted based on individual trajectory information (Seibert et al., 1994), however the statistical approach for trajectories have been improved especially by Stohl (1996). In the current studies, mainly trajectory statistics methods which are based on the combination of the air parcel trajectory information and trace gas measurements to represent the distribution of pollution sources have been used.

Exception of atmospheric dispersion and decay processes of test species such as radioactive decay, chemical reactions and deposition are the main assumptions of trajectory statistics procedure. Test specie concentrations are assumed be correct and fully representative for study region. Furthermore, it is supposed that air parcel trajectory data interprets atmospheric transport procedure accurately (Fuelberg et al., 1996; Stohl and Seibert, 1998; Wotawa and Kröger, 1999; Seinfeld and Pandis, 2006; Nyanganyura, 2008).

Many different types of statistical procedures have been improved to characterize the source areas of pollutants by applying trajectory and long-term air pollution measurements (Stohl, 1996). Flow climatology (FC), potential source contribution function (PSCF), cluster analysis, concentration weighted trajectory (CWT) are some of the important and widespread types of trajectory statistics methods.

### **2.3.1 Flow Climatology**

Among the trajectory statistics methods, firstly flow climatology has been discovered and implemented. The main aim of the flow climatology technique is identifying the airflow characteristics and pollution information of specific region which is far away from the source of pollution. Flow climatology approximately classifies “regions of influence” for particular site; on the other hand detection of the special source areas cannot be properly computed. A number of years of back trajectories are estimated for a specific receptor and based on the direction and speed information they are sorted (Miller, 1981a,b). In addition to this classification, precipitation chemistry information is taken into account by many scientists such as Henderson and Weingarten (1982), Colin et al. (1989) and Miller et al. (1993).

With the 10-day back trajectory information of Bermuda and related flow climatology which continuous 7 years, the pollutant transportation in North America have been analyzed. Then, it was stated that the contribution of chemical data was more effective in rainy periods. In addition, the research includes the chemical data information obtained from Bermuda (Miller and Harris, 1985).

Katsoulis and Whelpdale (1993) sorted the 5-year trajectory data for Greece EMEP station and it was shown that main flow sectors did not change in years. Therefore, the possible source regions of pollutants were studied by using the back trajectory and the transport sectors information.

Airflow climatology information, especially impact of temperature and precipitation, for Michigan during 40 years was operated by using GIS based tools. Then, the

comparison of the results of this study and previous results implied that the developed methodology was remarkable on detection of source regions (Shadbolt, 2006).

In order to identify why the Antarctic Peninsula is a rapidly warming region, flow climatology approach, especially focusing on the climatology of weather system, was applied with research project conducted by University of Leeds and British Antarctic Survey (URL 7).

### **2.3.2. Potential Source Contribution Function**

The study of Ashbaugh (1985) which is conducted at Grand Canyon National Park is the one of the main studies in order to define potential source contribution function (PSCF) approach. As chemical mass balance (CMB) and positive matrix factorization (PMF), PSCF is a receptor-oriented method which has been widely used to justify pollution-control decisions (Zeng and Hopke, 1989). The chemical concentrations of pollutants at the receptor site and air back trajectories for this receptor are the relevant information to apply the PSCF. In order to determine source areas to receptor sites, trajectory statistical methods such as PSCF are used (Ashbaugh et al., 1985; Zeng and Hopke, 1989). Probability of an air mass with a pollutant above a criterion value which arrived at the receptor site after having passed through a particular geographical area can be explained by PSCF. For this approach, all pollutants are assumed as conservative species because of the exception of chemical transformation, atmospheric scavenging and loss through diffusion (Acadia National Park). In order to identify the locations which may have a higher possibility of being source areas of substances in the study region, PSCF approach is an effective concept.

In the literature, PSCF has been successfully carried out in many studies. One of the prior studies has been performed by Hopke and his colleagues (1995) to define the possible sources and pathways for biogenic and non-sea-salt sulfur in Arctic region. Cheng and Lin (2001) have determined the source sites by applying the PSCF

approach to data of 1998 Central American smoke events. In the study of Begum et al. (2005), potential sources and the testing of the ability of the PSCF analysis with the forest fire whose source location was clearly sighted have been identified by using the analysis. The research performed at China (Jinan, China) has indicated that higher potential source regions for sulfate are seen at some specific provinces and agreement on PSCF results with cluster analysis results is apparently observed. Moreover, a new modified method of PSCF has been developed by Jeong et al. (2013) in order to evaluate the contribution of long range transport that alters the mean mixing ratio of test species at receptor site. The conditional potential source contribution function (CPSCF) has focused on inter-annual differences in the change in mean SO<sub>2</sub> mixing ratio due to the long-range transport in Seoul.

In the construction of PSCF, the trajectory endpoint lies at an *i* by *j* array grid cell and the trajectory collects pollutants emitted in the cell. The pollutant is assumed to transport through the trajectory to the receptor without any atmospheric removal and chemical change. Based on the geographical scale of the problem and the length of trajectory segment, the grid cell size is selected (Hopke et al., 1995).

The calculation of PSCF can be defined as below;

$$P[A_{ij}] = \frac{n_{ij}}{N} \quad (2.7)$$

The probability of falling of trajectory segment endpoints into the specific cell (*i,j*), in other words the potential transport of material to the receptor site, is notated as  $P[A_{ij}]$ . The number of endpoints that falls in the  $ij^{th}$  cell is represented as  $n_{ij}$ . And the total number of trajectory segment endpoints throughout the study period (*t*) is stated as *N*.

$$P[B_{ij}] = \frac{m_{ij}}{N} \quad (2.8)$$

The probability of falling of polluted trajectory segment endpoints into the same cell is notated as  $P[B_{ij}]$ . The number of polluted endpoints which are considered to be ending at receptor site at a time when measured concentration exceeds a selected criterion value for each species is represented as  $m_{ij}$ .

$$PSCF_{ij} = \frac{P[B_{ij}]}{P[A_{ij}]} = \frac{m_{ij}}{n_{ij}} \quad (2.9)$$

Additionally,  $PSCF_{ij}$  is the conditional probability function that identifies the spatial distribution of possible geographical source locations deduced by using trajectories (Hopke et al., 1995). The PSCF value ranges between 0 and 1. Cells with PSCF of 1 mean that the cells have high probability of being source region. The cells which contain pollution sources have high number of polluted trajectory segments ( $m_{ij}$ ), therefore the PSCF values of these cells are higher than the others.

The  $n_{ij}$  values are different for each cell. For example some cells have small number of trajectory segments and it causes an uncertainty. When there are only two trajectory segments in a cell and one of them is polluted segment, the PSCF value is 0.5. Due to small number of trajectory segment, it cannot represent the possibility of the source region correctly. In order to reduce the effect of small number of  $n_{ij}$ , weighting function is applied. Based on the average value of the  $n_{ij}$ , the weight function 2.10 have been applied at many studies (Zhao and Hopke, 2006; Xu and Akhtar, 2009). In addition, similar weight functions which depend on average  $n_{ij}$  and different weighting coefficients have been used in the researches of Poissar and Hopke (Hopke et al., 1995; Poissar et al., 2001).

$$w(n_{ij}) = \begin{cases} 1.0 & n_{ij} > 2 \cdot n_{avg} \\ 0.75 & n_{avg} < n_{ij} \leq 2 \cdot n_{avg} \\ 0.5 & n_{avg}/2 < n_{ij} \leq n_{avg} \\ 0.15 & n_{ij} \leq n_{avg}/2 \end{cases} \quad (2.10)$$

Instead of the weighting function, by using the non-parametric bootstrapping technique, PSCF results can be modified with the minimization of the uncertainties (Lupu and Maenhaut, 2002; Wehrens et al., 2000; Vasconcelos et al., 1996). In this technique, concentrations are assumed to be independent and identically distributed. While  $C = \{c1, c2, \dots, cN\}$  implies the concentration of original data set,  $B$  implies random subsamples of size equal to the length of the data set.  $C^* = \{c1^*, c2^*, \dots, cN^*\}$

is drawn with substitution and the corresponding PSCF spatial distribution,  $P^*k;ij$ , is calculated ( $k$  is the each bootstrapped sample). These values are ordered as  $P^*(1);ij < \dots < P^*(B);ij$ , where  $k = 1, \dots, B$ , and  $\alpha$  is the chosen significance level. If

$$P_{ij} \geq P^*_{((B+1)(1-\alpha/2))ij} \quad (2.11)$$

the null hypothesis, in which there is no association between concentrations and trajectories, is rejected at  $(1 - \alpha)$  100% confidence level. In that case, for further analysis, only the PSCF values satisfying Equation 2.11 are taken into consideration (Lupu and Maenhaut, 2002).

Unidentified and background sources, mixing factor of air parcels during transposition from source to receptor and differential loss of species such as deposition are the main uncertainties in trajectory calculation. Both these uncertainties and assumptions of the PSCF calculations are the weak aspects of this method (Stohl, 1998; Stohl et al., 2002).

## 2.4 Sources and Transport of Sulphur Compounds

The important anthropogenic sulphur sources include power plants, industrial boilers, municipal or industrial incineration, ore processing, pulp and paper industry, plastics and paint manufacture, motor vehicles and air craft. On the other hand, volcanoes, biogenic emissions from soils, plants, wetlands and the ocean, biomass burning and sea-spray are the main natural sources of sulphur. While the electric utilities generate approximately 60% of the man-made sulfur dioxide, industries form about 30% of it. The rest consists of the other types of man-made source of sulfur dioxide such as mobile sources (Girish, 2007). Mainly, 90-95% of total sulfur is emitted from anthropogenic activities, and the 5-10% of sulfur is formed by natural activities (Cullis and Hirschler, 1980). Particularly, the ratio is prevalent for industrial countries like North American and European countries. On the other hand, natural sources of sulfur oxides have a more important role in eastern countries. Lucas and

Akimoto imply that about 69% of the SO<sub>2</sub> forms from man-made surface emissions, 20% from the oceans and 10% from volcanoes (Lucas and Akimoto, 2007).

Sulfates include a charged group of sulfur and oxygen atoms. SO<sub>4</sub><sup>2-</sup> is a salt and fundamental component of sulfuric acid. Based on diameter, approximately 0.1 to 1.0 micrometer sulfates exist in atmosphere and more concentrated values are detected in industrial areas (Charlson et al., 1992). By the oxidation of sulfur dioxide which is produced from combustion of fossil fuels, a great deal of sulfate aerosol occurs. In addition, as an origin of dust, sea salt and compounds of marine, natural sulfate aerosols are present. When the concentrations of natural and industrial sulfates are compared, it is seen that anthropogenic (industrial) types have been increasing from 1950s while natural types stay almost constant. Lung irritation, contribution to acid rain and haze formation are the main negative side effects of the sulfates (Charlson and Wigley, 1994).

Andreas et al., (1988) have studied the possibility of material being transported from Asia to North America by examining the composition of the atmospheric aerosol and gases over the western North Pacific Ocean. They have concluded that dimethylsulphide (DMS) concentration over the Pacific Ocean is controlled by marine rather than continental processes. The vertical profiles of SO<sub>2</sub> and nss-SO<sub>4</sub><sup>-</sup> from the work of Andrea et al. (1988) suggest that, significant amounts of SO<sub>2</sub> and nss-SO<sub>4</sub><sup>-</sup> are produced by the oxidation of DMS within the boundary layer. The study of Eliassen and Saltbones (1983) implies that the deposition of sulphur due to foreign sources acts as an important contribution to the total deposition in most of European countries.



## CHAPTER 3

### METHODOLOGY

#### 3.1 Study Area

In this study, the study area was described depending on the locations of Antalya, Çubuk, Ashdod and Corsica stations and movement of trajectories. The rectangular study area extended from 20° West to 60° East longitudes and 71° North to 14° North latitudes. It means that the boundary longitudes reached from west of Iceland to east of Caspian Sea and the boundary latitudes included from north of Scandinavian countries up to south of Red Sea. The study domain consists of Europe, western part of Asia, North Africa and Middle East.

##### 3.1.1. Stations Selected for PSCF Calculations

Four sampling points which were selected to represent the study area are given in Figure 3.1. Among the four stations, two of them, namely, Antalya and Çubuk stations were used in PSCF calculations, because these were the stations where  $\text{SO}_4^{2-}$  data were available for long enough time periods. Antalya station was established in 1991, and first research was conducted by Güllü (1996). Related to the selection of this site, it is implied that selection of reference stations is an important stage in study of long range transport. However, such regional stations are expected to fulfill certain siting criteria. The stations should be away from local sources. According to the availability of power, having trained personnel to change samples and being on the grounds of a governmental property where it can be protected, the site of the

Antalya station was selected (Güllü, 1996). The Çubuk Station was selected to represent the Central Anatolian atmosphere, so that potential source regions which affect the Anatolia can be investigated.



**Figure 3. 1 Locations of sampling stations (Google Earth, 2013)**

### **3.1.1.1 Southern Anatolia Station (Antalya)**

Antalya Station is on the coast, approximately 20 km to the west of Antalya city. The geographic coordinates of the station is 31.0° East longitudes and 36.8° North latitudes. The location of the station was established at distant place from populated region in order to minimize the influence of local emissions. The station was built on the rock structure near the sea and it is 20 m above the sea level. Picture of the sampling platform is shown in Figure 3.2.



**Figure 3. 2 Antalya Station, Hi-Vol sampler (Öztürk, 2009)**

### **3.1.1.2. Central Anatolia Station (Çubuk, Ankara)**

The Çubuk Station (33.1°E and 40.1°N) is at one of the remote areas of Ankara city. It is approximately 50 km away from city center and also height above sea level of the station is 1169 meters. Çubuk Station was the only operational European Monitoring and Evaluation Programme (EMEP) station in Turkey and thus it was the best equipped station in the country. The station operated between 1993 and 2006 by the Ministry of Health. It was transferred to the Ministry of Environment and Forestry in the year 2006 and terminated due to operational problems. During this period of time, generated data were transferred to the EMEP secretariat. Data, from Turkey and other countries were used to calibrate EMEP models. EMEP avoided interpretation of data from individual stations.

### **3.1.2. Stations Selected for RoI Calculations**

The RoI approach does not depend on availability of pollutant data at the receptor. This means that we were not confined with stations where data were available for RoI calculations. Pollutant information in RoI calculations consisted of emission data compiled by EMEP.

Four stations were selected for RoI calculations, which represent different regions in the Mediterranean Basin. Antalya, Çubuk, Ashdod (Israel) sites were selected to represent Eastern Mediterranean region and Corsica station was selected to represent the Western Mediterranean atmosphere. Corsica and Ashdod are the two locations where extensive aerosol and rainwater research was conducted in the past. Site characteristics were easily accessible in literature. Application of RoI calculations to Antalya and Çubuk stations in Turkey allowed us to compare the results obtained by PSCF and RoI calculations.

### **3.1.2.1. Western Mediterranean Station (Corsica, France)**

The third station (8.72°E, 42.53°N) is located at the Corsica island of France, which is approximately 90 km away from the Italian coast and almost 150 km away from the French Riviera. The station is situated on the coast and at the sea level.

### **3.1.2.2. Eastern Mediterranean Station (Ashdod, Israel)**

In order to represent the eastern end of the Mediterranean basin, the Ashdod Station (34.655°E, 31.804°N) was selected. The station was located on the Mediterranean coast of Israel, 40 km south of Tel Aviv. Sampling equipment was installed approximately 20 m above ground level and 2.5 km away from the coast. It should be noted that it is not possible to find any site on the Israel coast that is entirely free from anthropogenic emissions. Because of this, Ashdod represents a site which is under the influence of a mixture of natural and anthropogenic sources.

## **3.2. Description of Study Domain**

Two different grid systems were used in PSCF and RoI calculations. The first grid system, which was used in PSCF calculations, extended from 20° West to 60° East in E-W direction and from 71° North to 14° North latitudes in N-S direction. The area between these grids was divided into 1° to 1° grids. The grids, which are on the

seas, were ignored because this first grid system was used to calculate the potential source contribution function for  $\text{SO}_4^{2-}$  only. Grids on the sea should be included in calculations when PSCF was calculated for ions and elements with marine sources, such as Na, Cl. Since seas are not a strong source of anthropogenic  $\text{SO}_4^{2-}$ , we did not include marine grids in our PSCF calculations. There were 3150 grid cells in the defined study area.

The second grid system was used in RoI calculations. The reason for using a different grid system in RoI calculations was the need for exact math with EMEP grid system in RoI computations. Emission data from EMEP data base was used in RoI calculations. Emission data in EMEP data-base are given in EMEP grid system, which does not exactly matched with the grid system we used for PSCF computations. The difference is not very large. EMEP grid system is  $0.25^\circ$  shifted version of our PSCF grid system. This second grid system, which is shown in Figure 3.3, extended from  $20.25^\circ$  West to  $59.75^\circ$  East longitudes and  $71.25^\circ$  North to  $14.25^\circ$  North latitudes. The grid size in this system was also  $1^\circ$  to  $1^\circ$ . RoI grid system is generated by moving PSCF grid system  $0.25^\circ$  northwest direction. Number of grids in RoI grid system was 4560. Both grid systems were created with “Grid Maker (Version 1.3)” application of MapInfo 7.5 program (MapInfo Corp, 2003).

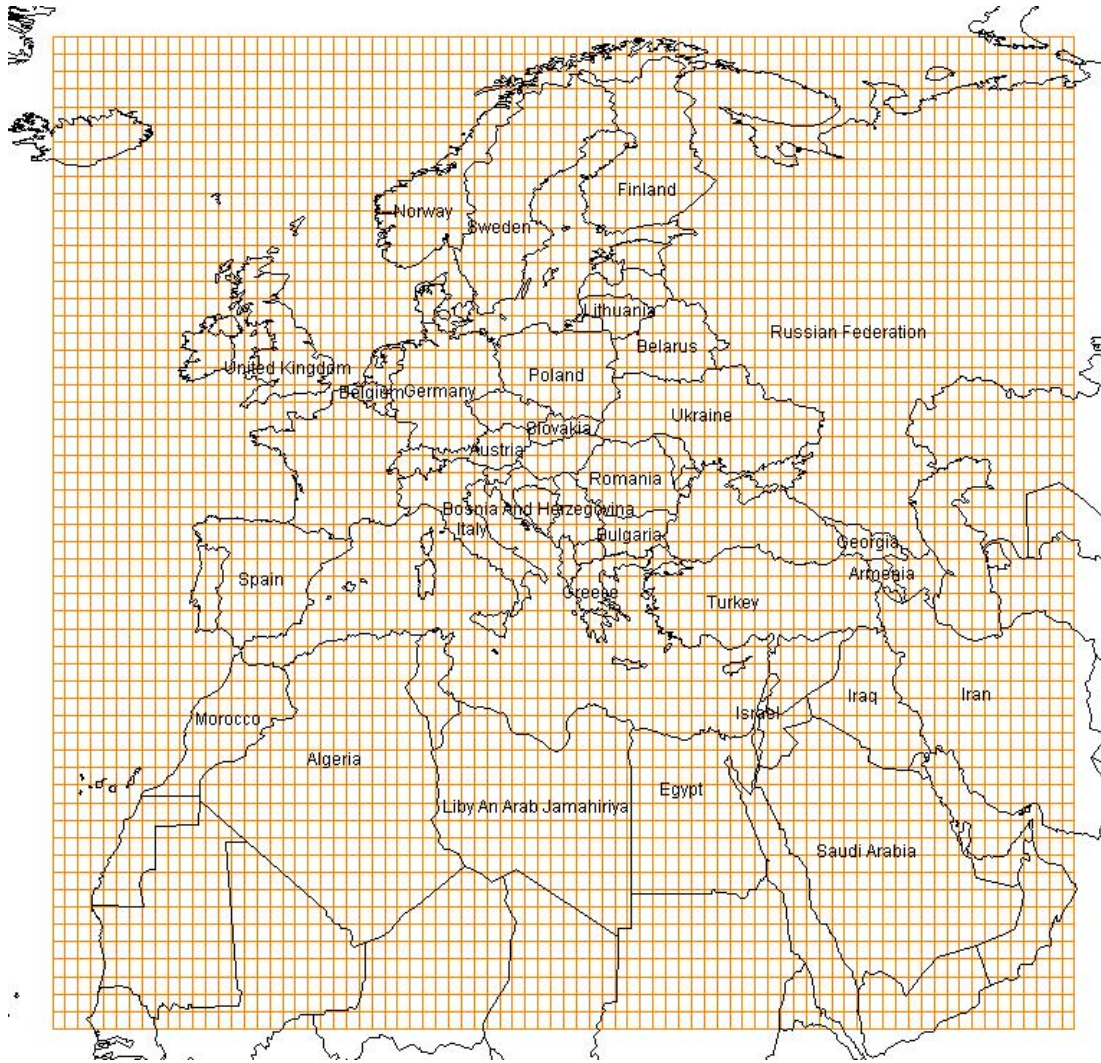


**Figure 3. 3 Second grid system (gridded domain of  $1^{\circ} \times 1^{\circ}$ )**

### **3.3. Data Preparation**

There are only two data sets were used in this study. Those were pollutant data, or  $\text{SO}_4^{2-}$  data and back trajectory data generated by back trajectory modeling. While  $\text{SO}_4^{2-}$  concentrations were obtained from Antalya and Çubuk stations,  $\text{SO}_2$  emission concentrations were taken from EMEP database for Antalya, Çubuk, Ashdod and Corsica. On the other hand, back trajectory data were calculated by using TrajStat program for each station and every day. The detailed information related to the data preparation is given in Section 3.3.1 and Section 3.3.2.

### 3.3.1. Pollutant Data

Sulfate is an important ion in the Eastern Mediterranean for two reasons; (1) it is the most important ion for acidification of environment through acid rain formation and (2) its concentration in the Eastern Mediterranean is higher than  $\text{SO}_4^{2-}$  measured anywhere else around the world. These are the two main reasons for why we wanted to understand how source regions of  $\text{SO}_4^{2-}$  affecting Eastern Mediterranean changed in time.

In Turkey  $\text{SO}_4^{2-}$  was measured in a number of stations, but data that is long-enough to be used for the assessment of temporal variations in source regions of this ion are only available at Çubuk and Antalya.

At Çubuk station daily aerosol sampling for ion measurements took place between 1993 and 2006. The station was operated by the Ministry of Health very successfully. The station was transferred to the Ministry of Environment and Forestry in 2006. Unfortunately no data was generated since then.

Samples at Çubuk station were collected on cellulose filters using a high volume pump. Sampling was daily. After sampling filters containing ions are transferred to the Central Laboratory in the Refik Saydam Institute of Public Hygiene in the Ministry of Health. In the lab major ions are measured by ion chromatography. The laboratory was equipped with two Dionex 120 ion chromatographs. One of them was fitted with a Dionex AG9-HC anion exchange column and the other one was equipped with Dionex CS12A cation exchange column.

Sulfate was not the only parameter measured in Çubuk station. All major ions including  $\text{SO}_4^{2-}$ ,  $\text{NO}_3^-$ ,  $\text{Cl}^-$ ,  $\text{Na}^+$ ,  $\text{Mg}^{2+}$ ,  $\text{K}^+$ ,  $\text{Ca}^{2+}$ ,  $\text{NH}_4^+$  and  $\text{H}^+$ , were measured in aerosol samples. In addition to these,  $\text{NO}_2$ ,  $\text{SO}_2$  were measured using filter pack technique. These data were generated without any significant interruption between 1993 and 2006. Only  $\text{SO}_4^{2-}$  data from Çubuk station were used in this work. A total of 3686  $\text{SO}_4^{2-}$  data were available from Çubuk station for this study. Sulfate data were obtained from the Ministry of Health through a special protocol signed between the university and ministry.

Station at Antalya was located approximately 20 km to the W of the city of Antalya. The station was established by METU, Department of Environmental Engineering in 1992 and remained operational until 2001. It was shut down in 2000 due to funding problems. Sampling was conducted on a daily basis using a high volume sampler. Sulfate was measured with a Varian Model 2010 HPLC ion chromatograph, equipped with a model VYDAC 302 IC anion exchange column and a model JASCO UV-VIS 875 detector (Öztürk, 2009).

Like in Çubuk station,  $\text{SO}_4^{2-}$  was not the only ion measured in Antalya station as well. In the same aerosol samples other major ions and approximately 50 trace elements were measured using a Perkin Elmer ICP-MS. Rain were also collected and analyzed for ions and trace elements. Only  $\text{SO}_4^{2-}$  data were used in this study. There were approximately 1370 daily  $\text{SO}_4^{2-}$  data were available from Antalya station.

In addition to the sulphate measurements at the Antalya and Çubuk Stations, when applying regions of influence approach,  $\text{SO}_2$  emission data were also needed.  $\text{SO}_2$  emissions were obtained from EMEP website.  $\text{SO}_2$  is the precursor of sulfate, and  $\text{SO}_x$  mainly consist of  $\text{SO}_2$ . Therefore,  $\text{SO}_x$  data obtained from EMEP directly related with sulfate data. EMEP gives the emission data information for whole EMEP region. Emission data in EMEP website are available for the years 1980, 1985, and from 1990 to 2010. Parameters, which are necessary to get emission data, are summarized in Table 3.1. In EMEP website, emissions are given in “emission database” (WebDab).  $\text{SO}_2$  emissions in EMEP data base were downloaded for all countries for the target years. Data obtained from EMEP were given in  $0.5^\circ$  to  $0.5^\circ$  grids for 10 source sectors, which includes:

S1: Combustion in energy and transformation industries (stationary sources),

S2: Non-industrial combustion plants (stationary sources),

S3: Combustion in manufacturing industry (stationary sources),

S4: Production processes (stationary sources),

S5: Extraction and distribution of fossil fuels and geothermal energy,

S6: Solvent use and other product use,

S7: Road transport,

S8: Other mobile sources and machinery,

S9: Waste treatment and disposal,

S10: Agriculture.

In this study data from all sectors are combined

**Table 3. 1 Summary table for getting emission data from EMEP**

<b>Data Information Section</b>	<b>Desired Data</b>
Countries/Areas	ALL (except international shipping)
Years	1980, 1985 and from 1990 to 2010 (all years)
Output formats	Grid (0.5o x 0.5o), Semicolon-Separated (CSV file)
Main Pollutants	SO <sub>x</sub> (as SO <sub>2</sub> )
Available Sectors	National Total (without other sources and sinks)

The gridded emission data covers the longitudes from 29.5°W to 60°E and latitudes from 30.5°N to 75°N. The region where the emission data information is defined contains Iceland, Scandinavian countries, all European countries, Western Russia, Turkey, Georgia, Armenia, Azerbaijan, west parts of Kazakhstan, Uzbekistan and Turkmenistan, Syria, Israel, Lebanon, North parts of Iraq and Iran and Jordan, small portion of northern Algeria, Tunisia, Libya and Egypt. In this study, emission data for all years were downloaded one by one via using the information explained in Table 3.1. The text file format data was converted to excel so that it can be uploaded to GIS software (MapInfo). A small part of the gridded emission data are given in Table 3.2 as an example. In the table, SO<sub>x</sub> values are given with grid center coordinates for the year 2002. The column of Number/Flag identifies the numerical value of SO<sub>x</sub> emission in megagram (Mg).

**Table 3. 2 Example for SO<sub>x</sub> emission data format, EMEP**

Country Code	Year	Sector	Pollutant	Longitude	Latitude	Unit	Number/Flag
PL	2002	Snap National	SO <sub>x</sub>	19	53.5	Mg	3423.958
PL	2002	Snap National	SO <sub>x</sub>	19	54	Mg	4145.48
PL	2002	Snap National	SO <sub>x</sub>	19	54.5	Mg	13764.39
PL	2002	Snap National	SO <sub>x</sub>	19	55	Mg	927.0188
PL	2002	Snap National	SO <sub>x</sub>	19.5	48.5	Mg	0.1991
PL	2002	Snap National	SO <sub>x</sub>	19.5	49	Mg	55.7621
PL	2002	Snap National	SO <sub>x</sub>	19.5	49.5	Mg	5294.446

Before uploading emission data to MapInfo software, only the year, longitude, latitude and number/flag columns were kept and remaining columns shown in the table were deleted. The excel file was updated to MapInfo program, from “Table” section, the data was visualized by using the “Create Points” application. The main part of distribution of SO<sub>2</sub> emission data in EMEP grid system is given in Figure 3.4. Based on the longitude and latitude values, SO<sub>2</sub> emission data was obtained for each point.

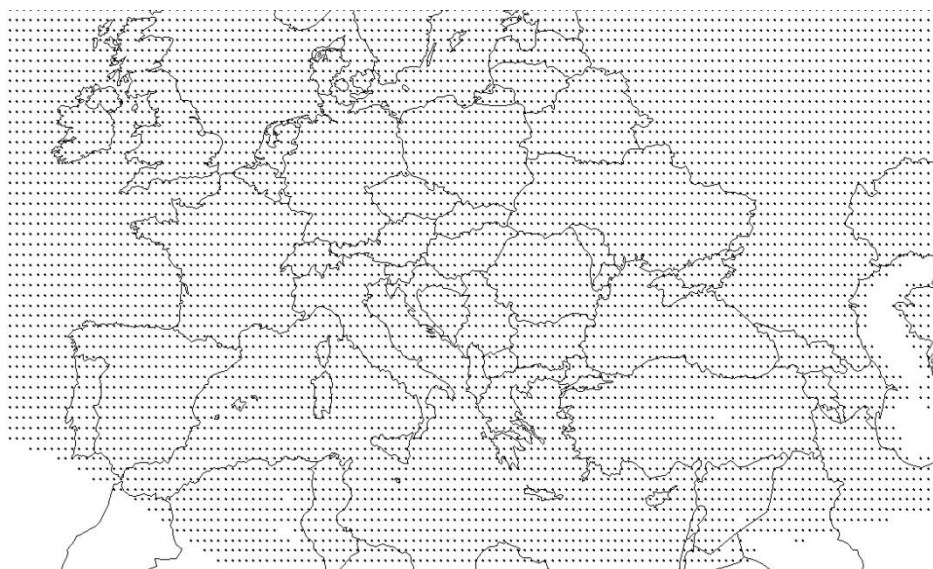


**Figure 3. 4 Distribution of SO<sub>2</sub> data at EMEP grid system**

### 3.3.2. Back Trajectory Data

In this study, Air Resources Laboratory's (ARL's) "HYbrid Single-Particle Lagrangian Integrated Trajectory Model" (HYSPLIT) (Draxler and Hess, 1998) was used to calculate back trajectories. The model was developed by the U.S. National Oceanic and Atmospheric Administration (NOAA) for the studies related to air quality, atmospheric dispersion, and climate.

The HYSPLIT model is a complete system for computing simple air parcel trajectories, complex dispersion and deposition simulations. The model computes the advection of a single pollutant particle, or simply its trajectory without the additional dispersion modules. The calculation method of the model based on a hybrid between the Lagrangian approach (using an air parcels move from their initial location as a reference moving frame) and the Eulerian approach (using a fixed three-dimensional grid as a reference frame). While the Lagrangian approach focuses on the advection and diffusion calculations, the Eulerian approach computes the pollutant air concentrations. The model has also dispersion modules to calculate transported concentrations of pollutants, but that module was not used in this study.

HYSPLIT web site allows computation of one trajectory at a time (in our case one day at a time). This makes back trajectory calculations a very slow process if trajectories are to be calculated for several years, as we did in this study.

A supporting program, namely TrajStat, which is GIS-based software (Wang et al., 2009), allows computation of trajectories in monthly batches. The trajectory calculation module of HYSPLIT is included in TrajStat as an external process to calculate trajectories. TrajStat software which became available in last three years significantly reduced our calculation time. Calculated trajectories were converted to GIS line shape file. In this shape file, trajectories are defined by its longitude (x), latitude (y) and height (z) datum. The two dimensions trajectories are shown based on the x and y coordinates.

TrajStat is free software. It also includes various trajectory statistical analysis methods such as Potential Source Contribution Function (PSCF), Concentration Weighted Trajectory (CWT) and Cluster Analysis.

In order to obtain back trajectories, in this study TrajStat software was used. Firstly, the TrajStat desktop application was downloaded, but Microsoft.NET Framework 3.5 had to be installed before using TrajStat in windows system. “Calculation” icon of “Trajectory” segment which is at the toolbar of TrajStat window was used to get back trajectories. The information of year-month, starting location, run time, starting hours, meteorological information, start and end days were entered to the system. When the “Multi\_Locations” option was selected, latitude, longitude and height data were entered one by one for three different starting height, so all trajectories were downloaded with only one run. The related meteorological files depending on the desired month of trajectory were added.

The meteorological data were obtained from gridded meteorological data archives of ARL. The required meteorological data were downloaded by using NOAA ARL FTP Server of (The National Weather Service's National Centers for Environmental Prediction) NCEP/NCAR Reanalysis (1948-2010) data set. The execute file was also definite and constant. The output file was created and path of the file was selected. The ‘hyts\_std.exe’ file obtained from HYSPLIT was used in calculation. The file names were set automatically to ‘yymmddhh’, such as ‘95072914’. Every trajectory was rewritten to the format with column titles as fist row and comma-delimited data with clicking the ‘Convert’ button. The extension names of the files were changed to ‘.tgs’. Finally, using ‘Combine’ button, ‘.tgs’ files were converted to one file.

A sample TraStat dialog interface to calculate back trajectory for Çubuk Station in July 1995 is given in Figure 3.5.

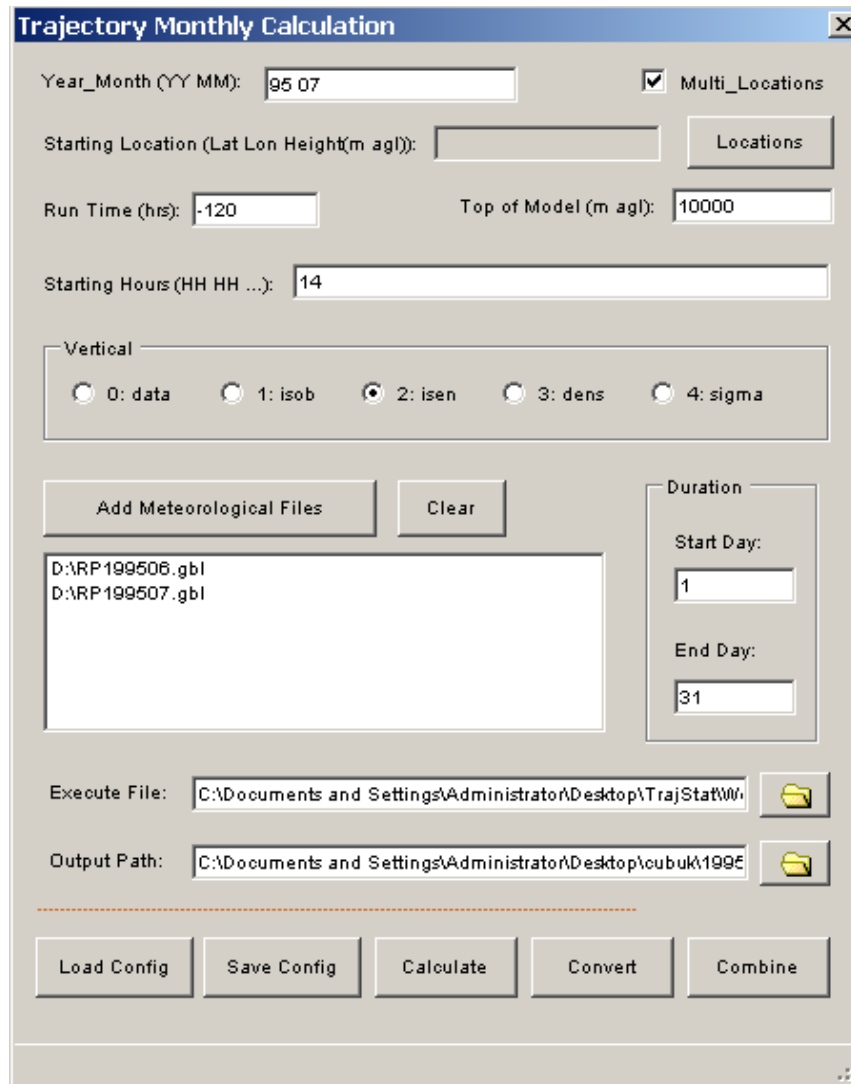


**Figure 3. 5 Example of trajectory monthly calculation window of TrajStat**

The combined monthly back trajectory data named as ‘9507’ was converted to Excel file format because Excel is an appropriate format to transfer trajectory segment coordinates to MapInfo for spatial calculations. The small part of prepared data format is given in Table 3.3 as an example.

**Table 3. 3 Example of back trajectory data format, TrajStat**

start year	st. month	start date	start hour	year	month	day	hour	age hour	Latitude	longitude	height	press
95	7	1	14	95	6	27	14	-96	59.21	28.477	2382.8	758.8
95	7	1	14	95	6	27	13	-97	59.4	28.231	2372.4	760.2
95	7	1	14	95	6	27	12	-98	59.585	27.973	2362.3	761.5
95	7	1	14	95	6	27	11	-99	59.777	27.699	2355.5	762.3
95	7	1	14	95	6	27	10	-100	59.985	27.403	2376.5	759.9
95	7	1	14	95	6	27	9	-101	60.215	27.08	2400.2	757

In order to get annual total trajectory data, the monthly files (such as 9501, 9502, 9503 etc.) were also be combined by using ‘Join TGS Files’ command of TrajStat. Therefore data with 132495 trajectory segments was produced.

HYSPLIT also provide rainfall information for every trajectory segment. If the precipitation data is needed, the unconverted daily data files are used. The format of files is undefined and size of each file is 40 KB. The daily trajectory data files cannot be combined since they are not in ‘.tgs’ format. They are combined by using Command Prompt which is an execution of Microsoft Windows. By using the command of ‘copy/b’, the desired days are combined in a new text document file format, then it is again converted to excel format. In this study we worked on weighting trajectory segments with rain, because rain effectively washes pollutants and if a trajectory passes through a rain event, history of pollution transport, from that segment backwards is erased. We did not use our attempts for rain weighting in this study because there were no good methods to test the accuracy of weighting used.

In this study, the 5-days back trajectories for the starting height of 100 m, 500 m and 1500 m were calculated for each station (Antalya, Çubuk, Corsica and Ashdod) during 23-years period (for 1980, 1985 and from 1990 to 2010) by using TrajStat software. Vertical motion was selected as isentropic because of the assumption of

trajectories which is related to constant temperature potentials. Trajectories started at 14 pm for every day and calculated 120 hours backward in time.

### 3.4. Potential Source Contribution Function (PSCF)

As defined in Section 2.3.2, the PSCF calculation was based on the Equation 3.1. The  $m_{ij}$  implies the total number of polluted trajectory segments, while  $n_{ij}$  is the total number trajectory segments for  $ij^{\text{th}}$  grid cell.

$$\text{PSCF}_{ij} = m_{ij} / n_{ij} \quad (3.1)$$

In PSCF calculation, the first grid system identified from 20° west to 60° east longitudes and 71° north to 14° north latitudes with cell size of 1° to 1° grid system was created.

Principally, altitude of trajectory segment is not taken into consideration in PSCF calculation. All trajectory segments which are at different altitudes have same potential of picking up pollutants. However, in this study, PSCF calculation was done by applying altitude weightings in order to add the effect of trajectory segments' height. It is assumed that the trajectory segment at high altitude has lower probability of picking up pollutants from surface sources, than trajectory segments that are close to the surface. We believe that uncertainties in assigning source regions are minimized by weighting trajectory segments depending on their altitudes. In the study of Doğan (2005) and Yıkılmaz (2010), the altitude effect on PSCF calculations were discussed. They implied that the trajectories which are far from the receptor have high altitude levels; hence, possibility of being potential source region decreases.

Three different altitude weightings, which are shown in Table 3.4, were tried. For instance, at altitude weighting type 1, if trajectory segment's height is between 0 and 500 meters, the segment is counted as 1.0. The weighing factor 1.0 means that segment totally contributes to the transportation of pollutant, and it was used for

segments which are close to the surface. When the height ranges between 500 and 1000 meters, it is weighted by 0.8. Finally, if the height is greater than 1000 meters, it is weighted by 0.5. It means that its effect of determining sources of pollution was decreased by 70%.

**Table 3. 4 Height weightings used in calculations**

	0 m < altitude < 500 m	500 m < altitude < 1000 m	1000 m < altitude
weighting factor of <b>altitude weighing type 1</b>	1.0	0.8	0.5
weighting factor of <b>altitude weighing type 2</b>	1.0	0.5	0.3
weighting factor of <b>altitude weighing type 3</b>	1.0	0.3	0.1

In order to calculate altitude weighted PSCF, the trajectory data files were prepared. The weighting factors were added to the new column of the file according to the altitude of each segment. The sulfate measurements were sorted in descending order. The highest 40% sulfate concentrations were defined as polluted days, therefore the back trajectories belonging the polluted days were determined. The same weighting approach was also used to prepare polluted trajectory data file.

At this stage, the total trajectory data file and polluted trajectory data file were prepared. The grid file was also ready to perform the PSCF. These files were opened at MapInfo. While  $n_{ij}$  was calculated by counting the altitude weighting factors of total trajectory segments in the  $ij^{\text{th}}$  grid cell,  $m_{ij}$  was counted by summing the altitude weighting factors of polluted trajectory segments. These were counted by using ‘SQL (Structured Query Language) Select’ technique, which is a way of questioning in the GIS software. Summations of altitude weighted factors (for altitude weighting type 3) of total trajectory segments in each grid cell for the years of 1999 and 2000 are shown in Figure 3.6 for Antalya data, as an example. The trajectory data file

(99\_00\_ant\_1\_altAB) and grid file (sonhakkin2003) were seen, also the summation of altitude weighted segments (P column) were written as in SQL Select window. As consequence, the program was run and the values were presented in ‘Query1’ browser. Same procedure was performed for polluted trajectory segments, hence the altitude weighted  $m_{ij}$  for  $ij^{\text{th}}$  cell was found. Then the values (Query1 and Query2) were updated to grid file by using the ‘Update Column’ section, and the  $m_{ij}$  values were divided by  $n_{ij}$  values as indicated in Figure 3.7. Thus, the altitude weighted PSCF values for each grid cell were computed.

As defined in Section 2.3.2, the numbers of total trajectory segments are different for each grid cell. If the value is small, the PSCF value has high uncertainty and assigned source regions become equally uncertain. This problem appeared particularly at the edges of the study area, where number of trajectories and trajectory segments are few. An approach developed by Zhao and Hopke (2006) was used to down-weight the contribution of grids with few segments in apportionment of source regions.

Hence, the weighting coefficients used in the research of were applied in this study. The approach depends on a weighting of number of trajectory segments in a particular grid  $ij$  with fractions of 1.0 depending on the difference between number of segments in that grid ( $n_{aj}$ ) and average number of trajectory segments in all grids in the study domain ( $n_{avg}$ ). The weighting scheme is given in Equation (3.2).

$$w(nij) = \begin{cases} 1.0 & nij > 2 \cdot navg \\ 0.75 & navg < nij \leq 2 \cdot navg \\ 0.5 & navg/2 < nij \leq navg \\ 0.15 & nij \leq navg/2 \end{cases} \quad (3.2)$$

This equation implies that no weighting is used if the number of trajectory segments in a grid is higher than twice the average number of trajectory segments in whole grid system. Number of segments in a grid is multiplied with 0.75 if the  $n_{aj}$  is between twice the average number of segments and average number of segments etc. This approach down weights the contribution of segments at the peripherals of the

grid system that have small number of segments on assigning source regions based on the PSCF values.

In PSCF approach one trajectory is calculated for each sample. Since there is not necessarily 360 samples collected in every year, number of measurements and thus number of trajectories are not large enough to calculate statistically significant PSCF values in some of the years when sampling is not complete due to various problems in the stations. To avoid this PSCF calculations, in this study, were performed with two-year increments.

All back trajectories, for the days with  $\text{SO}_4^{2-}$  data, were combined in an excel file, which was then opened with MapInfo software and trajectory segments were distributed based on their longitude and latitude values, using the Create Points option. Also the prepared grid file was opened by using Update Column option.

Another factor affecting the PSCF values is rainfall amount of trajectory segments. When the rainfall amount of trajectory segment is high, the pollutants which are transported with air masses are washed out. In other words, previous segments are no longer effective for calculation of pollution sources. The probability of being a pollution source before the segment is low because of the washout of pollutants. Yılmaz (2010) developed a weighting scheme, which attempts to down-weight the contribution of pre-rain segments to identification of potential source areas. In that study, the best result was obtained by selecting the rainfall weighting as 0.2 mm.

At the beginning of the study we started the weighting scheme used by Yılmaz (2010). Thus, 0.2 mm rainfall weighing was used. This means that if a trajectory passes through a rain event, which is  $> 0.2$  mm all segments before that point are multiplied by zero (deleted) and they do not contribute to segment counts in their respective grids.

The use of rain weighting was completely abandoned because there were no way to check the accuracy of the weighting scheme and uncertainty of rainfall calculations

at each grid was high and we were not sure if the altitude of rain event matches with the altitude trajectory segment. However, the logic for the need for rain weighting is valid and we may work on such weighting in the future.

### **3.5. Regions of Influence (RoI) Approach**

Regions of Influence approach was originally developed by Yilmaz (2010). In this study altitude weighting was added to original RoI method and the method is used to understand how source regions changed in time in four locations in the Eastern and Western Mediterranean basins.

RoI can be considered as source oriented trajectory statistics, which is different from most of other methods involving trajectory statistics as most of them are receptor oriented statistical tools.

While conducting RoI, SO<sub>2</sub> emissions were used as an input. EMEP has a database where emissions of SO<sub>2</sub> and other pollutants are kept in gridded form. Emission data is available for the years 1980, 1985 and from 1990 to 2010. Because of this these are also the years for which we calculated RoI distributions. And, back trajectory information for each of these years was generated using TrajStat code for each of the four stations. The grid system used in RoI calculations were discussed before and will not be repeated here.

RoI is a very simple computational scheme. Number of trajectory segments in each grid cell was counted and multiplied with the SO<sub>2</sub> emissions in that cell. We applied altitude weighting in as we did for PSCF calculations. For each station, yearly back trajectory data with altitude weighting constants were prepared for each of the grids in the system. This altitude weighted segment count in each cell is multiplied with the SO<sub>2</sub> emission value obtained from EMEP data base for that particular cell. This procedure can be formulated as:

$$\text{RoI}_{ij} = n_{ij} \times E_{ij} \tag{3.3}$$

Here  $RoI_{ij}$  is the region of influence value for grid cell  $ij$ .  $n_{ij}$  is the number of altitude weighted segments in grid  $ij$  and  $E_{ij}$  is the  $SO_2$  emissions in grid  $ij$ .

Advantage of the RoI distributions over PSCF calculations is that RoI does not require measurement data and thus can be used for wherever and whenever there is  $SO_2$  emission and trajectory data. That is why we calculated RoI distributions for four selected stations (Çubuk, Antalya, Ashdod (Israel) and Corsica (a site in the Western Mediteranean)).

Although RoI calculations were performed in a gridded format, we also took the average of all calculated RoI values in all grids of countries in Europe. In this way we also generated country based distributions of RoI in Europe.

## CHAPTER 4

### RESULTS AND DISCUSSIONS

#### 4.1. Investigation of Weighting Trajectory Segments, Based on Their Altitude

As explained before, altitude of a trajectory segment (or an air parcel) directly affects its potential to pick up a pollutant from a source region and transport it to the receptor. Because of this, equal treatment to all trajectory segments without paying attention to their altitude can increase uncertainty in identification of source regions. This is overcome by weighting trajectory segments depending on their altitudes. The need for altitude weighting is also depicted in Figure 4.1. Results of a PMF study performed on Antalya aerosol data (Öztürk et al., 2012) was used in Figure 4.1. In any PMF study one of the outputs is G-scores, which correspond to factor scores in conventional factor analysis. G-scores of a factor are a measure of the weight of that factor in that particular sample. When G-score of a factor  $i$  for a particular sample  $j$  is multiplied with the factor loading of an element in that factor  $x$ , result is the contribution of factor  $i$  to concentration of element  $x$  in sample  $j$ .

We have selected G-scores of marine (factor 4) and anthropogenic (factor 2) factors in Antalya PMF study to demonstrate the rationale for altitude weighting in PSCF and RoI calculations. We selected marine factor, because sources are well defined (Black Sea or Mediterranean Sea). Anthropogenic factor was selected to show that source regions are different from marine factor. In both cases trajectories that correspond to the highest 20% of factor scores are plotted in Figure 4.1.

Top views of the trajectories that are associated with the highest 20% of the marine factor are depicted in Figure 4.1a. In this top view, trajectories cannot be directly related to a marine source at first sight. However, when same trajectories are viewed from one of the sides, as shown in Figure 4.1b, it becomes clear that all of the trajectories touch to the surface of either Mediterranean or Black Sea. This clearly demonstrates that location of low lying trajectories is more important to identify the marine factor.

Figure 4.1b shows side-view of trajectories that are associated with the highest 20% of the pollution factor (Factor 2) in the same exercise. In this case none of the trajectories touches to sea surface, but their segments are close to the surface over Turkey, Balkan countries, Ukraine and Russia, which are the source regions of pollution aerosols affecting almost all parts of Turkey. Discussion of source regions found in that PMF exercise is beyond the scope of this study. However, figures clearly demonstrate the need for altitude weighting applied in this study. Side-view of trajectories is plotted using software of PloTra (version3.0).

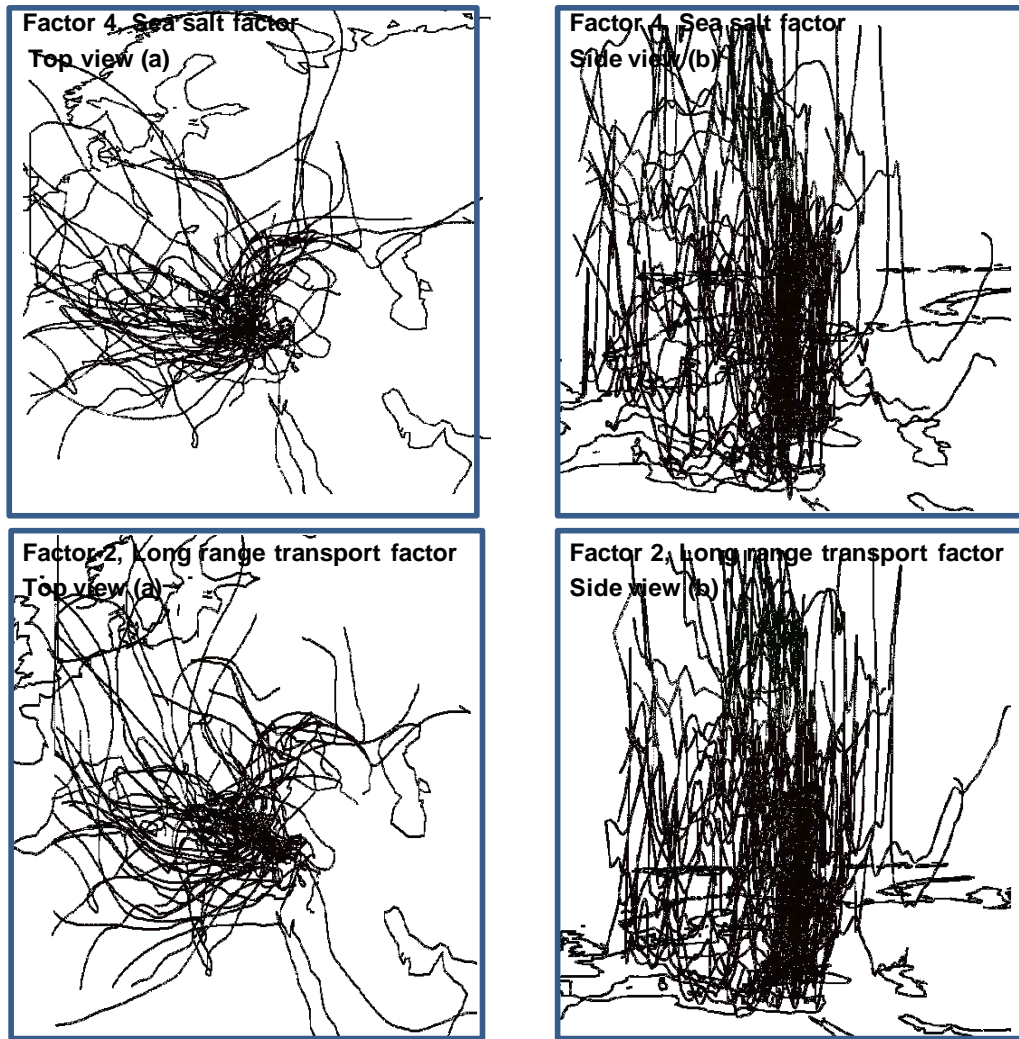


**Figure 4. 1 Top and side view of trajectory groups associated with highest 20% of pollution and marine factor scores in PMF study performed on Antalya aerosol data (Öztürk et al., 2012)**

PSCF, as a receptor-oriented trajectory statistics method, is commonly used to identify regions having higher potential to be source of pollution for a given receptor. In basic calculation of PSCF method, the air motion mechanisms such as diffusion, chemical transformation or atmospheric scavenging are omitted and these omissions make the model qualitative. In other words PSCF provide information on the locations of potential source regions, but cannot quantitatively tell how much a pollutant (such as  $\text{SO}_4^{2-}$ ) is transported from identified source region to receptor. The model has also some uncertainties in locations of source regions, which is mainly due to (1) uncertainties in trajectories (or uncertainties in the coordinates of

segments) and (2) equal weighting of segments at all altitudes and (3) ignoring the effect of scavenging on particle loadings of air masses.

There is not much can be done on horizontal and vertical uncertainties of trajectories. There had been several studies in the past to assign horizontal uncertainty as a function of distance from starting point (Walmsley and Mailhot, 1983; Kuo et al., 1985; Kahl and Samson, 1986; Merrill et al., 1986; Rolph and Draxler, 1990; Schoeberl et al., 1992; Bowman, 1993; Doty and Perkey, 1993; Seibert, 1993; Stohl and Wotawa, 1995; Stohl and Seibert, 1998; Bourqui, 2006; Davis and Dacre, 2009). Although there is no agreement between studies, it is typically accepted that horizontal uncertainties can be as high as 20% of the distance traveled (Stohl, 1998).

In this study influence of equal treatment of segments at all altitudes were investigated and a weighting scheme was developed to minimize the uncertainties in identification of source regions due to this treatment. Once weighting criteria was selected it was then used in all subsequent PSCF and RoI calculations.

Although we also worked on the rain weighting and attempted to develop another weighting scheme to reduce uncertainties arising from ignoring rain scavenging, eventually we decided not to use it in this study because (1) there were too many assumptions involved and (2) it was difficult to test the accuracy of the results.

Because of the different capacity of picking up pollutants at different altitudes, much more pollutants are collected at the low altitude segments than the high altitude segments. It is assumed that application of altitude weighting in PSCF calculation reduces the uncertainties forming from altitude differences. Therefore, altitude weighting function was applied in PSCF calculations. While applying weighting function, altitude of segments was divided into three parts between, 0-500m, 500-1000m, and (greater than)>1000m, and weighted each part separately. Each trajectory segment according to its altitude belongs to one part, so it is multiplied with related coefficient. Therefore three different altitude weighting types were created with different coefficients and these were mentioned at Table 3.4.

As shown in Table 3.4, the segments whose altitudes range between 0 m and 500 m were multiplied by 1.0, segments ranging between 500m and 1000m were multiplied by 0.8, and segments higher than 1000m were multiplied by 0.5 for the first weighting function. On the other hand, at second weighting function, the weighting constants were defined as 1, 0.5, and 0.3 for the same altitude ranges. Segments located between 0 m and 500 m, segments located between 500 m and 1000m and segments located higher than 1000m were weighted with the constants of 1, 0.3, and 0.1, respectively at third weighting function.

In order to understand results of the three weighting functions, PSCF values of Çubuk station for the combined years 1993 and 1994 were calculated. The calculations were repeated by every three weighting functions. The obtained results were shown in Figure 4.2.

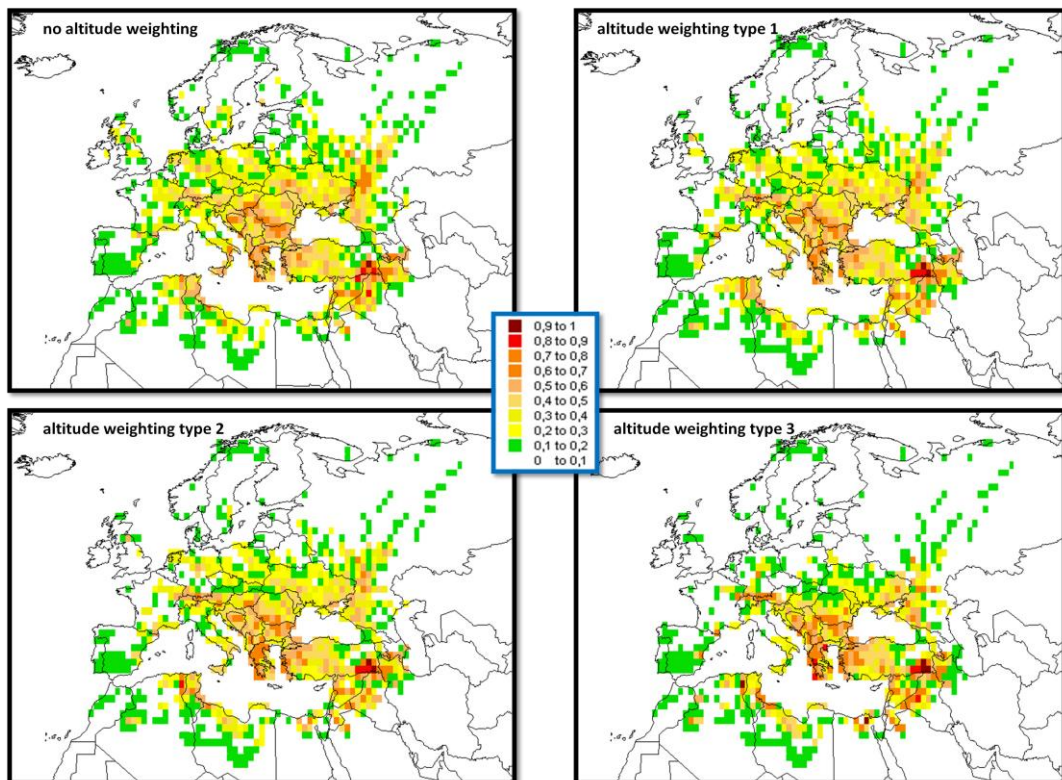


**Figure 4. 2** Effect of three different altitude weighting preferences to distribution of PSCF values at Çubuk station for the combined years 1993 and 1994

At such methods based on trajectory statistics, the accuracy of results depends on the segment numbers in grids. In order to have an opinion on uncertainties at grids, segment numbers in each country stated in the grid system are shown in Table 4.1.

**Table 4. 1** Number of total trajectory segments without altitude weighting and with three different altitude weightings for countries in grid system used at PSCF calculation

Country	Total trajectory segments w/o altitude weighting	Total trajectory segments w/ altitude type1 weighting	Total trajectory segments w/ altitude type2 weighting	Total trajectory segments w/ altitude type3 weighting
Saudi Arabia	290	181.9 (-37.2%)	145.6 (-49.8%)	119.6 (-58.7%)
Algeria	1328	776.7 (-41.5%)	553.5 (-58.3%)	349.7 (-73.6%)
Liby An Arab Jamahiriya	1335	894.4 (-33%)	697.6 (-47.7%)	533.6 (-60%)
Egypt	548	337 (-38.5%)	276.7 (-49.5%)	224.9 (-59%)
Iran	678	452.3 (-33.3%)	373.3 (-45%)	305.9 (-54.8%)
Morocco	86	46.6 (-45.8%)	30.4 (-64.6%)	14.4 (-83.2%)
Jordan	328	243.8 (-25.6%)	206.9 (-37%)	181.1 (-44.7%)
Iraq	1329	823.8 (-38%)	678.7 (-49%)	569.7 (-57%)
Tunisia	561	341.9 (-39%)	230.6 (-58.8%)	134.6 (-76%)
Israel	45	30.5 (-32.2%)	25.6 (-43%)	21.2 (-52.8%)
Syrian Arab Republic	1784	1267.2 (-29%)	1028.7 (-42.3%)	854.1 (-52%)
Lebanon	223	165.7 (-25.7%)	132.9 (-40.4%)	109.5 (-51%)
Spain	399	208.7 (-47.7%)	133.2 (-66.6%)	59.6 (-85%)
Turkey	37014	25161.2 (-32%)	19821.7 (-46%)	15315.1 (-58%)
Portugal	45	22.5 (-50%)	13.5 (-70%)	4.5 (-90%)
Italy	1304	703.6 (-46%)	444.5 (-66%)	199.1 (-84.7)
Greece	1366	820.9 (-40%)	552.6 (-59.5%)	310.6 (-77.2%)
Armenia	93	60.9 (-34.5%)	45.4 (-51%)	32.2 (-64.4%)
Azerbaijan	125	74.4 (-40.5%)	49.1 (-60.7%)	26.1 (-79%)
Albania	230	127.6 (-44.5%)	87.5 (-62%)	50.1 (-78.2%)
Macedonia	186	99.8 (-46.3%)	69.6 (-62.5%)	42 (-77.4%)
Bulgaria	1991	1077.7 (-45.8%)	693.3 (-65%)	336.3 (-83%)
Georgia	514	331.8 (-35.4%)	240.1 (-53.2%)	165.5 (-67.8%)
Russian Federation	10567	5893.7 (-44.2%)	3897.2 (-63%)	1999.6 (-81%)
Kazakhstan	379	220.1 (-42%)	154.1 (-59.3%)	94.3 (-75%)
Andorra	23	11.5 (-50%)	6.9 (-70%)	2.3 (-90%)
France	1301	708 (-45.6%)	445.6 (-65.7%)	197.2 (-84.8%)
Yugoslavia	1191	711.5 (-40.2%)	498.5 (-58%)	303.5 (-74.5)
Bosnia And Herzegovina	400	232.4 (-42%)	153.7 (-61.5%)	80.3 (-80%)

**Table 4. 1 (contd) Number of total trajectory segments without altitude weighting and with three different altitude weightings for Countries in grid system used at PSCF calculation**

<b>Country</b>	<b>Total trajectory segments w/o altitude weighting</b>	<b>Total trajectory segments w/ altitude type1 weighting</b>	<b>Total trajectory segments w/ altitude type2 weighting</b>	<b>Total trajectory segments w/ altitude type3 weighting</b>
<b>Croatia</b>	412	220.2 (-46.5%)	138.9 (-66.3%)	61.5 (-85%)
<b>Romania</b>	2808	1489.6 (-47%)	968.5 (-65.5%)	465.1 (-83.4%)
<b>Ukraine</b>	6262	3403.8 (-45.6%)	2235.3 (-64.3%)	1109.9 (-82.3%)
<b>Switzerland</b>	207	118.8 (-42.6%)	91.4 (-55.8%)	64.6 (-68.8%)
<b>Austria</b>	448	253.4 (-43.4%)	169.5 (-62%)	88.9 (-80%)
<b>Slovenia</b>	48	25.7 (-46.4%)	17.5 (-63.5)	9.7 (-80%)
<b>Hungary</b>	703	356.9 (-49.2%)	221 (-68.5%)	87.4 (-87.5%)
<b>Moldova</b>	429	221.1 (-48.4%)	136.2 (-68.2%)	53 (-87.6%)
<b>Germany</b>	1101	569.9 (-48.2%)	367.7 (-66.6%)	170.3 (-84.5%)
<b>Slovakia</b>	220	114.6 (-48%)	72 (-67.3%)	29.6 (-86.5%)
<b>Luxembourg</b>	20	10.6 (-47%)	6.4 (-68%)	2.4 (-88%)
<b>Czech Republic</b>	279	129.9 (-53.4%)	78 (-72%)	26.4 (-90.5%)
<b>Poland</b>	1331	664.1 (-50%)	408.7 (-69.3%)	156.5 (-88.2%)
<b>United Kingdom</b>	407	207 (-49%)	127.4 (-68.7%)	47.8 (-88.2%)
<b>Belgium</b>	19	9.5 (-50%)	5.7 (-70%)	1.9 (-90%)
<b>Netherlands</b>	79	37 (-53%)	22.2 (-72%)	7.4 (-90.6%)
<b>Belarus</b>	719	384 (-46.6%)	250.5 (-65.2%)	119.5 (-83.4%)
<b>Ireland</b>	69	34.5 (-50%)	20.7 (-70%)	6.9 (-90%)
<b>Lithuania</b>	93	46.5 (-50%)	27.9 (-70%)	9.3 (-90%)
<b>Denmark</b>	94	47 (-50%)	28.2 (-70%)	9.4 (-90%)
<b>Sweden</b>	730	365 (-50%)	219 (-70%)	73 (-90%)
<b>Latvia</b>	118	59 (-50%)	35.4 (-70%)	11.8 (-90%)
<b>Norway</b>	348	177 (-49%)	106.4 (-69.4%)	36.8 (-89.4)
<b>Estonia</b>	62	31 (-50%)	18.6 (-70%)	6.2 (-90%)
<b>Finland</b>	402	201 (-50%)	120.6 (-70%)	40.2 (-90%)
<b>Total Trajectory Segments</b>	83071	51205.2 (-38%)	37580.7 (-54%)	25332.1 (-69%)

As seen in Figure 4.2, the PSCF results prepared by using altitude weighting types 1 and 2 are not so different than PSCF distribution obtained without any weighting. On identification of source regions, these two altitude weighting schemes had minimum effect because of the small weighting factors (coefficients). Since trajectory segment altitudes are expected to higher at the edges of our study domain, we were expecting

to avoid artifacts in those regions by down-weighting high-altitude segments. This would also be more in agreement with literature. Source regions of pollutants (not necessarily  $\text{SO}_4^{2-}$ ) were investigated extensively by our group and other researchers by using a variety of techniques (Doğan et al., 2010; Gullu et al., 1998; 2005; Im et al., 2014; Karaca et al., 2009; Koçak et al., 2004a; 2009; Ozturk et al., 2012; Traub et al., 2003). Results in most of these studies suggest that anthropogenic sources affecting concentration of pollutants at Eastern Mediterranean are quite local, namely Balkan countries, Russian Federation Ukraine etc. Consequently, a distribution of PSCF values after weighting segments should be consistent with this general conclusion. However, with weighting scheme #1 and #2, it did not work out that way. The outside regions are not properly cleaned. Distribution obtained by using weighting scheme 3 is more in line with the literature. Based on this argument, among three weighting types, third one was selected to be used in the rest of the study.

How segments in countries that take part in different parts of the study area are affected by three weighting schemes is given in Table 4.1. Also percent difference of total trajectory segments of each type with respect to total trajectory segments without altitude weighting is given in parenthesis. There is approximately a total of 83 000 segments when there is no altitude weighting was applied. That number is reduced to 51 000 when weighting system # 1 is used and to 37 500 when #2 weighting scheme was applied and to 25 000 when # 3 weighting scheme was applied. Naturally larger fraction of segment reduction (or down-weighting) was observed at the edges of the study domain. For example, number of segments decrease by a factor of five when altitude weighting scheme 3 was applied to segments in Bulgaria. However, corresponding reduction was an order of magnitude in the United Kingdom and Norway. It is clear from segment counts that trajectory segments in a grid which are located  $>1000$  m from surface has very little contribution to PSCF value calculated for that grid.

From this point on, in all PSCF or RoI calculations, PSCF and RoI values were computed using weighting scheme #3. That is to say, in every grid cell number of

segments whose altitudes range between 0 m and 500 m are multiplied with 1.0, number of trajectory segments whose altitudes range between 500 m and 1000 m are multiplied with 0.3 and number of segments with  $z > 1000$  m were multiplied with 0.1.

Usually visualization of PSCF values in their distribution over the study domain is also important. We tried three different legends to depict distribution of PSCF and RoI values in our grid system. These are given in Figure 4.3. Distributions shown in the figure are PSCF distributions calculated for Çubuk station and for the years 1993+1994.

In legend #1 PSCF values between 0.4 and 1.0 are colored. Values  $< 0.4$  are left white. In this legend scheme important and moderate source regions are shown and weak source regions are not significantly considered. Please note that PSCF value 0.4 for a grid  $ij$  means that if 100 trajectories that are interrupted at our station passes through grid  $ij$ , 40 of them are expected to correspond to high  $\text{SO}_4^{2-}$  concentration (top 40%).

Grids with PSCF values between 0.6 and 1.0 are color coded in legend #2. Only very strong source regions are depicted when you only color PSCF values  $> 0.6$ . Moderate source regions which are also important in terms of their influence on chemical composition of atmospheric aerosol at the receptor are ignored.

All PSCF values between 0 and 1.0 are color coded in legend #3. Although this legend scheme is being used by researchers, we feel that even very weak source region are colored and this may be confusing in many cases.

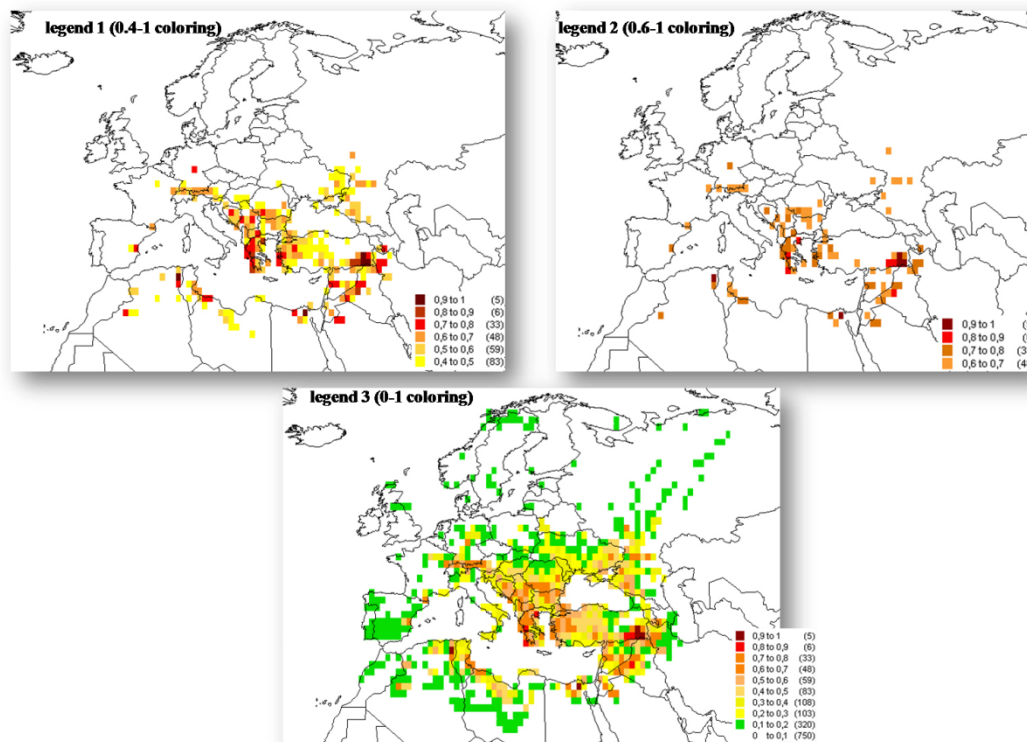


**Figure 4. 3** Distribution of PSCF values for a Çubuk Station for 1993+1994 using altitude weighting type 3 with legend 1, legend 2 and legend 3.

Based on the Figure 4.3, legend #1 which shows PSCF values vary between 0.4 and 1 was selected as most suitable visualization. Therefore the PSCF results were stated by using legend 1 in this study.

#### **4.2. Variation in $\text{SO}_4^{2-}$ Source Regions as Determined by PSCF Approach, Between 1993 and 2006**

The main objective in this study was to understand how sulfate source regions affecting  $\text{SO}_4^{2-}$  concentrations measured at different parts of Turkey and Mediterranean have been changed from 1980 to 2010. Since the beginning of 1970s, high sulfate concentrations have been measured in the Eastern Mediterranean region. Therefore the sulfate is a significant ion in this part of the world. At the beginning, in 80's and early 90's  $\text{SO}_4^{2-}$  concentrations measured in the Mediterranean area was comparable to the  $\text{SO}_4^{2-}$  concentrations measured in other parts of Europe. However, starting with 1990  $\text{SO}_4^{2-}$  concentrations measured in the EMEP network started to

decrease with actions taken to reduce SO<sub>2</sub> emissions. These actions proved very effective first in the Western Europe and then in Eastern Europe. Today SO<sub>4</sub><sup>2-</sup> concentrations in EMEP network is approximately 70% smaller than corresponding concentrations measured in 70s and 80s (Lajtha and Jones, 2013; Colette et al., 2011; Forsius et al., 2001).

However, it was seen that SO<sub>4</sub><sup>2-</sup> values measured in the Mediterranean region did not decrease at the same rate with Europe. Real reason of this situation is not known yet. Although, the high SO<sub>4</sub><sup>2-</sup> concentrations in the Eastern Mediterranean have been mentioned in many studies till today, there is not any article written about the potential cause of it.

In this study, the clarification of how the sulfate source regions affecting Eastern Mediterranean region changed in last 30 years was discussed. This is important because it provides information about past and current source regions affecting Eastern Mediterranean atmosphere.

Variation in source regions were discussed with both PSCF and RoI approaches. Results of the PSCF approach are discussed in this section. Time period covered by PSCF was shorter than that covered by RoI. Data from Çubuk and Antalya stations were used in the PSCF analysis. Fairly large SO<sub>4</sub><sup>2-</sup> data set is needed to apply PSCF technique to find SO<sub>4</sub><sup>2-</sup> source regions. Although there are many SO<sub>4</sub><sup>2-</sup> data sets generated in different parts of Turkey, there are only two stations which have long-enough data. One of the stations is about 20 km east of Antalya, a picnic area belonging to the Ministry of Forestry and Water Affairs and it is established and operated by the Department of Environmental Engineering of Middle East Technical University. This station is referred as “Antalya Station” in this study.

Aerosol and trace elements in rain water and ions collected at Antalya Station from 1993 to 2000 were analyzed. Sulfate concentrations obtained by aerosol samples from the ion measurement were used in this study.

There were data on  $\text{SO}_4^{2-}$  concentrations in rainwater in both Antalya and Çubuk stations those data were not used in this study, because rain data is generally fewer than aerosol data in most of the sampling locations. Annual number of rainy days in the Antalya region is fewer than 100 per year. Thus, the highest number of rain sample collected each year is 100. Whereas the number of aerosol sample collected annually ranges from 200 to 300. Because of higher statistical reliability of results, the aerosol data were preferred.

On the other hand, “Çubuk Station” was established and run by the Ministry of Health within framework of the EMEP program between 1993 and 2006. In 2006, the station was transferred to the Ministry of Environment and Urban Planning. Since 2006, the Ministry has not been successful so far for the operation of the station. Thus, daily  $\text{SO}_4^{2-}$  concentrations generated by the Ministry of Health from 1993 to 2006 were used for this station.

In order to understand how source regions have been changed in time, the PSCF technique was applied to two-year periods for these stations. Implementation of two-year period rather than one-year period was preferred because measuring data of the stations have some missing data for some years. If the PSCF was applied to annual periods, the statistical reliability of the results, at least for some years, would likely be too low. This is true for both stations.

In this way, the PSCF was applied to the period of four consecutive 2-year periods between 1993 and 2000 in Antalya Station. On the other hand, the period of seven consecutive 2-years between 1993 and 2006 was investigated in Çubuk Station.

The PSCF results were discussed in three different levels. First, distribution of PSCF values in our grid system was visually investigated and visible changes were discussed. Secondly, the PSCF values of each grid calculated for the first period was subtracted from PSCF values of the same grid calculated for the previous 2-year period or a reference 2-year period and percent change between them were plotted and discussed. Distributions of the percent change were also shown by using the GIS

software, MapInfo. With these figures, distributions of differences of PSCF between periods were examined. Obviously, this approach is more quantitative than the first level, which depends on visual assessment only. Finally, in the third level, the average PSCF value of each country was calculated based on the PSCF values of the grids covered by countries. The effects of countries or individual grids on sulfate concentrations measured at the two stations were analyzed for different periods of time, because data coverage was not the same in Antalya and Çubuk stations.

#### **4.2.1. Antalya Station**

For Antalya Station, PSCF values calculated for the two year periods were shown in Figure 4.4. While showing the distribution of PSCF values, the grids whose PSCF values are smaller than 0.4 are shown in white in order to avoid confusion and highlight only the moderate and high potential source regions. Therefore, a large part of Europe was shown as white which indicates that there is not large enough source region which can be classified as “moderate” or “high”, but, it does not mean that there is not any source in Europe.

When analyzing the source regions affecting the measured sulfate concentrations in Antalya station, it is seen that the important source regions include Balkan countries particularly Greece (especially Athens region), Bulgaria, Romania and the area to the North East of Turkey, which contains Georgia and Azerbaijan and eastern parts of Ukraine.

As seen in Figure 4.4, distribution of PSCF prepared for the years 1993-1994 shows that the source regions extend to the North of Italy and Central Europe. On the other hand, distributions of PSCF for the years of 1995-1996 and 1999-2000 implies that source regions affecting the Antalya Station and more generally Eastern Mediterranean region are more local. The source regions are limited to Balkan countries, eastern part of Ukraine, western part of Turkey and a region close to the North Eastern border of Turkey. It generally explains why  $\text{SO}_4^{2-}$  concentrations did not decrease in Eastern Mediterranean region contrary to Europe.

Distribution of PSCF values for years 1997-1998 is slightly different from distributions discussed for previous years. Although there were no significant source regions identified beyond Romania in the years 1993-1994, 1995-1996, Central European countries and southern parts of Germany appeared as moderately strong source regions in the years 1997-1998. These distant source regions did not appear in PSCF performed for 1999-2000. We do not know the reason for such unexpected modification in identified source regions for these two particular years, a different meteorological regime, which was specific for these years, was suspected.

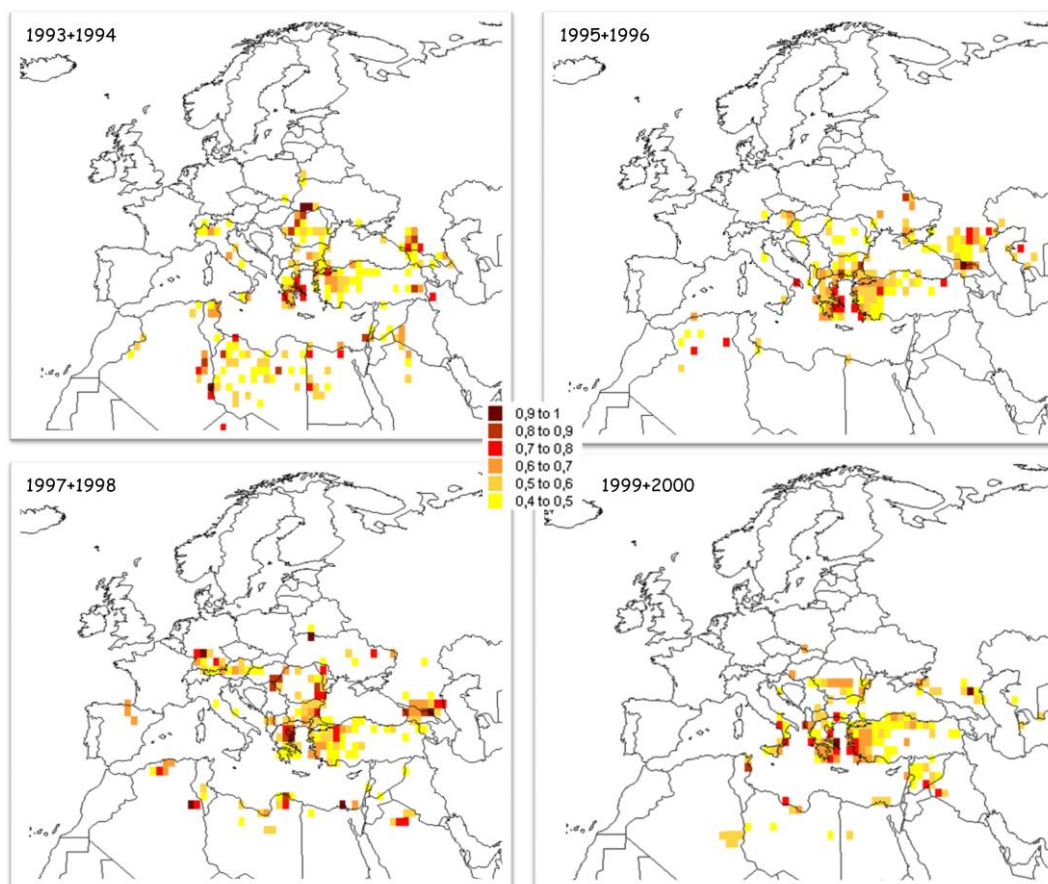


**Figure 4. 4** Distribution of PSCF values for Antalya Station with two year intervals between 1993 and 2000. Altitude weighting was used in PSCF calculations

Two important points stand out in terms of the distribution of the source regions in time. The first one is a marked region which is at east of Ukraine seems to be an important source. Although PSCF values calculated in this area has declined in time,

the area measurements made in recent years (1993-2000) indicate that the marked region has still been a major source for Antalya station.

There is also a similar region which covers Armenia, Azerbaijan and Georgia in Northeastern Turkey. This region seems to be an important source for Antalya and also still maintains its importance in 2000, which is the last year of the measurements. A series of industrial facility with high-emission exists at the Georgian border of Russia. In addition, Azerbaijan seems to be an important source of SO<sub>2</sub> until recent years.

At the second stage of the study, the difference of PSCF values between two-year periods and the period of 1993-1994 were calculated based on grids and the difference was expressed as a percentage change with respect to values of 1993-1994. The distribution of each period's difference compared to 1993-1994 on the basis of grids is shown in Figure 4.5. Different shades of green in the figure indicate that PSCF values in those grids are smaller than corresponding values in 1993+1994. Different shades of red, on the other hand indicate that emissions increased relative to base period.

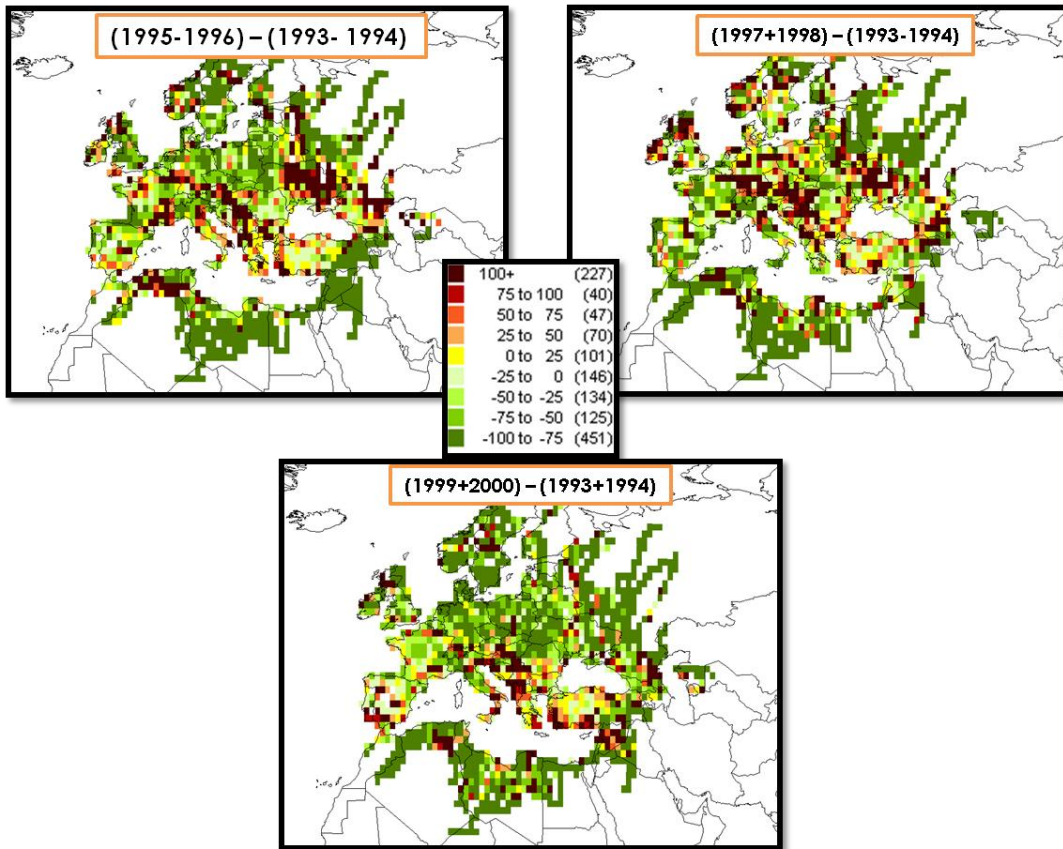


**Figure 4. 5 Grid-based percent differences between biyearly PSCF distributions. Differences were calculated between different years and 1993+1994.**

There are few interesting points at the distribution of PSCF differences. In the years following the period of 1993-1994, the green areas are in majority, particularly in Western Europe, indicating that PSCF values decreased compared to 1993-1994 period. However, there are increases observed in some of the grids. Most of these grids take place at former USSR countries. Both the decrease observed in western European countries and occasional increases observed in Eastern European countries are in close agreement with literature.

Sulfur protocol, which was formed as an annex to Long Range Transboundary Air Pollution convention, became effective in 1994. Most of the countries in Western Europe took necessary measures to reduce their SO<sub>2</sub> emissions. Eastern European countries, on the other hand, were economically weak after the collapse of the Soviet Union in 1991. Reductions in SO<sub>2</sub> emissions in Eastern Europe occurred later with the help of the Western European countries. Please note that all periods we used in

Antalya PSCF study is in 90's. Thus decreases observed in PSCF values in grids in the Western Europe and increases observed in Eastern Europe are in agreement with this scenario. When PSCF values calculated for the year 2000 are compared with base period (1993-1994), a general reduction in PSCF values is noticed in whole study area (except for a limited number of grid).

Another noteworthy point in Figure 4.5 is increase of PSCF values in Turkey over the years. This implies that the effects of Turkey's own sources on  $\text{SO}_4^{2-}$  concentrations measured at Antalya station increased in time. This is partly due to decreases in contributions of foreign sources. Unfortunately this weakens our hand in international platform, no matter what the reason is. Since  $\text{SO}_2$  emissions are decreasing in other Balkan Countries, like Bulgaria, Romania as they became members of EU and have to comply with EU directives, contribution of our country to  $\text{SO}_4^{2-}$  levels in Antalya station and elsewhere in the Eastern Mediterranean basin are expected to increase in time.

PSCF values of source regions detected in Azerbaijan, Georgia and Russia's border with Georgia do not decrease significantly in time. On the other hand, while Ukraine was the most important source region affecting Antalya at the beginning of the 1990s, the PSCF values compared to 1993 decreased substantially by the 2000s. Even though PSCF values of source regions located in eastern part of Ukraine decreased, the region is still important source region for  $\text{SO}_4^{2-}$  concentrations measured at Antalya.

In the third step in evaluating PSCF values calculated for Antalya station, Country averages of PSCF values were calculated for the first time. PSCF technique has been used in many thesis studies in our group; however PSCF results in terms of countries have not been discussed up to now. Country-based distribution of average PSCF values for Antalya Station is depicted in Figure 4.6, with two-year intervals. It is seen that the sources affecting  $\text{SO}_4^{2-}$  concentrations measured in Antalya are Italy, Ukraine, Romania, Greece, Georgia and Turkey in each period. Contribution of distant countries to  $\text{SO}_4^{2-}$  concentration measured in Antalya is less comparing with

the closest countries in all time segments. One feature of Figure 4.6, worth noting is that minor influence of distant countries, such as, Germany, Poland, Czech Republic and Hungary can be seen in the earlier time segments, such as, 1993-1994 and 1995-1996. However, contribution of these countries disappeared entirely in last time segments.

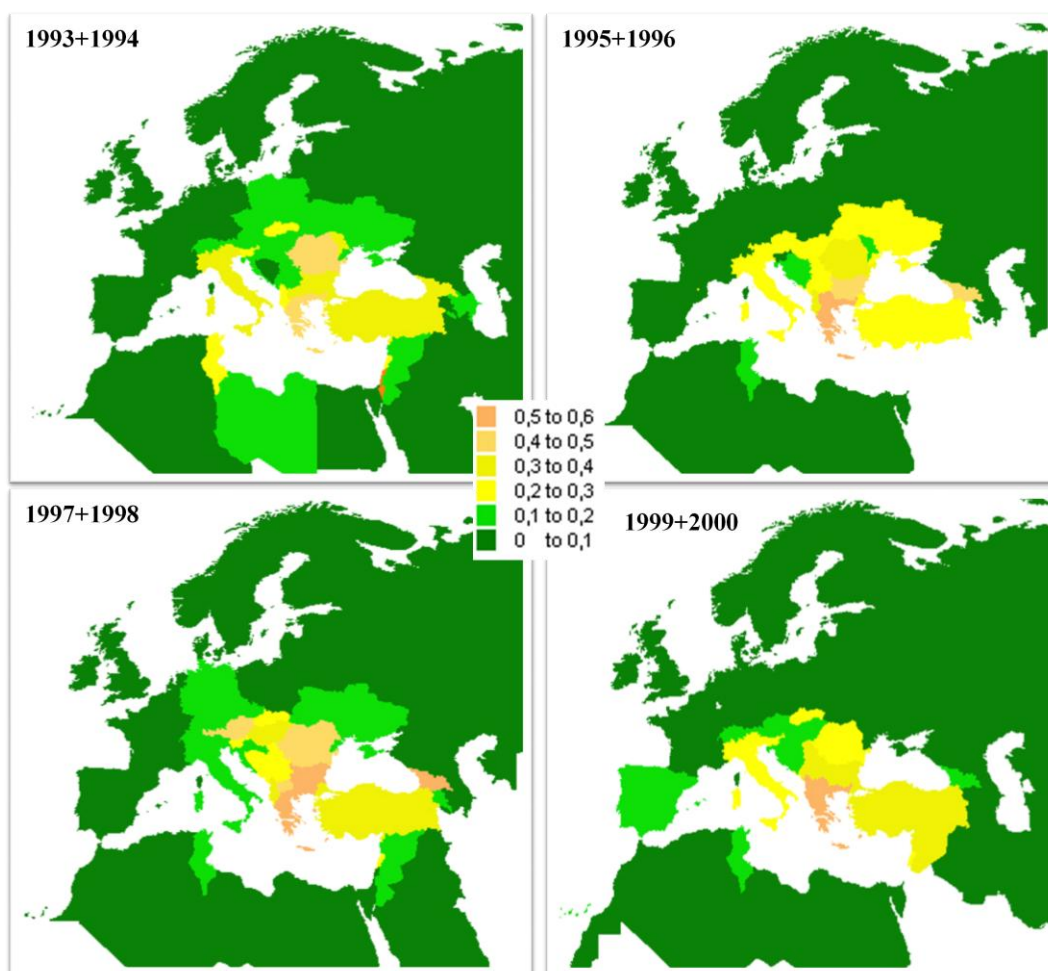


**Figure 4. 6 Country Average of two years period PSCF results using altitude weighting type 3 for Antalya Station between 1993 and 2000**

In 2000, source regions were limited with the Balkan countries. Ukraine seems to be a source until 1998; however it was not a major source in 2000. It is known that eastern region of Ukraine was also an important resource in 2000. However, when calculating the average for the whole of Ukraine, the high PSCF values calculated in the grids that correspond to eastern parts of Ukraine disappeared.

Georgia seems to be an important source region in 1993 and it was still a source in 2000. Since these countries are very small, the grids can cover more than one country. In fact, there is an industrial area in Russia Federation, which is very close to Georgia. Probably, Georgia appears as an important source area for  $\text{SO}_4^{2-}$  concentrations measured at Antalya because of this industrial area. Stevens et al (1984) also reported contribution of two high-emitting smelters in this industrial area on concentrations of anthropogenic elements and ions, including  $\text{SO}_4^{2-}$ , on their sampling point in Georgia.

#### **4.2.2. Çubuk Station**

Sulfate data is available at Çubuk Station between 1993 and 2006. Because of this, PSCF was run for these years. As given in Figure 4.7, the important source regions affecting  $\text{SO}_4^{2-}$  concentrations measured in Çubuk in the early 1990s (from 1993 to 1996) are almost all Balkans, eastern region of Ukraine, the border of Georgia and Russia Federation, western and southeastern parts of Turkey.

At the end of the 1990s (between the years of 1997 and 2000), Balkans are still an important source region. However PSCF values were not as high as in the early 1990s. Both eastern and western parts of Turkey were significant sources for Çubuk Station. Eastern region of Ukraine and the border of Georgia and Russia Federation were still source regions, but the PSCF values of these regions reduced compared to 1990.

In the period of 2000 to 2004, importance of eastern and western parts of Turkey as source regions increased. Balkans, eastern regions of Ukraine and the border of Georgia and Russia Federation were still source regions, but PSCF values have decreased compared to the early 1990s. The distribution of PSCF in 2005-2006 was not much different from the previous two years.

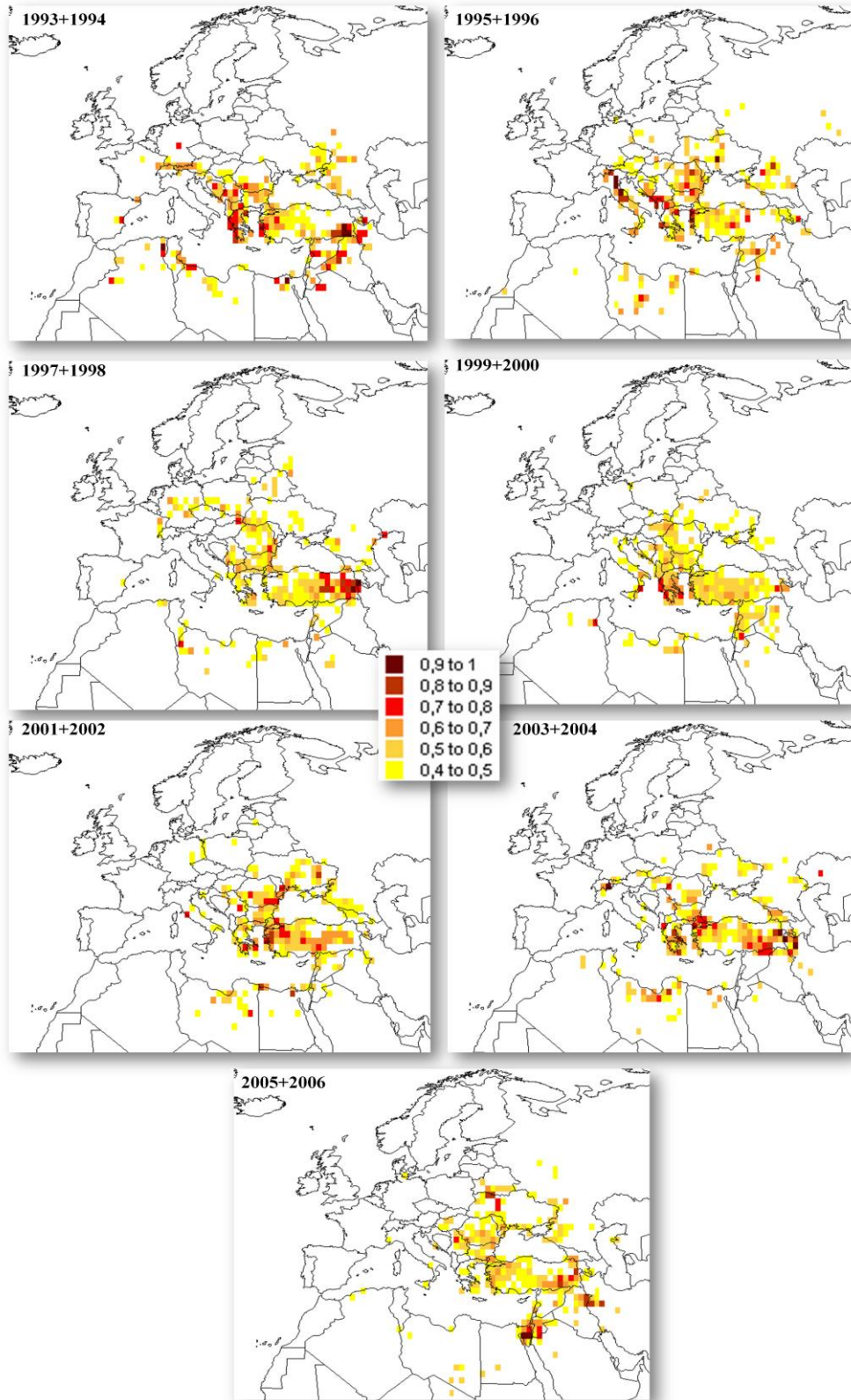


**Figure 4. 7 Two years period of PSCF results using altitude weighting type 3 for Çubuk Station between 1993 and 2006**

The difference graphics which are given in Figure 4.8 are interesting. In central European countries such as Poland, Czech Republic, Hungary and the western part of Russia Federation, the PSCF value of 1995-96 and 1997-98 were higher than PSCF value of 1993-94. Increase of the PSCF values at some parts of this mentioned regions continued up to 2006. This may be due well documented fact that SO<sub>2</sub> emission control in former USSR countries become effective after the emission control applied at the western European countries. There is another point that should also be considered. The PSCF values calculated for these regions may be higher than the previous year's PSCF value, but PSCF values in most of these regions were <0.4. Since these regions were not important source regions for SO<sub>4</sub><sup>2-</sup> concentrations measured at the central Anatolia, change of PSCF values with respect to time may not be so important.

Maybe more important point to note is that PSCF values for grids that include significant source regions, such as Balkan countries, Ukraine, Turkey and Georgia did not decrease significantly between 1993 and 2006. On the contrary, PSCF values calculated for regions like eastern regions of Turkey, Georgia, and western Ukraine was higher in 2006 than they were in 1993.

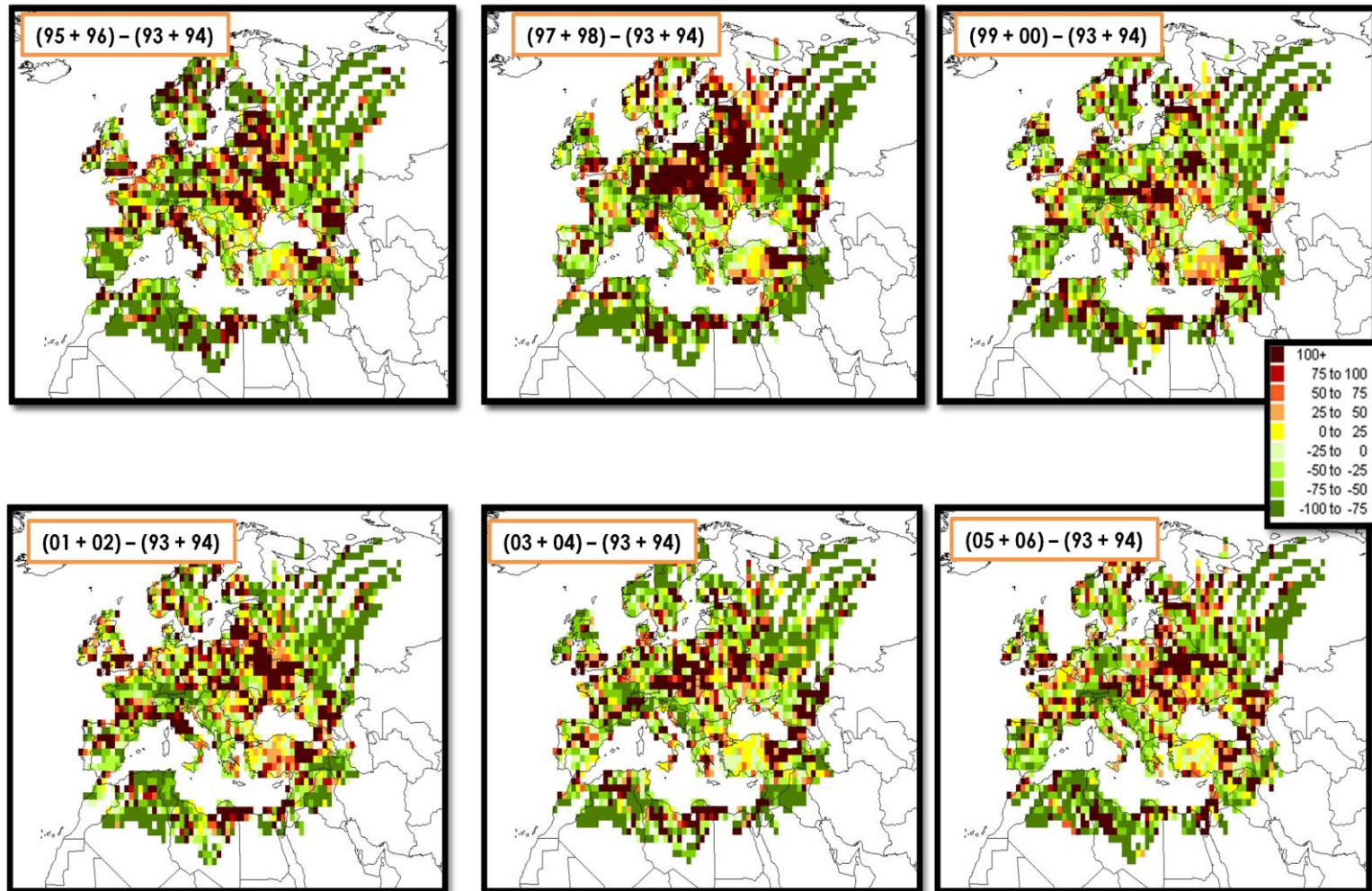
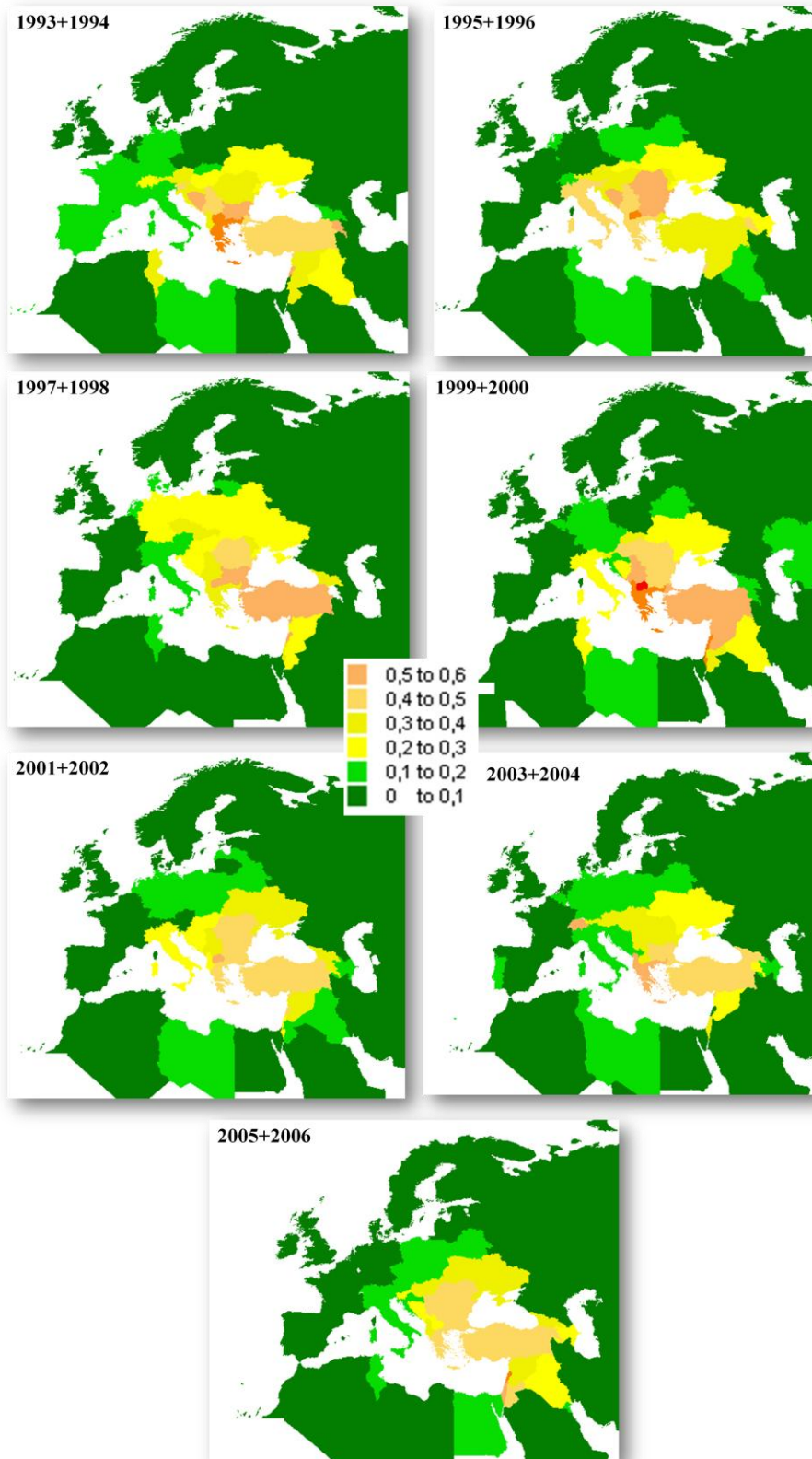


Figure 4. 8 Distribution of differences of PSCF values between each of the 2-yr-long intervals and (1993+1994) period

Trends observed for the Western European countries were different from trends observed in main source regions for Central Anatolia. The PSCF values in Western European countries decreased steadily after 1993. The point to be considered is that Western Europe was not an important source region in 1993 for Çubuk region. Decreasing tendency of the PSCF values calculated for Italy and some Balkan countries is more important than the decrease observed in Western Europe. Because these countries significantly contributed to  $\text{SO}_4^{2-}$  concentrations measured in 1993s in Çubuk. Their contribution decreased significantly in 2006.

Average PSCF values of countries are shown in Figure 4.9. Contributions of European countries to PSCF values in Çubuk do not show a significant change between 1993 and 2006. In 1993s, Central European and Balkan countries, Ukraine, and some Middle Eastern countries, especially Syria shown in yellow were the most important source regions. Looking at the average values of PSCF on the basis of countries in 2006, it is seen that same countries were still the most important countries affecting Çubuk station if European countries are no longer source regions. Principally, this explains why  $\text{SO}_4^{2-}$  ion concentrations in the Eastern Mediterranean region did not decrease until recent years.



**Figure 4. 9 Country Average of two years period PSCF results using altitude weighting type 3 for Çubuk Station between 1993 and 2006**

### 4.2.3. Relation between PSCF Values and SO<sub>2</sub> Emissions

Variation of source regions affecting SO<sub>4</sub><sup>2-</sup> concentrations measured at Antalya and Çubuk stations in time was discussed in Sections 4.2.1 and 4.2.2. In order to complete the PSCF part, three more questions should be addressed:

1. Is source regions identified for Antalya and Çubuk stations using PSCF distributions consistent with distribution of SO<sub>2</sub> emissions in Europe and near East?
2. Can the source regions found with PSCF calculations be related with known industrial activities in the study domain?
3. To what degree the source regions calculated for Antalya and Çubuk have similarities and differences.

The first two questions were discussed in this section, as they are related. The third question will be addressed in the following section, because it is independent from the first two questions.

SO<sub>2</sub> emission distribution maps and data in Europe for years, 1980, 1990, 1995, 2000, 2005, and 2010 were obtained from EMEP database, to see the variation of SO<sub>2</sub> emissions in Europe. Distributions of emissions in these years are given in Figure 4.10.

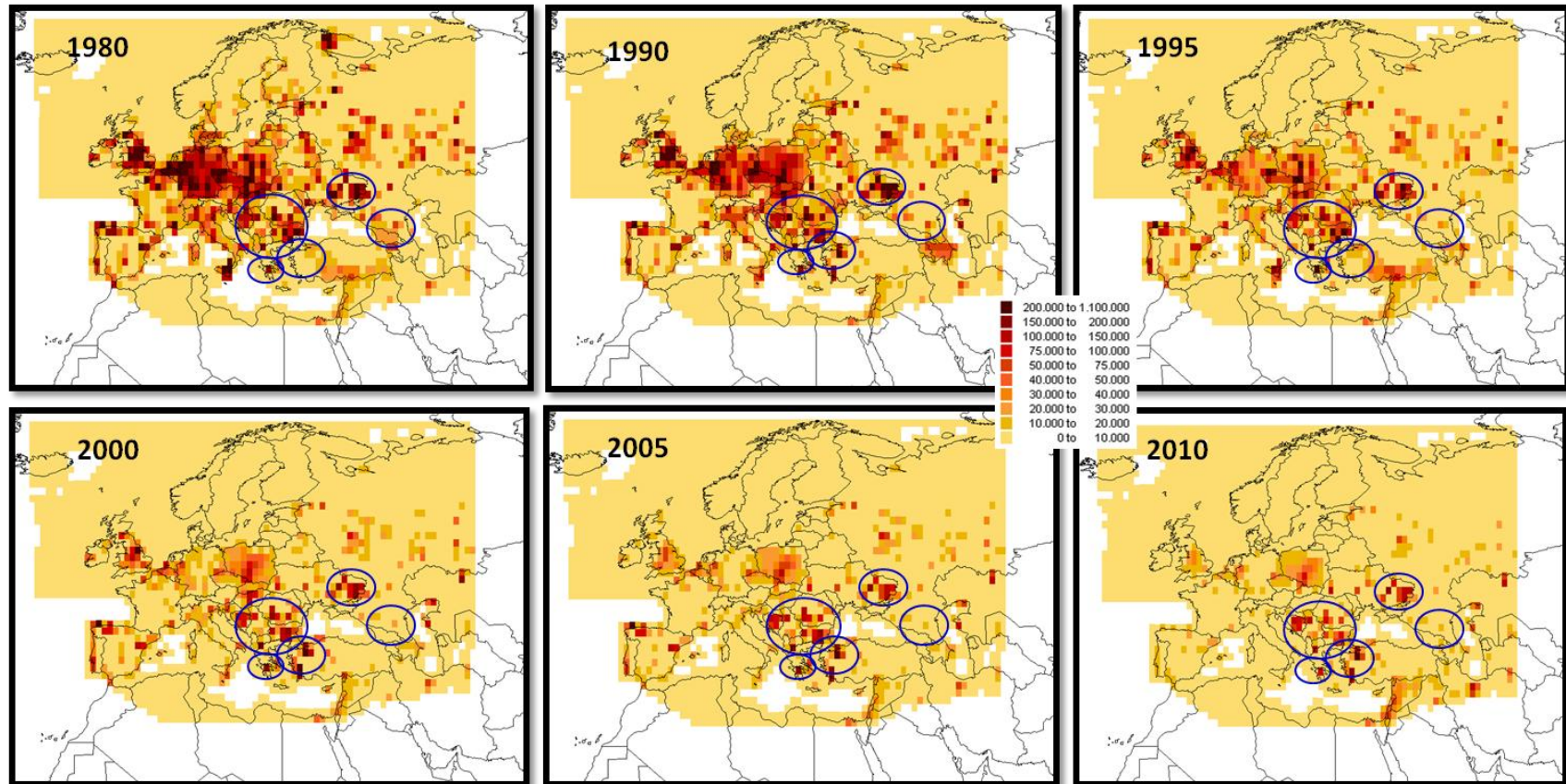


**Figure 4. 10** Variation of SO<sub>2</sub> emissions in Europe, between 1980 and 2010. High SO<sub>2</sub> emissions in the most potential source regions affecting Antalya and Çubuk stations are highlighted by blue circles.

Emission distribution maps show that the amounts of emissions have decreased in Europe, especially beginning from 1995. This is the information that has already been discussed widely in literature. However, the decrease did not start at the same time and was not with the same rate in all parts of Europe.

Because of becoming regional and global air pollution important after 70's, and increasing problems of acid rain in Europe, the first meeting related to the long range transport of pollutants was organized by United Nations Conference on the Human Environment in 1972. Transport of particles and gases via the atmosphere is the most important mechanism for dispersion of pollutants in the regional and global scales. Because of the absence of boundaries within the earth's atmosphere, gases and particles produced from one point source can be transported around the globe.

Therefore, as consequences of first sulfur protocol, more reduction in  $\text{SO}_4^{2-}$  concentrations in especially developed and industrial countries, Western European Countries which are more close the technological developments such as cleaner production techniques was reported. Totally the reduction of sulphur emissions between 30 and 60% by 1993 was satisfied with this protocol. Moreover effects-based approach, the critical load concept, best available technology, energy savings and the application of economic instruments became important in second sulfur protocol in 1998. Also it can be said that the second sulfur protocol was more effective for Eastern European Countries in comparison to first protocol. Because enforcements were more effective and technological developments were more accessible for all countries. Therefore, with the application of protocol, the critical acid loaded area decreased to  $15 \times 10^6$  ha in Europe.

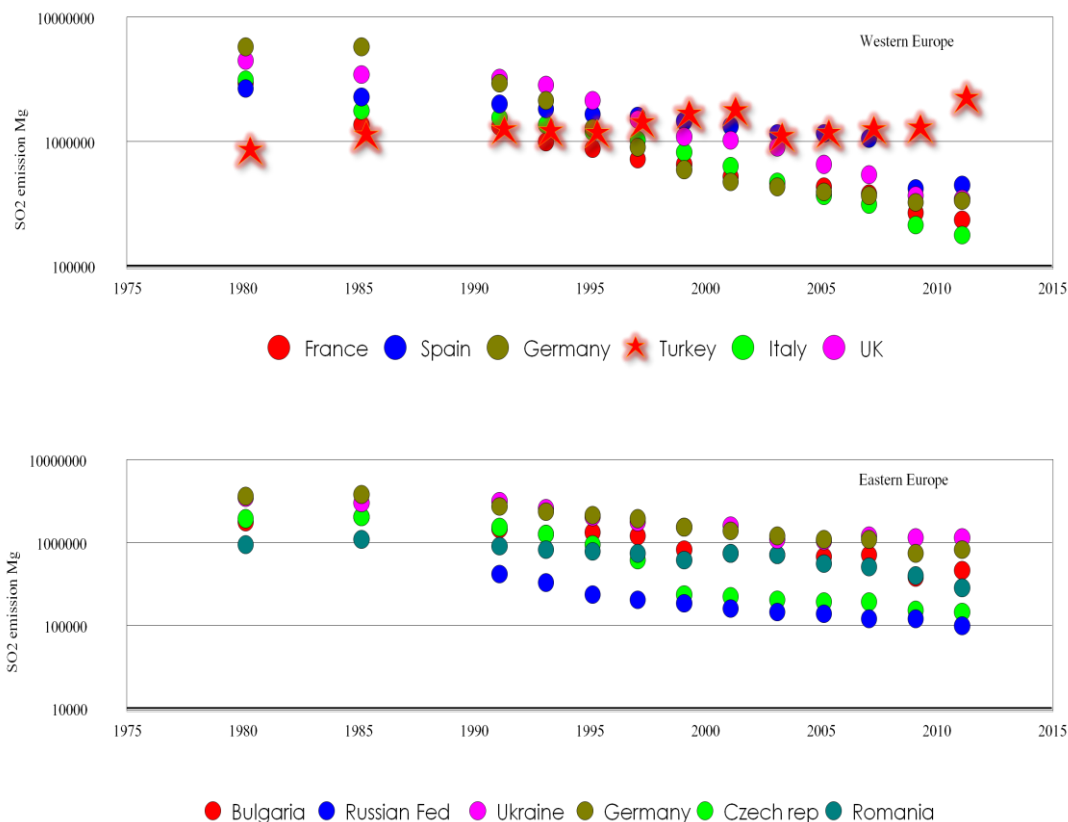


**Figure 4. 11 Variation in SO<sub>2</sub> emissions in selected Western and Eastern European countries**

Earlier and faster decline in emissions was observed in Western Europe. This is fairly obvious in Figure 4.10 and Figure 4.11, where country based emissions are plotted for selected western and eastern European countries with two year time intervals. On the other hand, decrease in emissions of Eastern European countries started later and is occurred at a slower rate. For example Poland has still high emissions in the year 2010. One interesting point in both figures is the unique pattern of Turkish emissions. Start of emission reduction and its rate in the Western Europe is not very important for the stations selected in this study for PSCF calculations, because Western Europe had never been important source regions for Antalya and Çubuk stations. Today Turkey is the only country in Europe whose emissions do not show any decreasing trend. This may have significant implications for our country if we do not something about our emissions. This variation or lack of variation SO<sub>2</sub> emissions in Turkey is very nicely picked up by our PSCF calculations. For both Antalya and Çubuk stations Turkey appeared as an important, but not the most

important source regions affecting  $\text{SO}_4^{2-}$  concentrations at Çubuk and Antalya stations. But it turned out to be the most important source region in the PSCF runs performed for the year 2000 in Antalya and 2006 at Çubuk stations. We are afraid that if this exercise is repeated in the future, Turkey will be the only source region.

As mentioned in Section 4.2.1 and 4.2.2, the source regions which have considerable importance for both Antalya and Çubuk Stations are Balkan countries (particularly Greece, Romania and Bulgaria because of their closer proximity to our stations in Turkey), the eastern regions of Ukraine, Georgia, and region of Russia Federation which is at the north of Georgia. Time-dependend variations in  $\text{SO}_2$  emissions in these regions are the ones we have to investigate carefully.

These source regions, (namely, Greece, Bulgaria, the east part of Romania and Ukraine, Georgia, and Russian side of Georgia Russia border) are marked by blue circles in Figure 4.10. Distributions of emissions in areas circled with red line in different years were then compared.

These regions remained as high emitting areas in Europe until 2005. They stand out as high emitting areas even in 2010. Please note that our PSCF calculations do not extend to the year 2010, due to lack of  $\text{SO}_4^{2-}$  measurement data in years after 2006. Variation in source regions in more recent years was discussed in coming sections using RoI approach. In the period for which we had measurement data, source regions that are common for both Çubuk and Antalya stations and identified using PSCF distributions are all high emitting areas. This agreement between emissions and PSCF values is impressive and a good demonstration of reliability of PSCF calculations. However there is an exception. One of the consistent source areas found by PSCF calculations is area around the border between Georgia and Russian Federation. This region had fair amount of emissions in 1980 and early 1990, but emissions decreased significantly in later years, but our PSCF calculations kept on showing that area as potential source area for  $\text{SO}_4^{2-}$  concentrations measured at Çubuk and Antalya. At this point it is not clear whether it is due to some sort of error

in PSCF calculations or it is due to, intentional or unintentional, poor quality emission reporting.

Another point is not the gradual increase in Turkish emissions, particularly in Northwestern Turkey. Northwestern Turkey was not a hot spot in terms of SO<sub>2</sub> emissions in 1980 and 1990, but starting with 1995 emissions started increase. PSCF calculations identified this area as an important SO<sub>4</sub><sup>2-</sup> source region since early 90's and it remained as important source region in PSCF calculations performed in all time segments. This obviously reflects the development of industry at Thrace and Istanbul–Kocaeli region. Whatever the reason, it is a dangerous development for the country. In time Turkey may be the sole high-emitter in the region.

Secondly, in order to see if we can relate PSCF-identified potential source areas (these areas were also turned out to be high emission areas) to known industrial areas in the region. High-emitting (SO<sub>4</sub><sup>2-</sup>) industries that are located in Ukraine, Turkey, Bulgaria and Russia are depicted in Figure 4.12. This data were obtained from EMEP data base and is not available for all countries surrounding Turkey. For example; it would be good if there were similar data for Romania, but unfortunately it is not available.

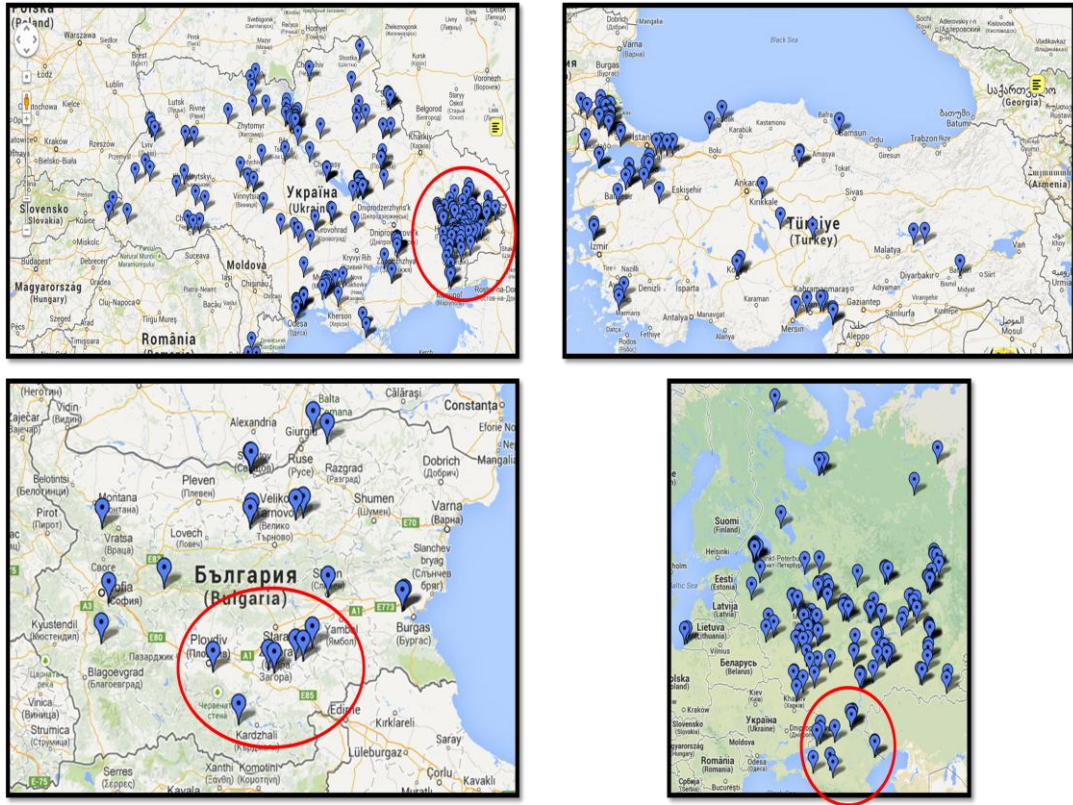


**Figure 4.12 Location of significant SO<sub>2</sub> point sources in some of the countries around Turkey.**

After the PSCF calculations mentioned at Section 4.2.1 and 4.2.2, the source regions affecting Antalya and Çubuk Stations are shown with red circles in Figure 4.12. The figure clearly demonstrates why Eastern part of Ukraine is an important source region in all time segments. It is seen that there is an important industrial region in east of Ukraine. Emissions of these industries have not decreased as much as other industries' emissions. Also this region is still an important source region for both stations until recent years.

#### **4.2.4. Comparison of PSCF Results Obtained for Çubuk and Antalya Stations**

One of the questions that should be answered about SO<sub>4</sub><sup>2-</sup> source regions affecting Eastern Mediterranean and Central Anatolia is the similarities and differences between locations of these source regions affecting the two stations. PSCF, for the two stations were run for time segments, because SO<sub>4</sub><sup>2-</sup> data available at Çubuk and

Antalya do not cover the same time interval. At Çubuk station  $\text{SO}_4^{2-}$  data existed between years 1993 and 2006, whereas at Antalya station data were available between 1992 and 2001. Since this 4 years difference in data coverage can be the reason for some of the differences, a new PSCF exercise was performed for the years between 1993 and 2000. Since the aim is to compare the results obtained for the two stations, one single run covering entire eight years were performed.

Obtained source regions of the two stations can be seen in Figure 4.13. Some common properties and some differences were determined when both figures were compared.

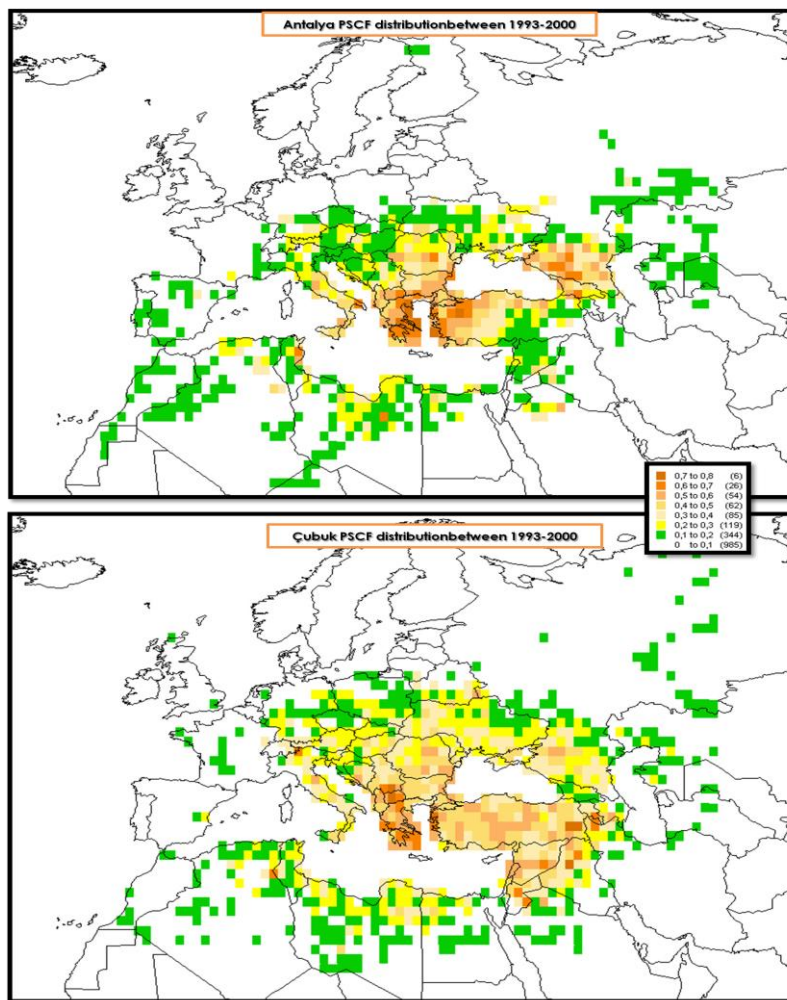


**Figure 4. 13 Distribution of PSCF values at Çubuk and Antalya Stations between 1993 and 2000**

Greece, Bulgaria, Romania, the western regions of Turkey, east of Ukraine, and north of Georgia seem to be important source regions affecting both stations. Especially Athens region of Greece, a few grids at the Turkey's Aegean Coast, a region at the middle part of Romania are the highest level of the source regions affecting these two stations.

On the other hand, there are some differences between the regions affecting these stations as well. The entire northern coast of Black Sea is a significant source region for Çubuk. However, only sources on northeastern Black Sea appear as significant sources affecting sulfate concentrations measured in Antalya.

The Western Turkey and Eastern Bulgaria are important source regions for both stations ( $PSCF > 0.4$ ); however these regions are more effective for Antalya. More frequent air mass movements from these regions to Antalya could be a reason for this.

For both stations, Western Europe is not a major source region because the emissions of Western European countries have been reduced before countries that appear as important source regions for sites in Turkey and Eastern Mediterranean. Another reason is the distance. Western European countries are further away from our sampling points than Balkan Countries and countries to the North of Turkey. This can have two important consequences; (1) air masses coming from Western Europe have a larger chance of being washed out by rain events. This is used to explain lower concentrations of pollution derived elements (not only  $SO_4^{2-}$ ) in winter season, at the Eastern Mediterranean, in many studies, (2) Since western European countries are further away, air masses, which we intercepted at our stations, are generally at higher altitudes and have smaller chance of picking up pollutants including  $SO_2$  from surface. Note that this was our rationale to use altitude weighting in PSCF calculations.

To simplify comparison, PSCF values of Antalya and Çubuk Stations were subtracted from each other and percent variations were calculated in order to see the

relative contribution of source regions on the two station. Results are depicted in Figure 4.14. Grids with green shading indicate areas that are more important source regions for Çubuk Station and grids with yellow shading are the areas that are more important source regions for Antalya station.

Please note that the distributions were plotted for the whole study domain. A given region may appear as a more important source region for one of the stations, but it does not mean that it is significant source region. For example, some Germany appears a green, indicating that it is a more important source region for Çubuk station, but we know that Germany is not a significant source area for any of the station. That means it's being more important for Çubuk is not meaningful. So, the regions that should be compared are the regions that affect  $\text{SO}_4^{2-}$  concentrations in both stations.

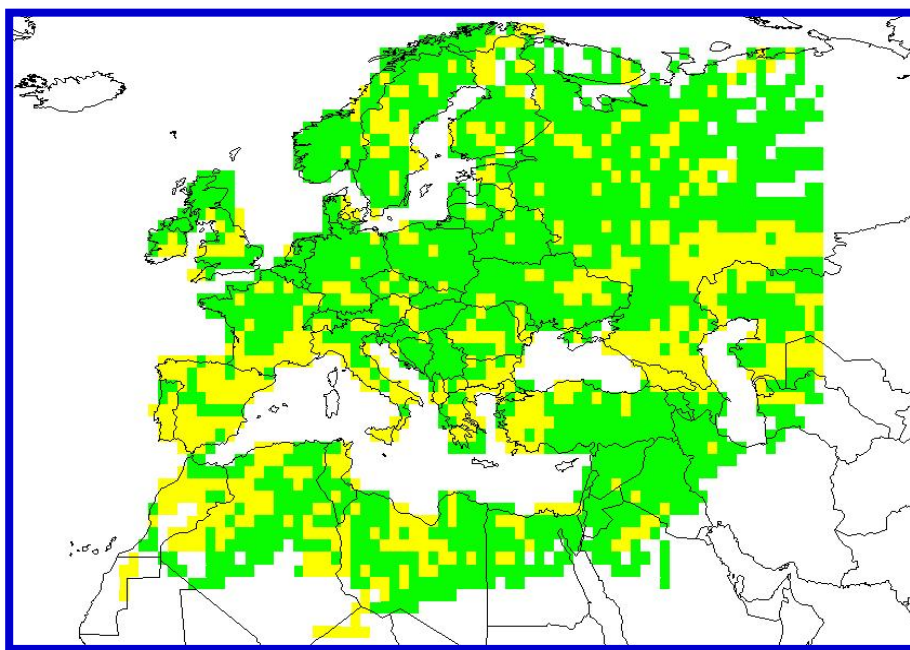


**Figure 4. 14 Percent difference between PSCF values at each grid calculated for Antalya and Cubuk stations.**

As shown in Figure 4.14, Romania and Ukraine contributes almost equally to  $\text{SO}_4^{2-}$  levels in both stations. Bulgaria, Greece and Western parts of Turkey have stronger influence on  $\text{SO}_4^{2-}$  concentrations measured at Antalya station. Sources located in the

Middle East and Eastern Turkey have stronger effect on  $\text{SO}_4^{2-}$  concentrations at Çubuk. These differences are probably dictated by air mass flow patterns affecting both stations.

These results demonstrate that major source areas affecting Central Anatolia and Eastern Mediterranean are the same but there are some minor differences. Generally source regions affecting both stations are very similar. This is not surprising because upper atmospheric air flow patterns at central Anatolia is not much different from air flow patterns affecting Eastern Mediterranean. However, Probability of these regions to be source areas affecting one of the stations may be different. For example Bulgaria is among main source regions affecting both Çubuk and Antalya stations. However, sources in Bulgaria have higher probability of affecting Antalya station.

#### **4.3. Region of Influence (RoI) Approach**

PSCF and similar techniques, such as, conditional probability function and distributed concentrations fields are collectively referred to as “trajectory statistics”. They are proven and reliable tools to identify regions that have high probability of affecting concentrations of a given pollutant at a receptor. However, all of these techniques require concentration information as input, which means that they can only be applied to receptors at which measurement results are available, or for time period during which concentration information exists. In many cases this is a drawback. For example there are many locations in Turkey for which we would like to have source information. In this study we were able to use only two of these and only between 1993–2000 (or 2006 for Çubuk station), because long-term  $\text{SO}_4^{2-}$  data were available only in these two stations. This limited PSCF part of this work, because (1)  $\text{SO}_2$  emissions in Europe is changing since early 80's, (2) we cannot learn how source regions modified after 2006 and (3) we would like to know how  $\text{SO}_4^{2-}$  source regions changed in other parts of Turkey, such as Eastern Black Sea, another locations in the Eastern and Western Mediterranean regions. There is no way to generate this information if we stick with measurement – dependent PSCF technique.

A new technique, which is called “Region of Influence” and which is independent of measurement data was developed and used to increase temporal and spatial coverage. “Regions of Influence” is also a method, which identifies the potential source regions affecting concentrations of pollutants, but it does not need pollutant concentrations at receptor. The approach needs few and simple input data, which includes emission data at the study domain and back trajectory information. Since back trajectories, in our study domain, are available back to 60’s, limiting factor is the availability of SO<sub>2</sub> emission data. Emission data for our gridded study area is available since 1980 in EMEP data-base. Initial emissions are available for years 1980 and 1985. After 1990 emission data is available on a yearly basis. Emissions are organized and presented in 0.5°x 0.5° grids (which is conventional EMEP grid system). Since our grids are 1°x 1°, we combined EMEP grids to make one grid in our system. Our grid system was also shifted 0.25°, so that combined grids in EMEP system exactly matches with our grids.

The “Regions of Influence” approach was developed by Yıkmaz (2010). It was only applied to find source regions affecting Antalya station in the years 1992, 1995 and 2000, as a case study. In this study, we improved methodology by applying altitude weighting to RoI calculations and apply it to determine how SO<sub>4</sub><sup>2-</sup> source regions affecting Antalya and Çubuk stations, so that we can compare the results with results of PSCF calculations in these stations. In addition to Antalya and Çubuk, RoI calculations were also performed at a site in Eastern Mediterranean, namely Ashdod, Israel and a site in the western Mediterranean, namely Corsica Island France. The altitude weighting was applied as described in Section 4.1. RoI calculations were performed for 1980, 1985, 1990 and every after 1990 until 2010.

As mentioned at Section 3.4, RoI approach is performed require back trajectory and emission data as input parameters. Number of trajectory segments in a grid is multiplied by the SO<sub>2</sub> emission for the same grid to generate a RoI value.

A weighting scheme, which is exactly identical to the one used PSCF calculations were used in RoI calculations as well. Corsica and Ashdod were selected for RoI

calculations, because (1) they are typical locations for Eastern and Western Mediterranean basins and (2) They are well-equipped atmospheric measurement sites and their characteristics are well known through large volume of publications that are available in literature.

#### **4.3.1. Variation in $\text{SO}_4^{2-}$ Source Regions as Determined by RoI Approach Between 1980 and 2010 in Four Stations at Eastern and Western Mediterranean**

In this part of the study, three different calculations were performed to discuss “Regions of Influence” calculation for every station. These three steps used were identical to approach adopted in PSCF calculations for Antalya and Çubuk stations. In the first step, annual variation of RoI distributions in our grid system was discussed for the years between 1980 and 2010. In the second step grid-based differences between each year from 1985 to 2010 and the base year, which is 1980, are plotted and discussed. Finally, in the third step, country based temporal variations in RoI distributions were discussed.

##### **4.3.1.1. At Antalya Station**

Yearly change of RoI distribution between 1980 and 2010 for Antalya Station is given in Figure 4.15. It can be seen in Figure 4.15 that emissions in most part of Europe including UK contributed to  $\text{SO}_4^{2-}$  levels at Antalya in 1980. Only the effect of France and Spain were lower compared to other regions, probably because frequency of air mass transport from W (West) sector is smaller than frequency of transport from NW (North West) and N (North) sectors. In 1980's,  $\text{SO}_2$  emission was high in all countries in Europe and source regions were determined primarily by the direction of air mass movements in the upper atmosphere.

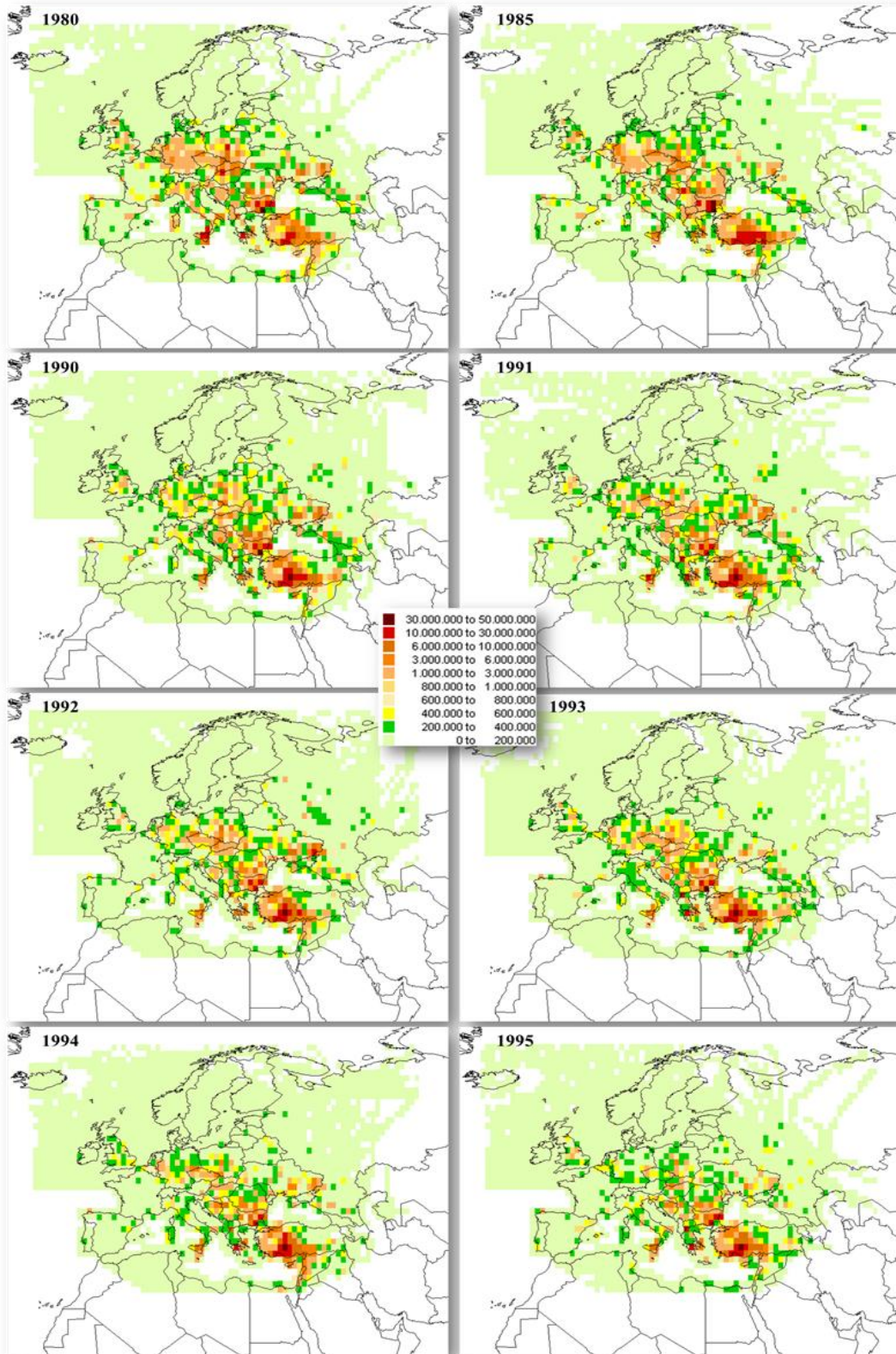


**Figure 4. 15 Yearly Change of RoI distribution between 1980 and 2010 calculated for Antalya Station**

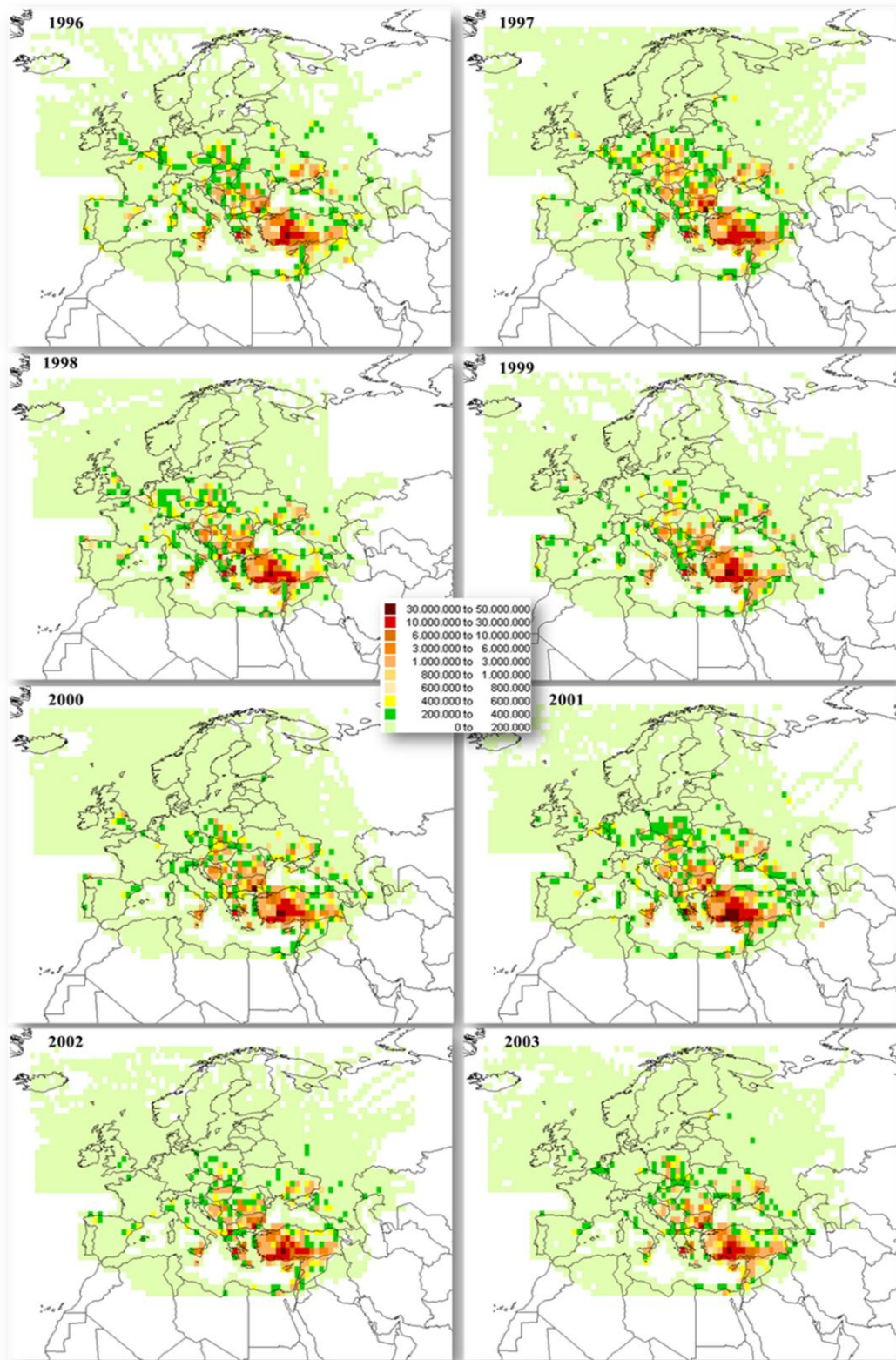


Figure 4.15 (contd). Yearly Change of ROI distribution between 1980 and 2010 calculated for Antalya station

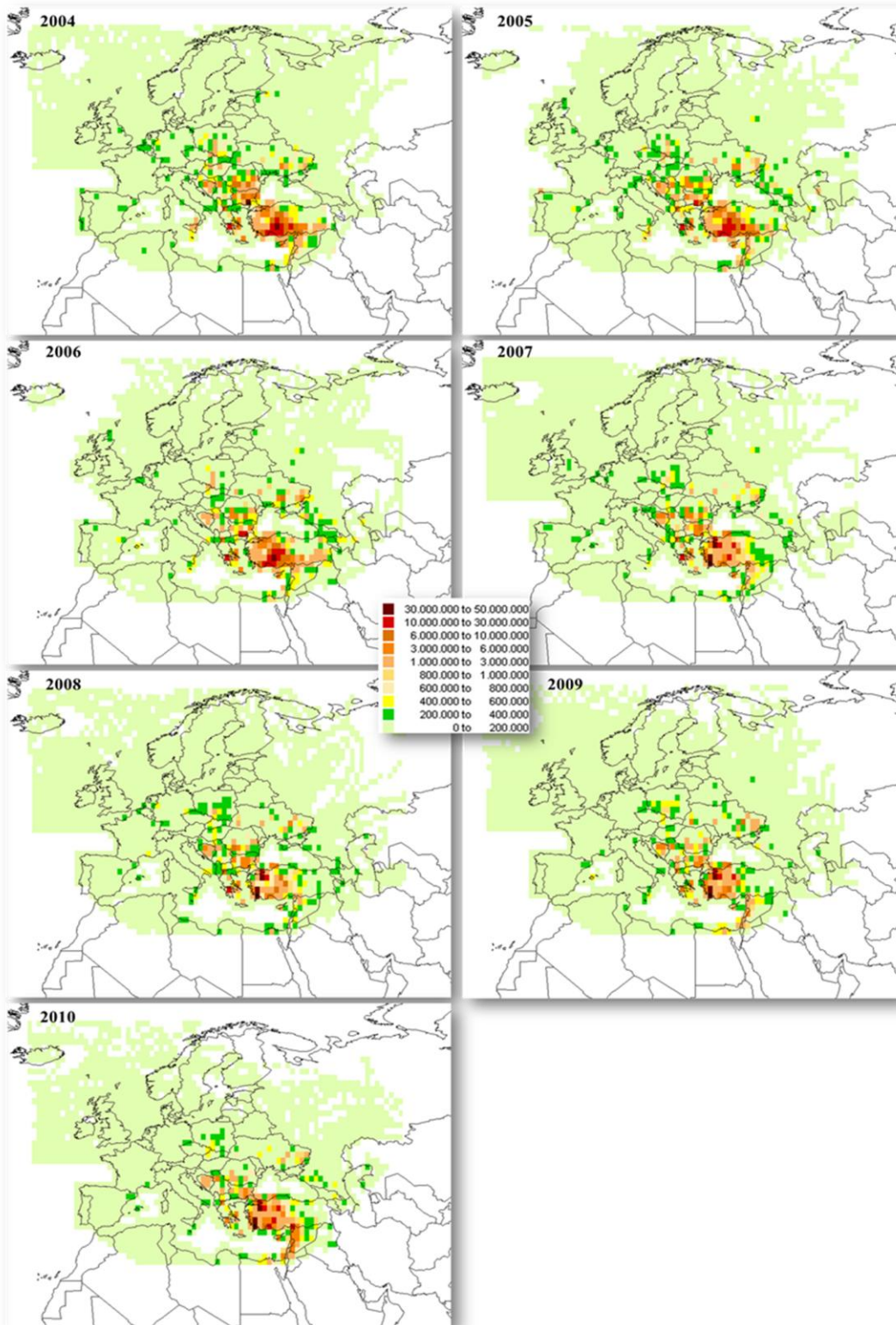


Figure 4.15 (contd). Yearly Change of ROI distribution between 1980 and 2010 calculated for Antalya station

Climatological studies in this region demonstrated that air mass movement is the most frequent from NW sector. This is depicted in Figure 4.16, which is taken from an earlier study in our group (Öztürk et al., 2012) and shows trajectories associated with transport of pollutants to Antalya station. As can be seen in the figure, trajectories that are associated with pollution transport shows an overwhelming preference to NW wind sector. That is why  $\text{SO}_4^{2-}$  potential source regions occur in NW sector if emissions are similar in all directions. This explains the brown channel, indicating reasonably strong source regions, in NW direction from Turkey in RoI maps for 1980 or 1985. However, this pattern changed when emission reductions became effective in later years.



**Figure 4. 16 Direction of back trajectories computed at an earlier work at Antalya station (Öztürk et al., 2012)**

Apart from the regions located in direction of the trajectory group, Ukraine, north of Georgia and Western Turkey were also important source regions in Europe. There were not significant changes in distribution of RoI results until 1995. Only effect of Germany was slightly reduced. Fundamentally, as will be discussed later in the manuscript, there is a reduction in many grids, but it cannot be distinguished by visual evaluation of RoI results. Effect of Western Europe significantly reduced after 1995, but changes that occurred in Eastern Europe and Balkans were not significant at that time.

RoI values in Balkan countries started to decrease only after 2005. In 2010, Western region of Turkey, Israel Coast, East of Ukraine and the some regions of Balkans were the most effective regions for Antalya station. Source regions in most of the Europe, which were important source regions in earlier years, are no longer significant source regions when we come to 2010.

Percent variation of Antalya RoI values at each grid, relative to 1980 RoI's, between 1985 and 2010 is given in Figure 4.17. Firstly, RoI values of each year were compared with previous year's values. The main advantage of this figure is that small changes, which cannot be seen by looking only RoI in Figure 4.15, values can be detected. Furthermore, not only decrease in RoI values but also increase of the values are observed.

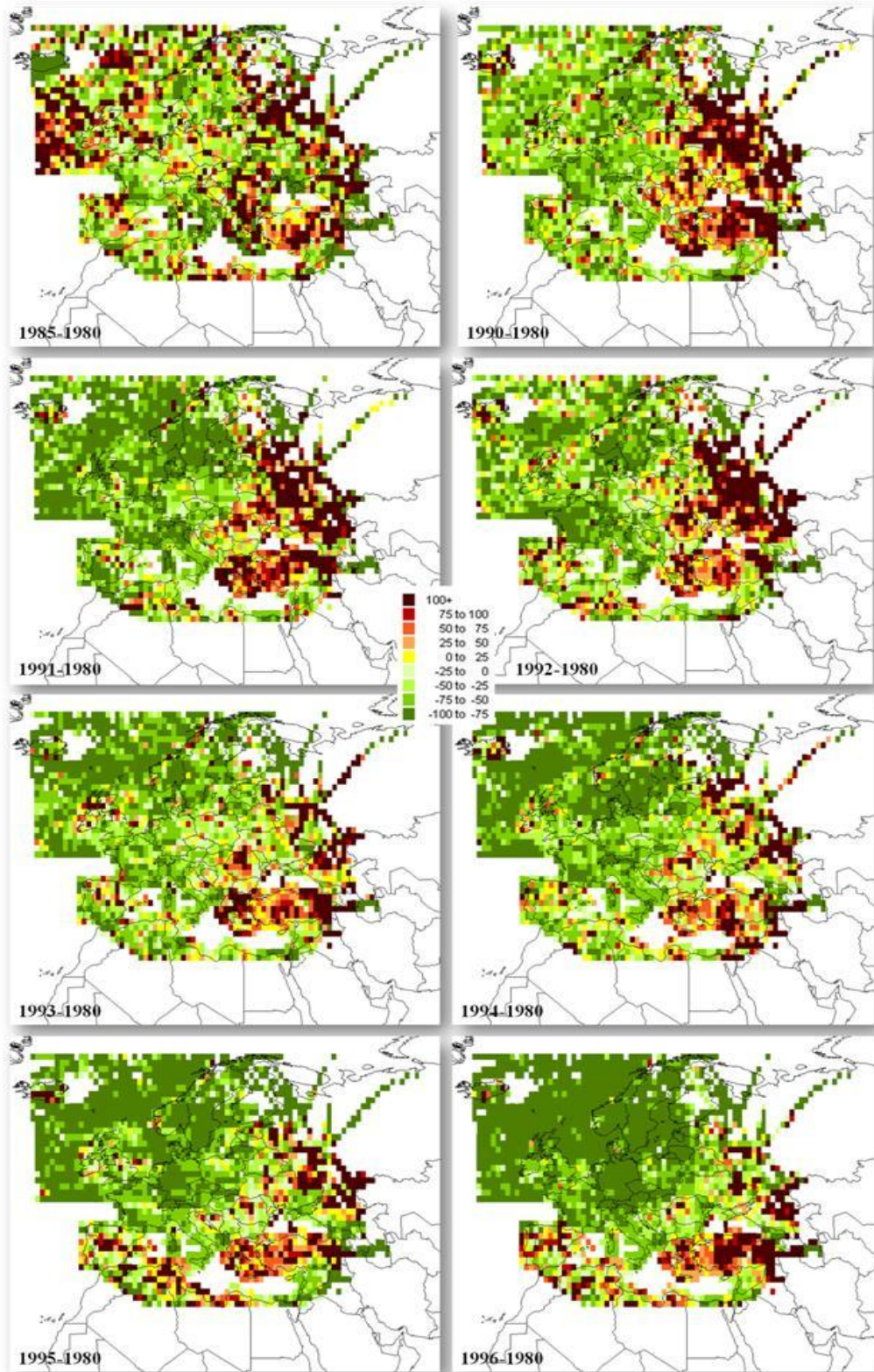


**Figure 4. 17 Percent variation of Antalya ROI values at each grid, relative to 1980 ROI's, between 1985 and 2010**

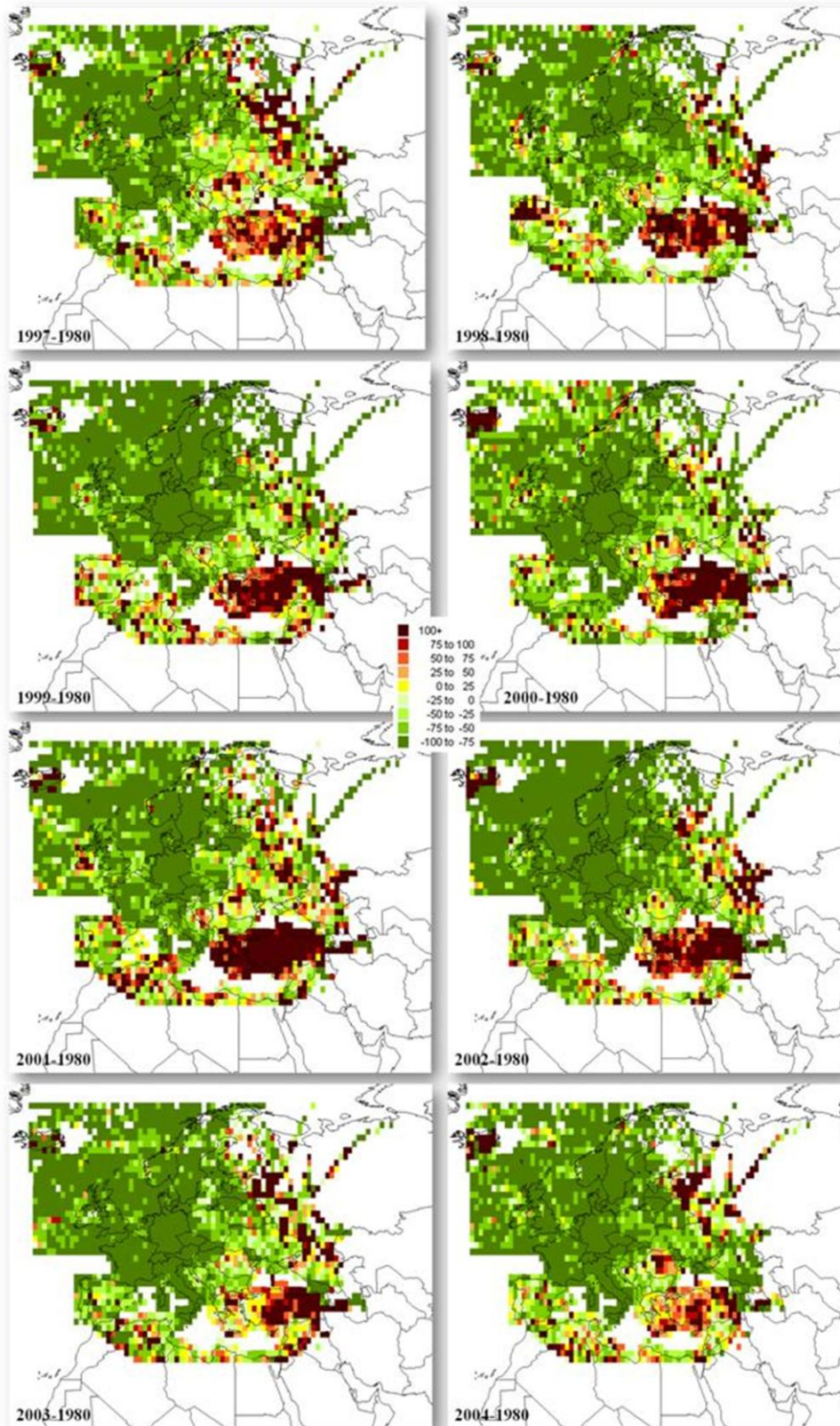
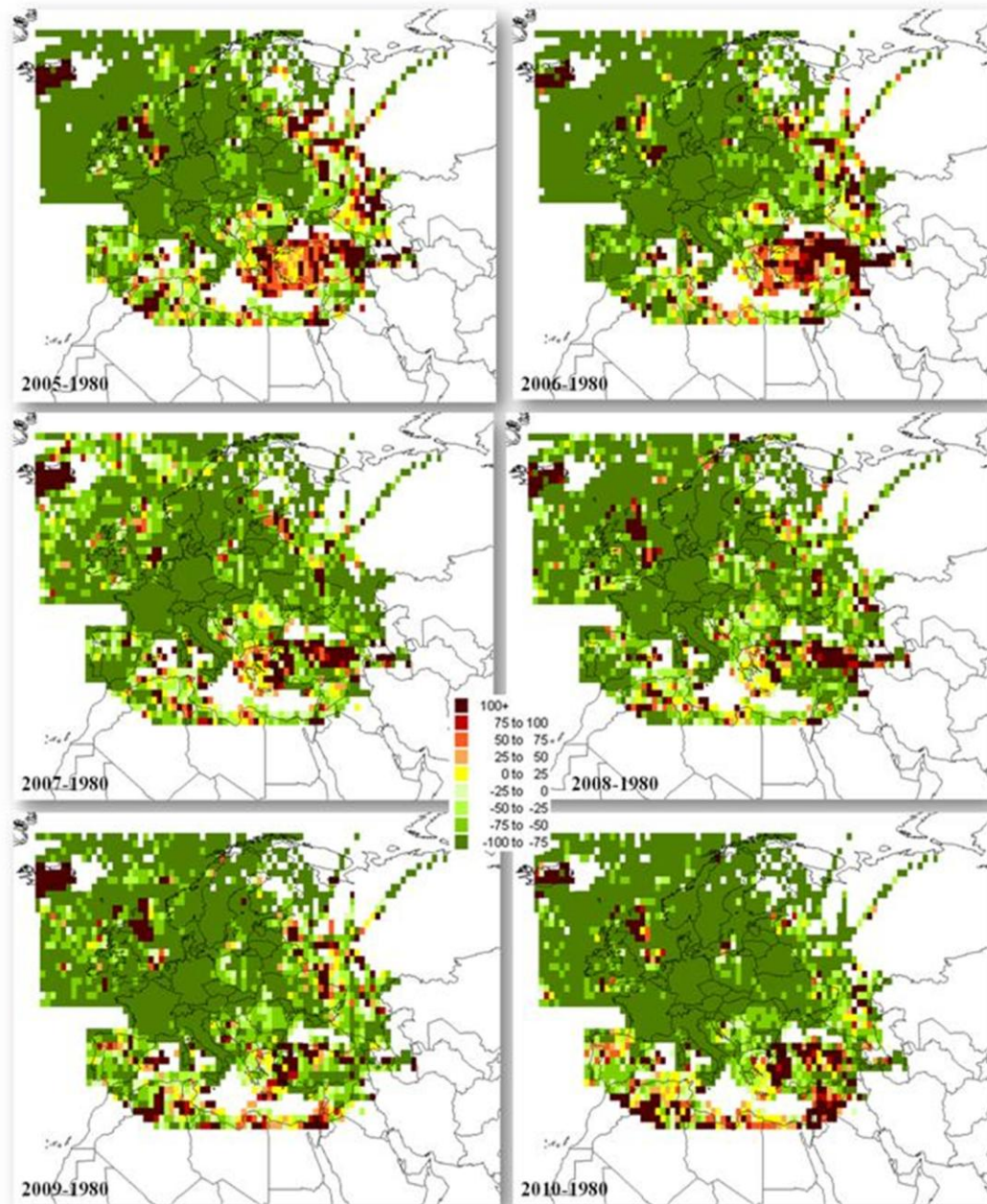


Figure 4.17 (contd). Percent variation of Antalya ROI values at each grid, relative to 1980 ROI's, between 1985 and 2010



**Figure 4.17 (contd). Percent variation of Antalya ROI values at each grid, relative to 1980 ROI's, between 1985 and 2010**

When the Figure 4.15 is discussed, it is stated that there was not any significant change in distribution of RoI until 1995. On the other hand, Figure 4.17 shows that it was not like that. Between 1980 and 1985, there was no significant difference. Until 1995, there was reduction in especially Western Europe. Increase in RoI values were observed in Eastern Europe, Balkan countries and Turkey.

After 1995, the regions which have higher RoI values than 1980's values decreased dramatically. After 2000, only some regions in Ukraine, especially intensive industrial region in the Eastern part, some regions in Poland and Romania and Most parts of Turkey, remained as regions with higher RoI values than corresponding RoI values in 1980. The decrease in RoI values with respect to 1980 varied between 75% and 100% in 2010. Besides, there were a reduction at RoI values in Romania, Bulgaria, Greece and Poland. However, the reduction was not as high as 75% reduction seen in other parts of Europe.

One very important point is the increasing significance of Turkey as a source region for Antalya station. This is partly due to very large number of trajectory segments in grids included in Turkey, due to close proximity to receptor site. However, since changes in annual flow pattern cannot vary dramatically over a 20 year period, increasing RoI values in time over Turkey cannot be explained by large number of segments, it is largely due to lack of decrease in SO<sub>2</sub> emissions in Turkey, as discussed in previous sections.

Variation of average RoI value at each country for Antalya station from 1980 to 2010 is given in Figure 4.18. Variation of RoI values at each country is not so different from discussion made on the basis of Figure 4.15. In years 1980 and 1985 all countries in Europe are potential source regions for Antalya SO<sub>4</sub><sup>2-</sup> levels. Contribution of Western Europe starts to decrease after 1990. Ukraine, Balkan Countries, Turkey and Middle East are the regions affecting SO<sub>4</sub><sup>2-</sup> concentrations at Antalya after the year 2000. Turkey is the main source region, Balkan Countries and Middle East, Particularly Israel are the secondary source regions when we come to year 2010.

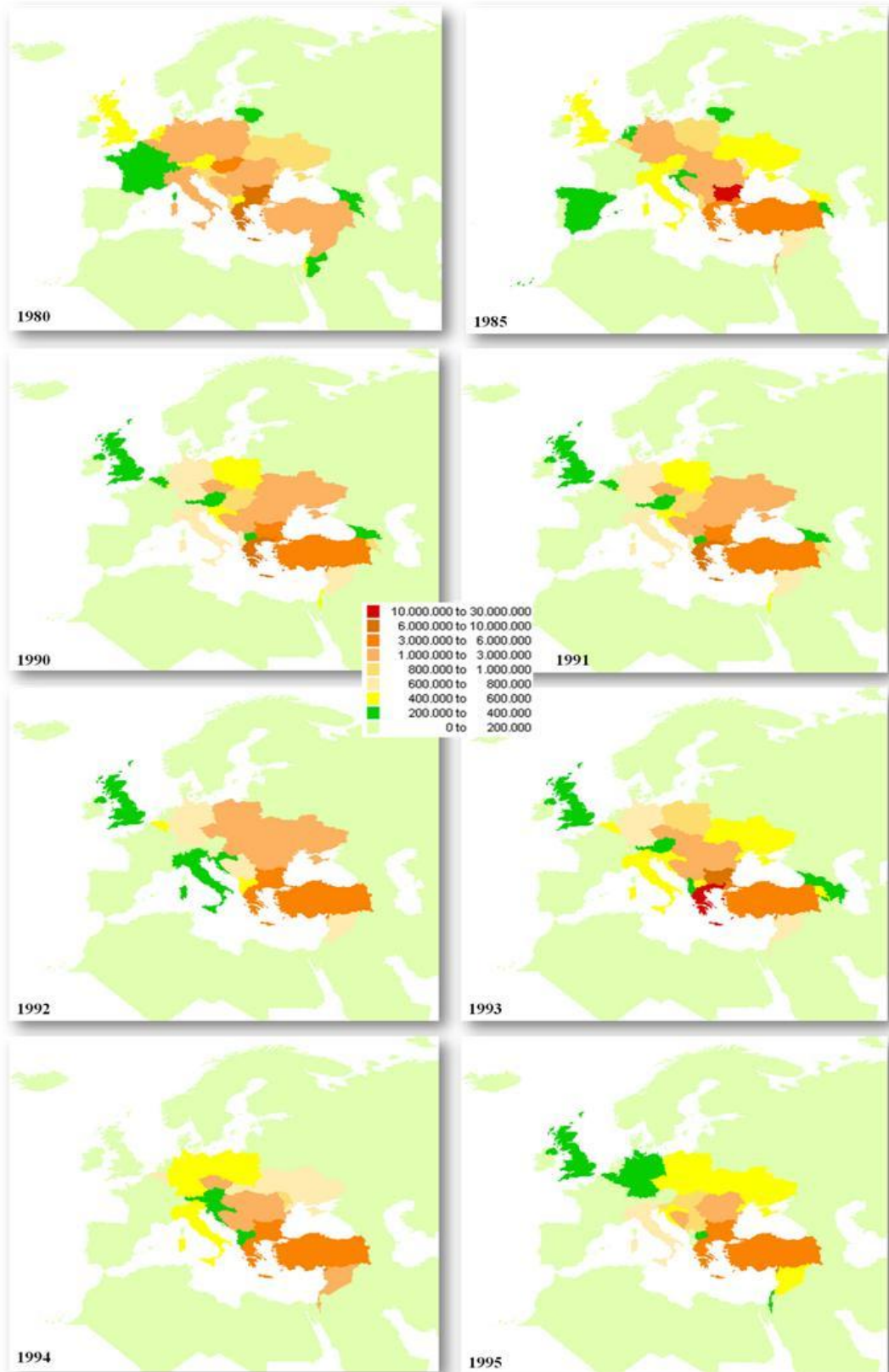


**Figure 4. 18 Variation of average RoI value at each country, between 1980 and 2010, for Antalya station**

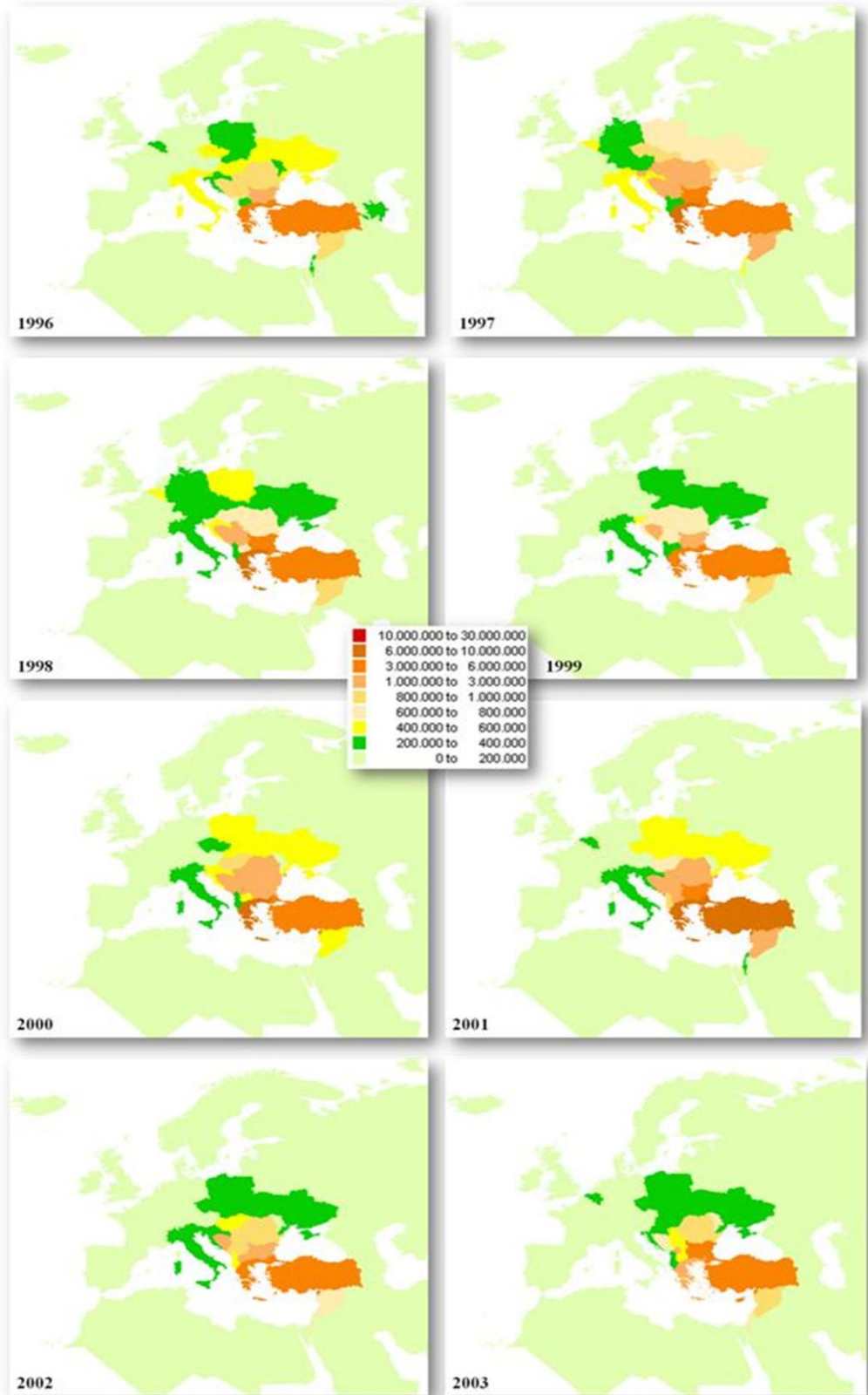


**Figure 4.18 (contd) Variation of average ROI value at each country, between 1980 and 2010, for Antalya station**

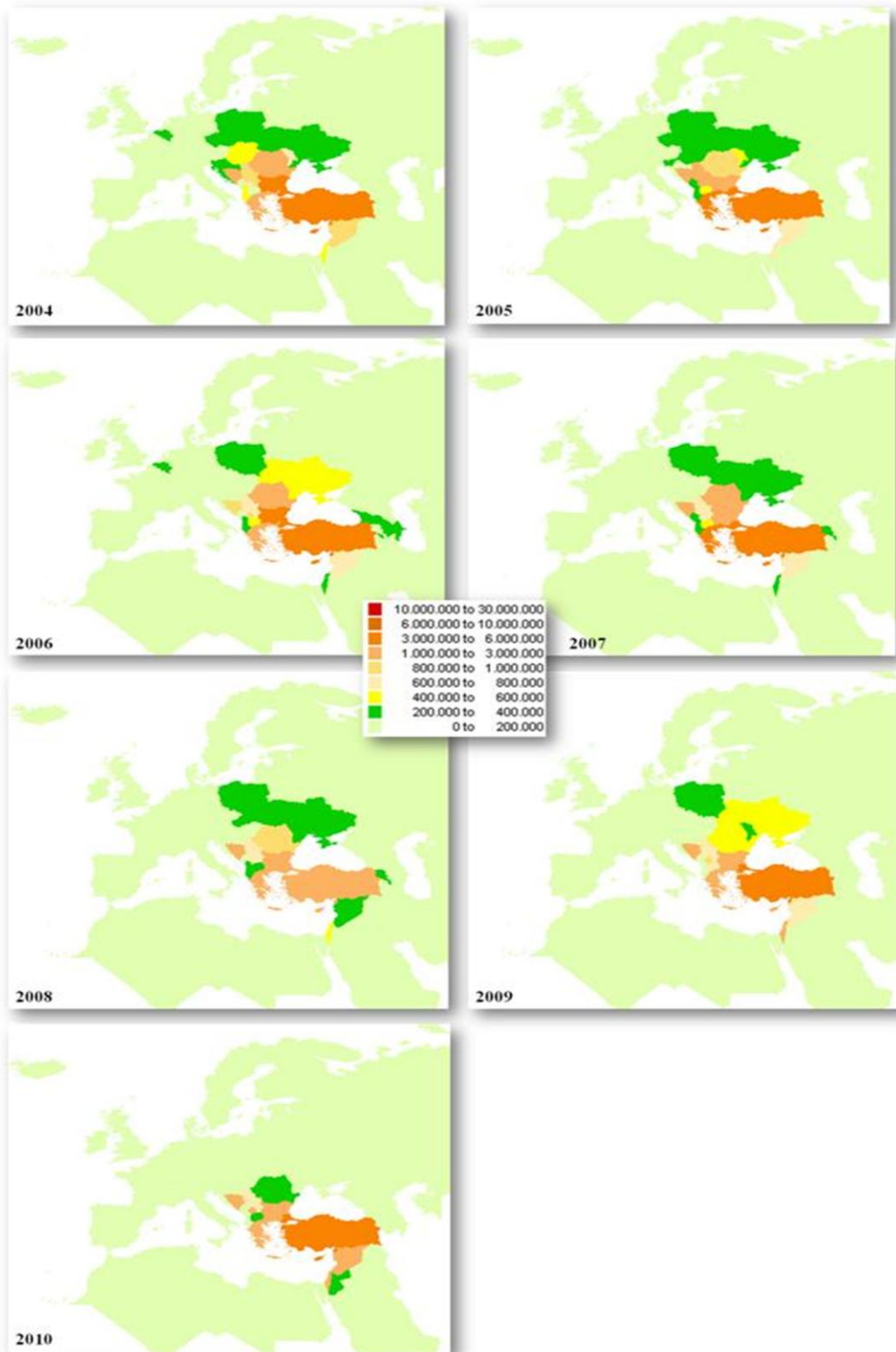


**Figure 4.18 (contd) Variation of average ROI value at each country, between 1980 and 2010, for Antalya station**

In 1980 and 1985, the countries mostly affecting Antalya were the Balkans (especially Bulgaria and Romania), Poland, Ukraine, Germany, and Turkey. After 1990, the effect of Western Europe, especially Germany, gradually decreased. But the effects of the Balkans, particularly Greece, and Turkey did not change and actually increased. After 1994, Middle East, particularly Syria and Israel, appeared as a moderate source region.

After 2000, the RoI values of Ukraine and Poland also decreased, but they remained as potential source regions. The effects of Balkan countries, namely Greece, Romania Bulgaria and Turkey on Antalya station were still predominant. In 2010, effect of Ukraine and Poland minimized, and RoI value of Romania decreased to the lowest level. Therefore; Bosnia Herzegovina, Greece, Bulgaria, Turkey and Syria were the most probable source regions affecting sulfate concentrations in Antalya.

#### **4.3.1.2 At Çubuk Station**

In Figure 4.19, yearly change of ROI distribution between 1980 and 2010 for Çubuk station is shown. According to the figure, in 1980, many regions of Europe including few grids in England contributed to Çubuk. All emissions of Western and Eastern Europe contributed to  $\text{SO}_4^{2-}$  concentrations measured in Çubuk. As in Antalya station, contributions of and Spain was not as high as the contributions of other countries on  $\text{SO}_4^{2-}$  levels at Antalya site, due to less frequent upper atmospheric air mass movements from W sector.

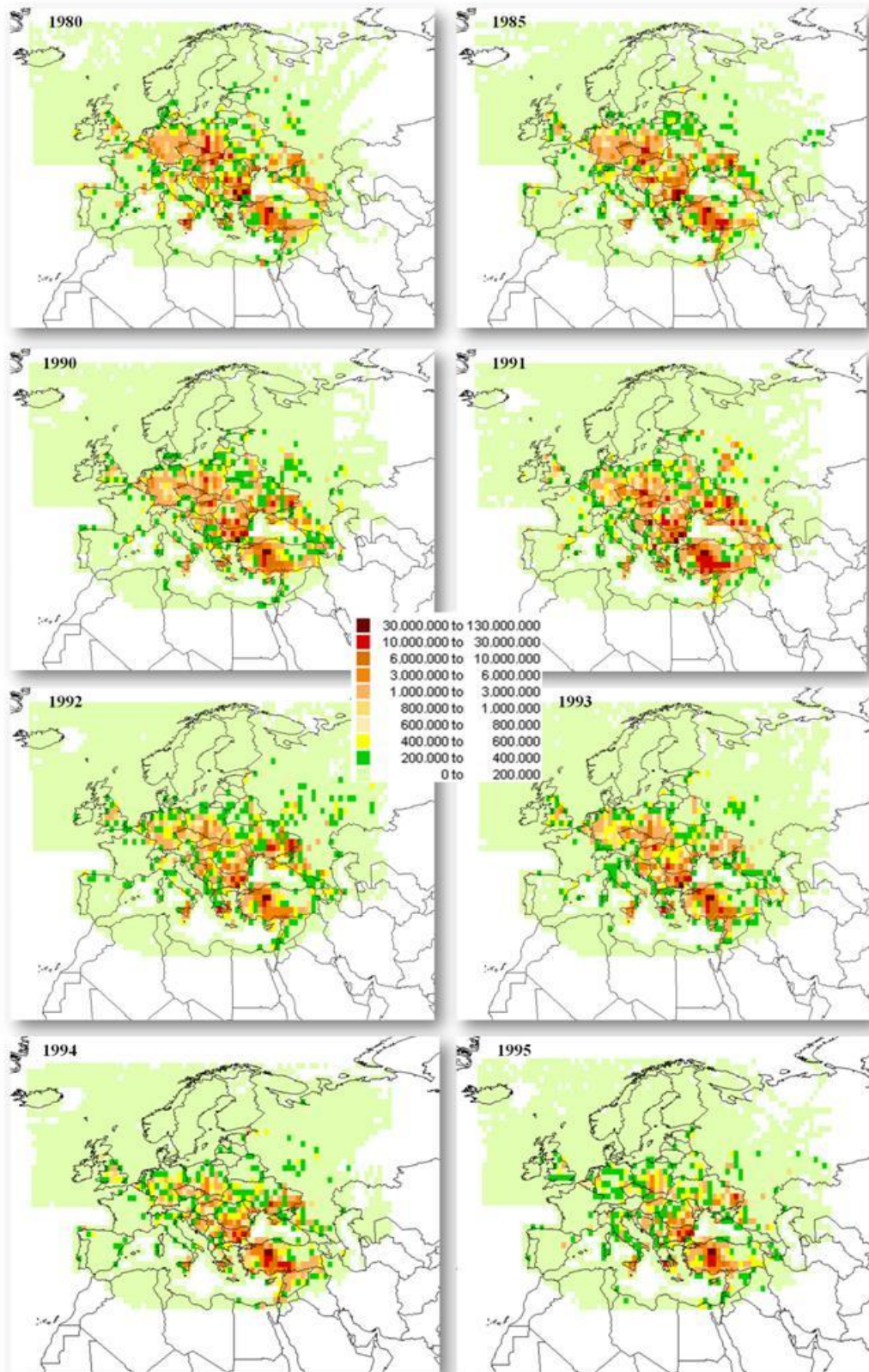


**Figure 4. 19** Variation of potential source regions affecting Çubuk station between 1980 and 2010

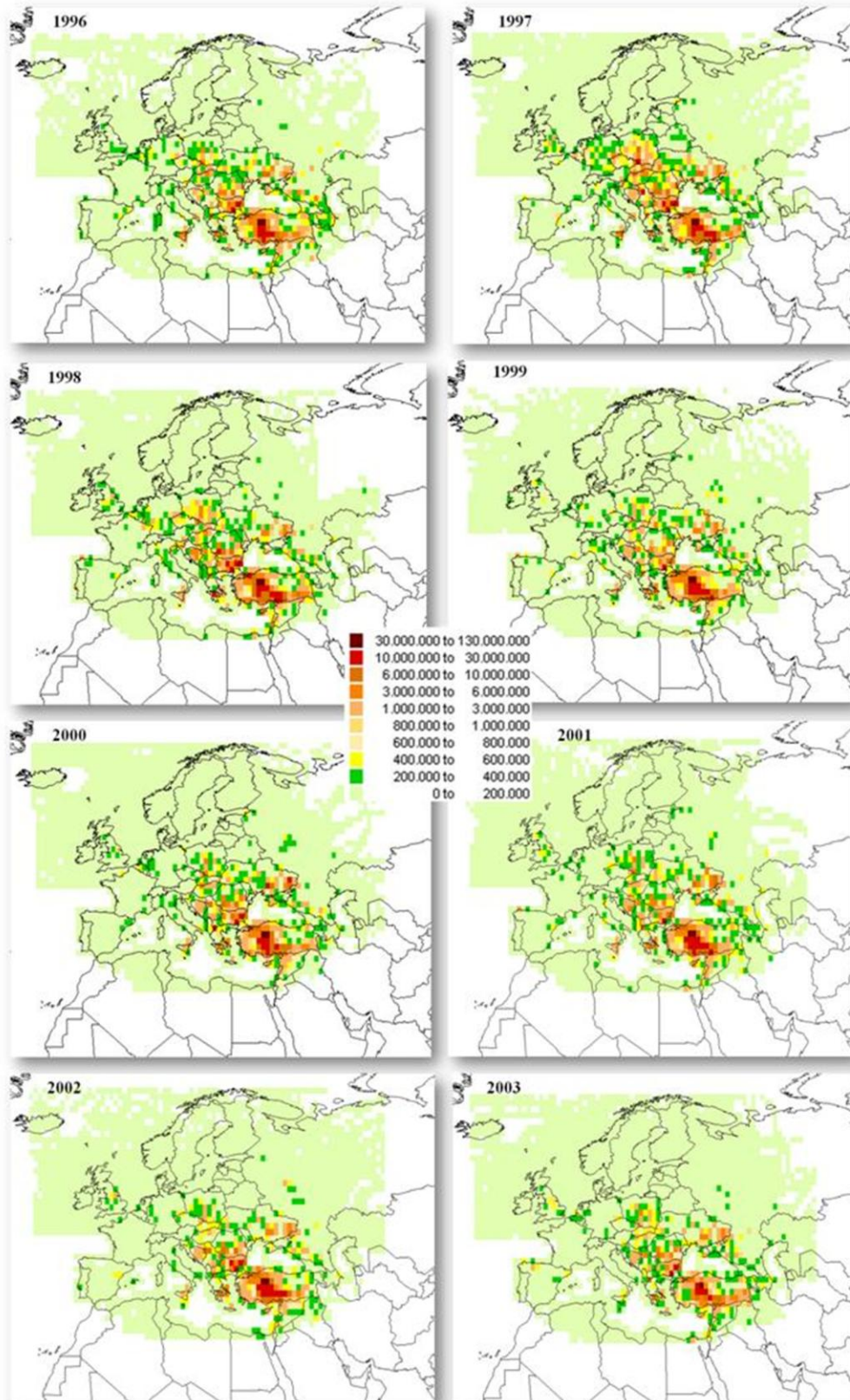
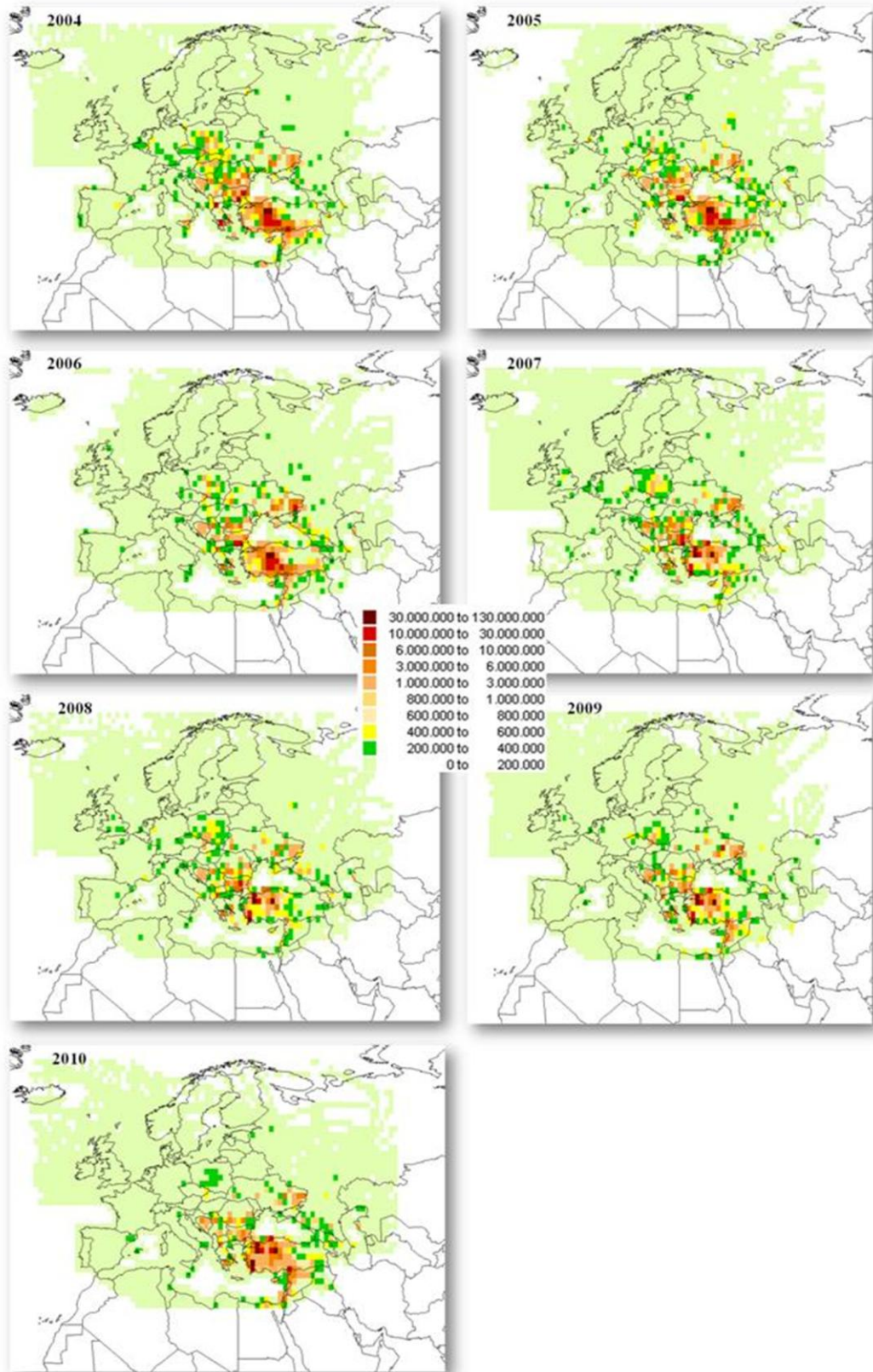


Figure 4.19 (contd) Variation of potential source regions affecting Çubuk station between 1980 and 2010



**Figure 4.19 (contd) Variation of potential source regions affecting Çubuk station between 1980 and 2010**

Ukraine, Georgia, Black Sea Coast of Russia and Southern Turkey were important source regions in Europe at that time. Effect of Western Europe gradually decreased after 1990. On the other hand, the effects of Balkans, especially Bulgaria, and Northern sources (especially emissions in Ukraine) did not change significantly. However, after 2000, the effects of Balkans on Çubuk gradually decreased. In 2010, Western and Northwestern regions of Turkey, Israel Coast, East of Ukraine and the some regions of Balkans were the most effective regions affecting sulfate concentrations of Çubuk.

In Figure 4.20, percent variation of Çubuk RoI values at each grid relative to 1980 RoI's is shown for the years from 1985 to 2010. It is seen that there was not any significant change in distribution of RoI values until 1993. Between 1980 and 1985, there was no significant difference. There were both grids with decreased RoI values and grids with increased RoI values. The regions which have higher RoI values than 1980's values have decreased dramatically since 1993. Also, after 2000, some grids with increased RoI values in Eastern part of Ukraine, the some regions in Poland and the some industrial regions in Romania and Western Turkey disappeared. In 2010, although general distribution of RoI values ranged from 75% to 100% reduction, west, north and northeast regions of Turkey, Armenia, Azerbaijan, Israel, and North border of Africa were the regions with increased RoI values compared to 1980's values.

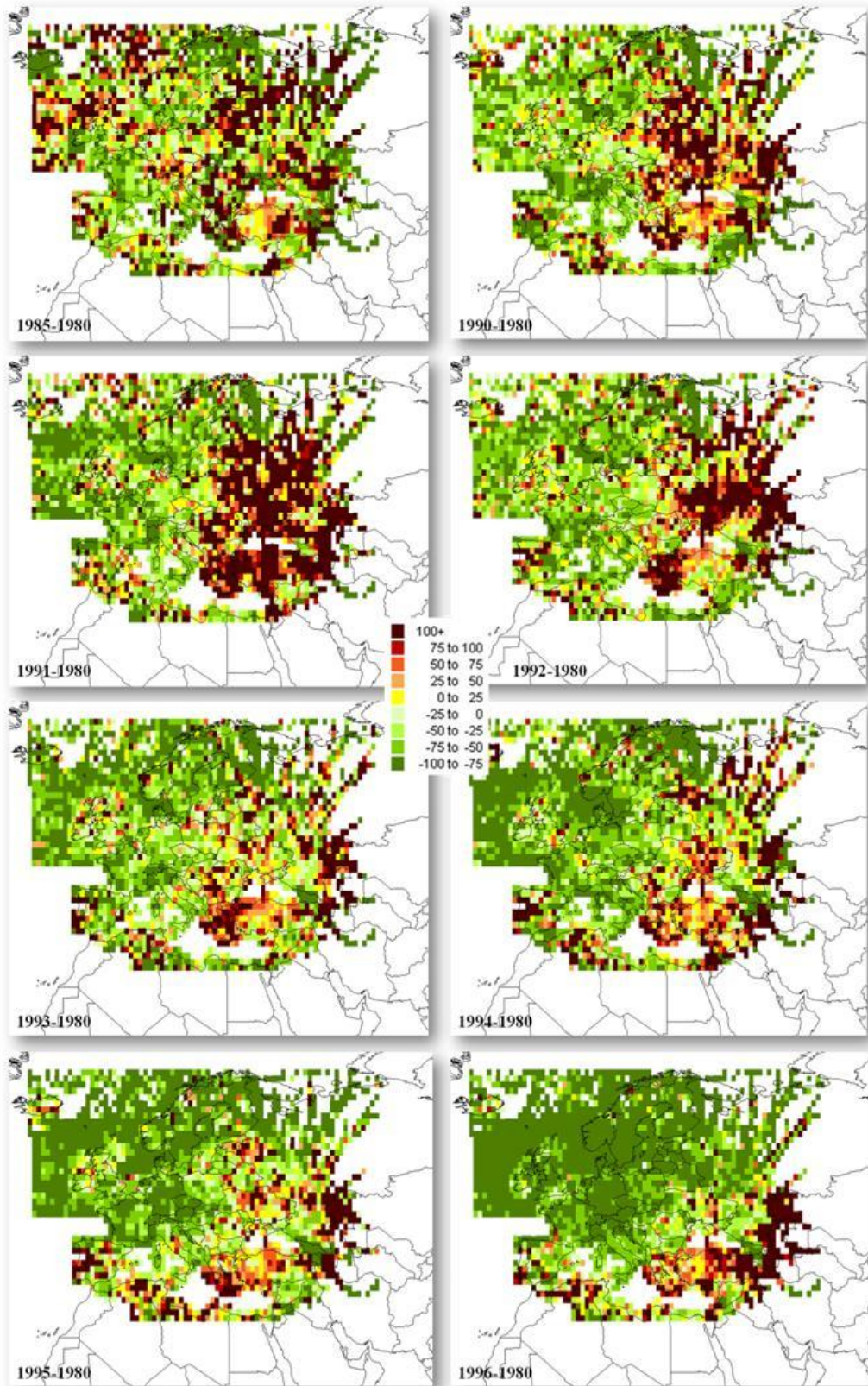


**Figure 4. 20 Percent variation of Çubuk RoI values at each grid, relative to 1980 RoI's, between 1985 and 2010**

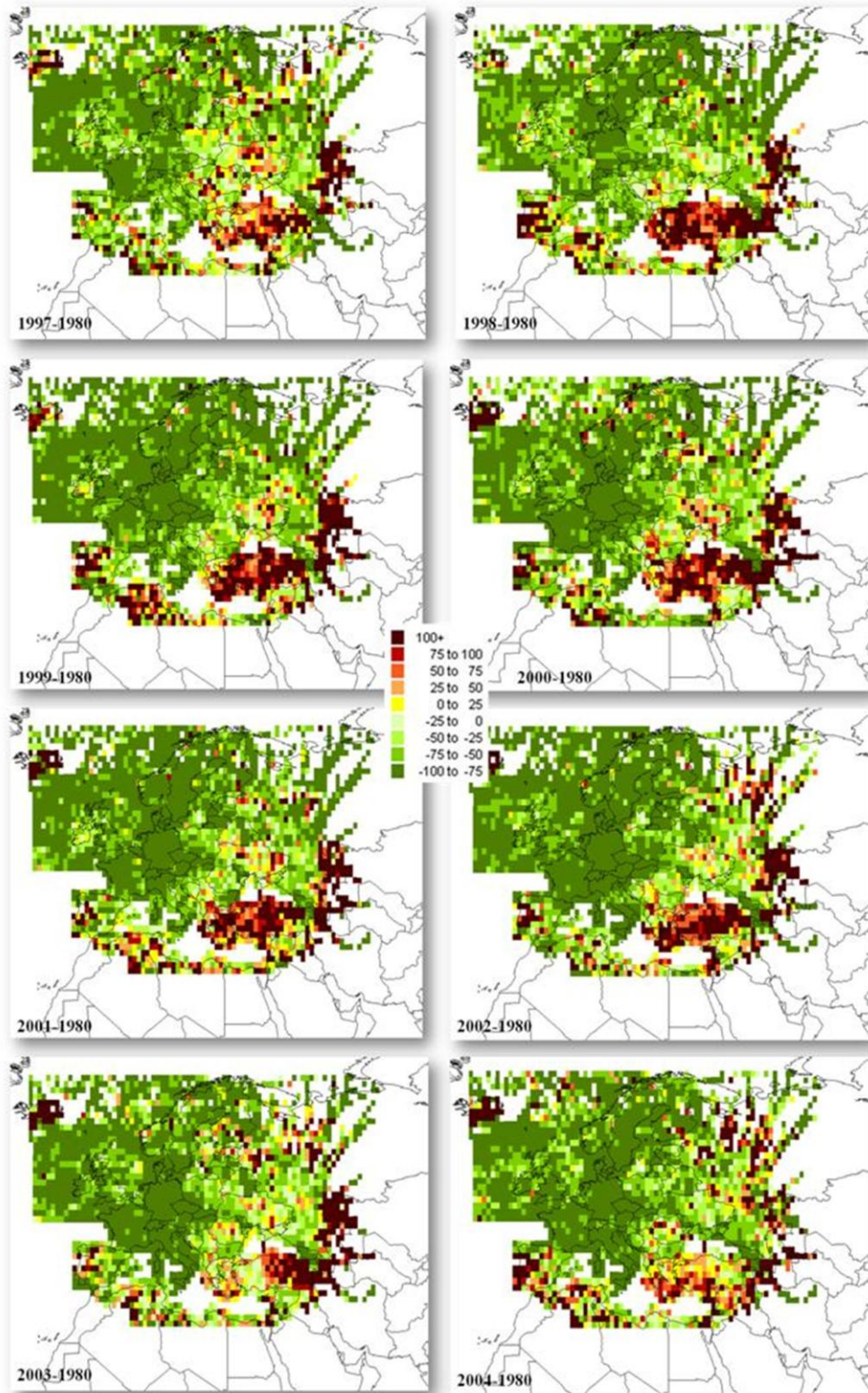
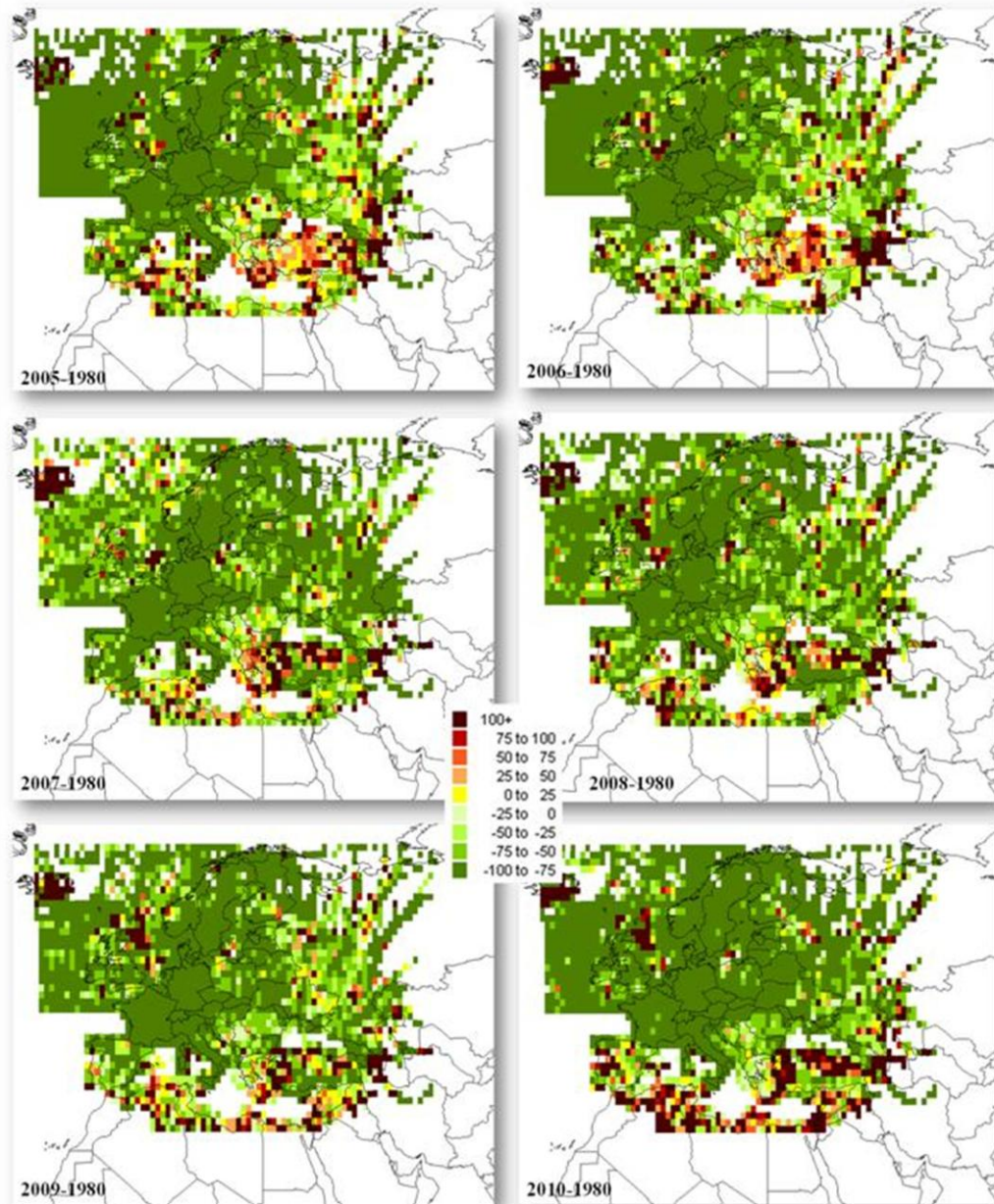


Figure 4.20. (contd) Percent variation of Çubuk ROI values at each grid, relative to 1980 ROI's, between 1985 and 2010



**Figure 4.20. (contd) Percent variation of Çubuk ROI values at each grid, relative to 1980 ROI's, between 1985 and 2010**

The distributions of RoI values for Antalya and Çubuk stations were very similar to each other. Also identification of small differences between source regions affecting  $\text{SO}_4^{2-}$  concentrations measured in the two stations was very difficult. Thus, RoI values of both stations were subtracted from each other in order to differentiate the small differences. The calculation was performed for 1980, 1990, 2000, and 2010. The difference between RoI results at each grid for Antalya and Çubuk Stations are given in Figure 4.21. While grids with orange shading indicate areas that are more

important source regions for Antalya Station, grids with blue shading define more significant source regions for Çubuk Station. In addition to this, grids with yellow shading indicate areas that are almost equally significant source regions for these stations.

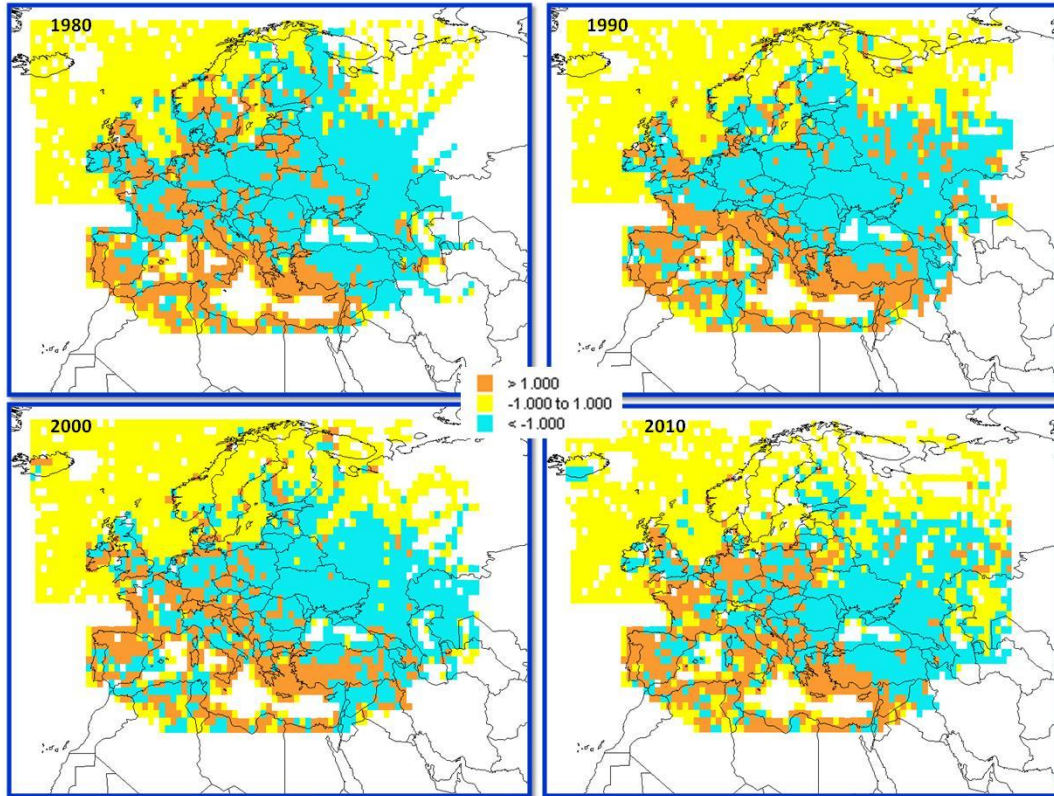


**Figure 4. 21** Difference between RoI values at each grid calculated for Antalya and Çubuk Stations. Grids with orange shading indicate areas that are more important source regions for Antalya Station and grids with blue shading are the areas that are more important source regions for Çubuk Station.

As seen in Figure 21, regions with orange, yellow and blue shading have not changed substantially from 1980 to 2010. Major difference is seen in France, Germany and Poland. While north of France, Germany and Poland were regions that are more effective sources for Çubuk Station in 1980, the regions became important source regions for Antalya Station in 2010. Moreover, southeast part of Turkey affected Antalya Station in 1990, but the region started to be important source region for Çubuk Station in 2010. Although there is not any significant source in the Southeastern Turkey, the region is an important source region for especially Çubuk.

In general, north part of the study area, especially, Scandinavian Countries, north of Russia, North Sea and Iceland do not predominantly affect Çubuk or Antalya Station. On the other hand, north of Africa, Spain, Italy, Greece, Aegean Sea and Western Turkey seem to be important source regions affecting Antalya stations. It can be supposed that coming of air masses to Antalya from these regions is predominant.

Bulgaria, Romania, Hungary, Ukraine, North and East of Turkey, Black Sea and Caucasian Countries (Georgia, Armenia, Azerbaijan, Black Sea part of Russia) are significant source regions affecting sulfate concentrations in Çubuk. While Greece had an important role on sulfate concentration of Antalya in 1980, grids which are located in most part of Greece became important source regions for Çubuk in 2010.

In Figure 4.22, variation of average RoI value at each country for Çubuk station from 1980 to 2010 is shown. Generally, comments related to Figure 4.19 are similar with discussion of Figure 4.22.

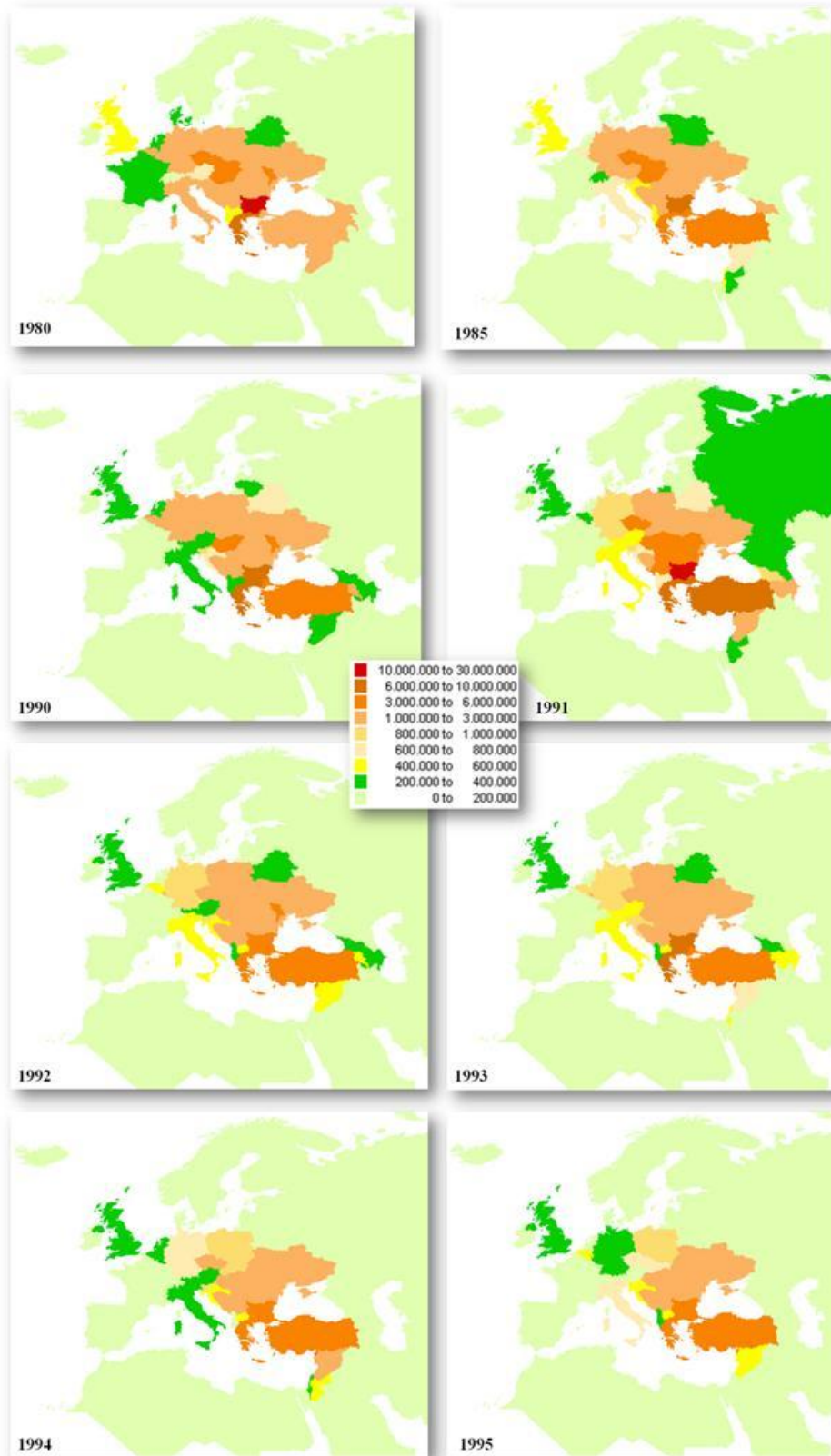


**Figure 4. 22 Variation of average RoI value at each country, between 1980 and 2010, for Çubuk Station**

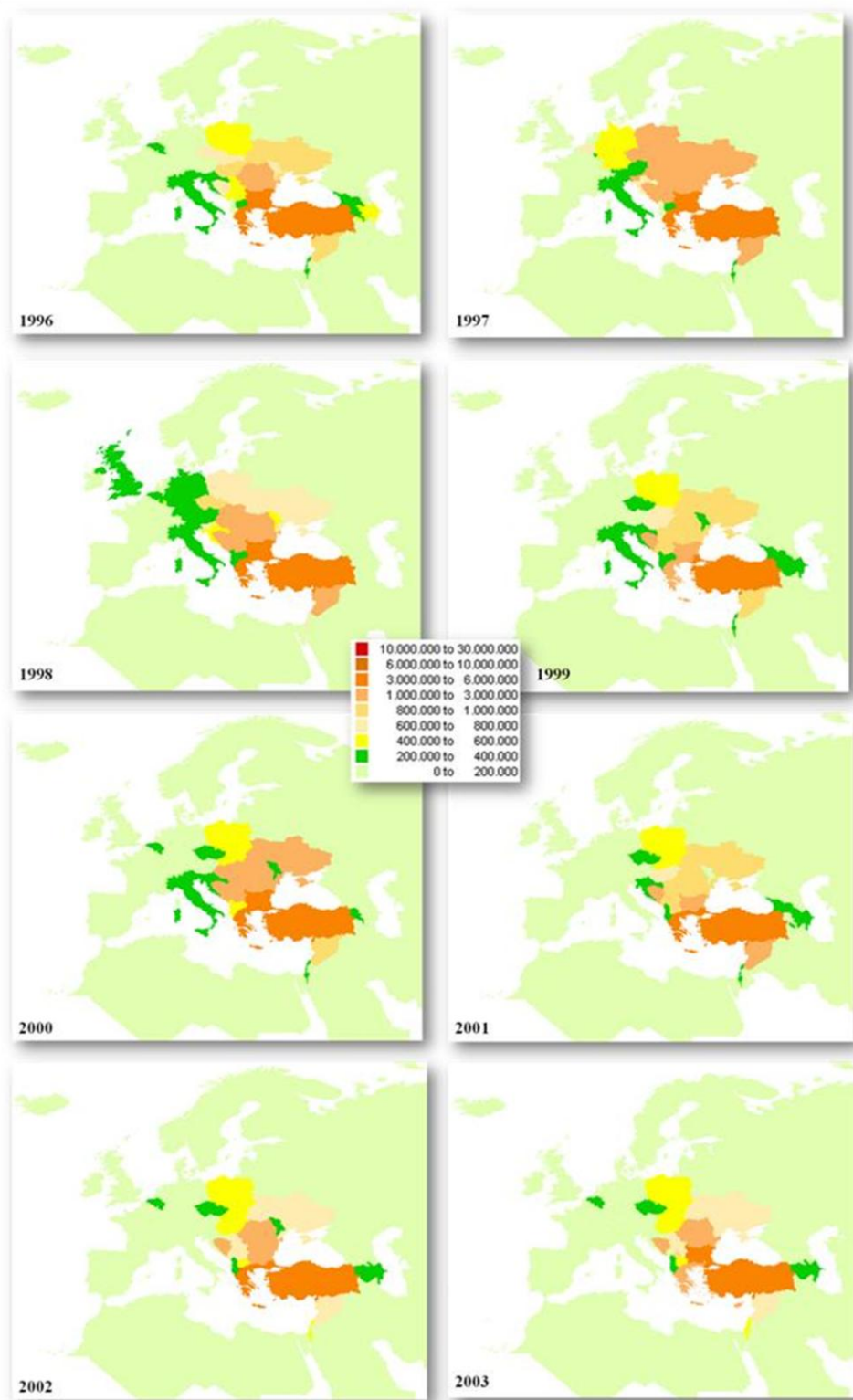


**Figure 4.22 (contd) Variation of average RoI value at each country, between 1980 and 2010, for Çubuk Station**

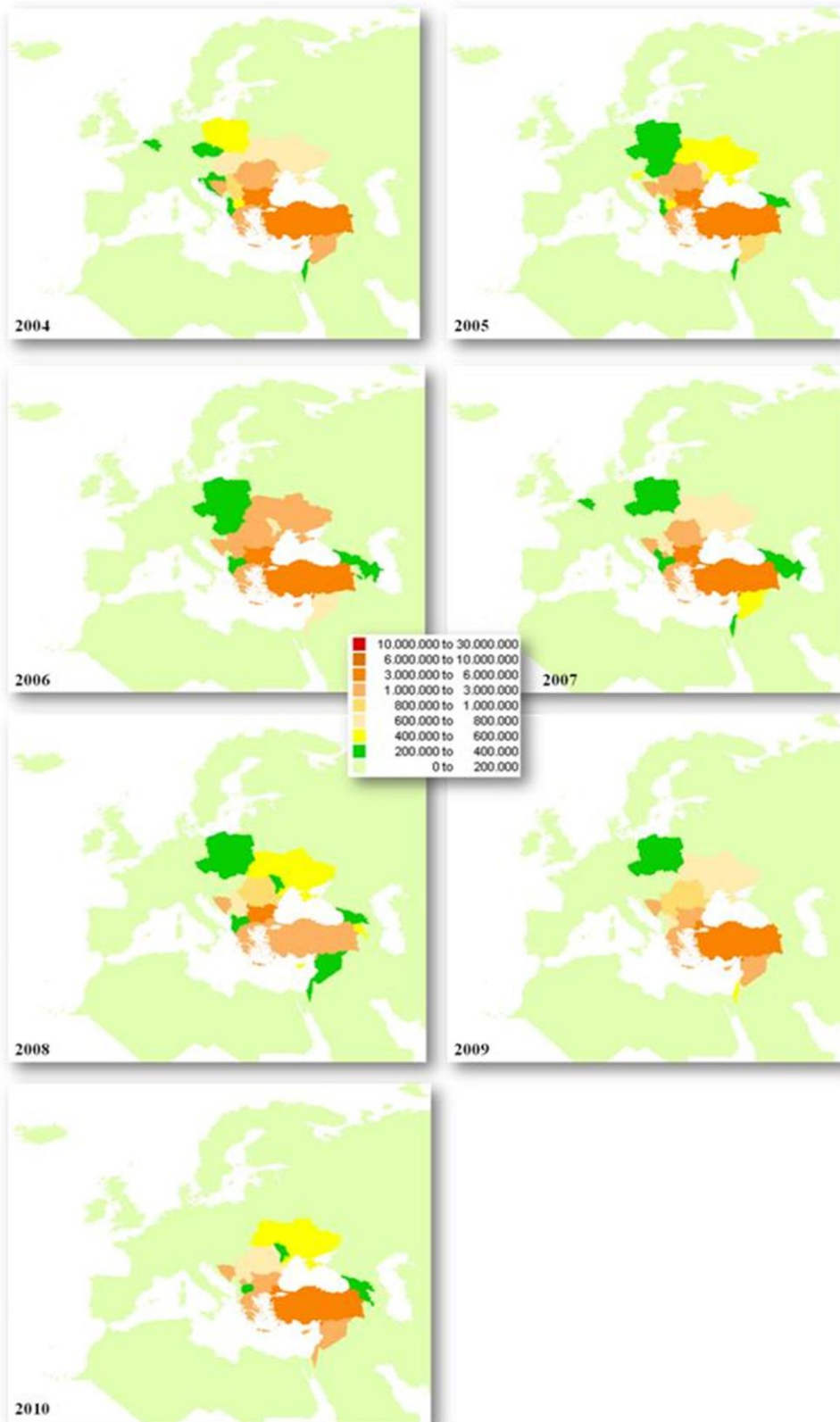


**Figure 4.22 (contd) Variation of average RoI value at each country, between 1980 and 2010, for Çubuk Station**

In 1980, especially Central and Eastern Europe contributed to sulfate concentrations in Çubuk. In Europe, Bulgaria had highest RoI value. As discussed in Figure 4.19, Western Europe has not affected Çubuk station especially since 1985. The effects of Germany and Poland slightly reduced until 1995. The RoI results of Balkans and Ukraine have dramatically reduced since 2000. In 2010, Turkey, Israel, Syria, Greece, Bulgaria, Bosnia Herzegovina were the significant source regions in terms of sulfate concentrations in Çubuk.

#### **4.3.1.3. At Middle East (Ashdod, Israel) Station**

During calculation of RoI approach, source regions affecting stations at Turkey and source regions affecting sulfate concentrations in other regions of Mediterranean could be compared. For this purpose, RoI values for two more stations which are located in Western Mediterranean and Israel Coast were calculated for the years between 1980 and 2010.

Yearly change of RoI distribution between 1980 and 2010 for Ashdod station is indicated in Figure 4.23. There are some differences and similarities between source regions affecting sulfate concentrations in Ashdod and source regions affecting Antalya and Çubuk stations. Ashdod is far from emissions of Europe, so effect of Western Europe on Ashdod is less than the effect on stations situated in Turkey. Even 1980, source regions in Europe did not affect Israel excessively. Locations of source regions for Ashdod were in direction of Northwest-Southeast (NW-SE) as for Antalya and Çubuk. However, RoI values were lower than the values of Antalya and Çubuk. The other similarity between Ashdod and Antalya, Çubuk was source regions in Ukraine. The RoI values in Ukraine were also high. West and south of Turkey were the important source regions affecting Ashdod station. In addition, significant RoI results were calculated along the Coast of Israel.

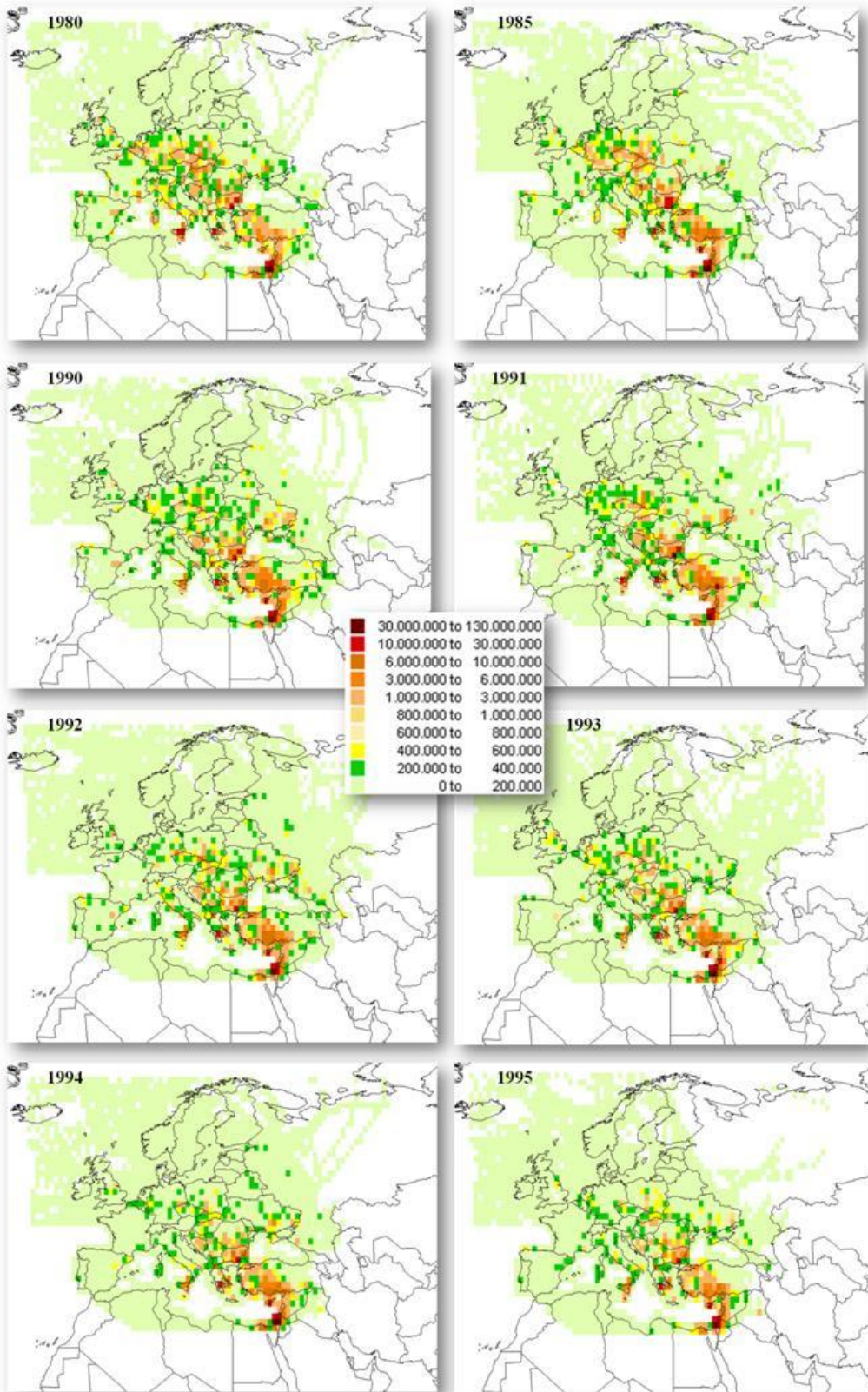


**Figure 4. 23 Yearly Change of RoI distribution between 1980 and 2010 calculated for Ashdod Station**

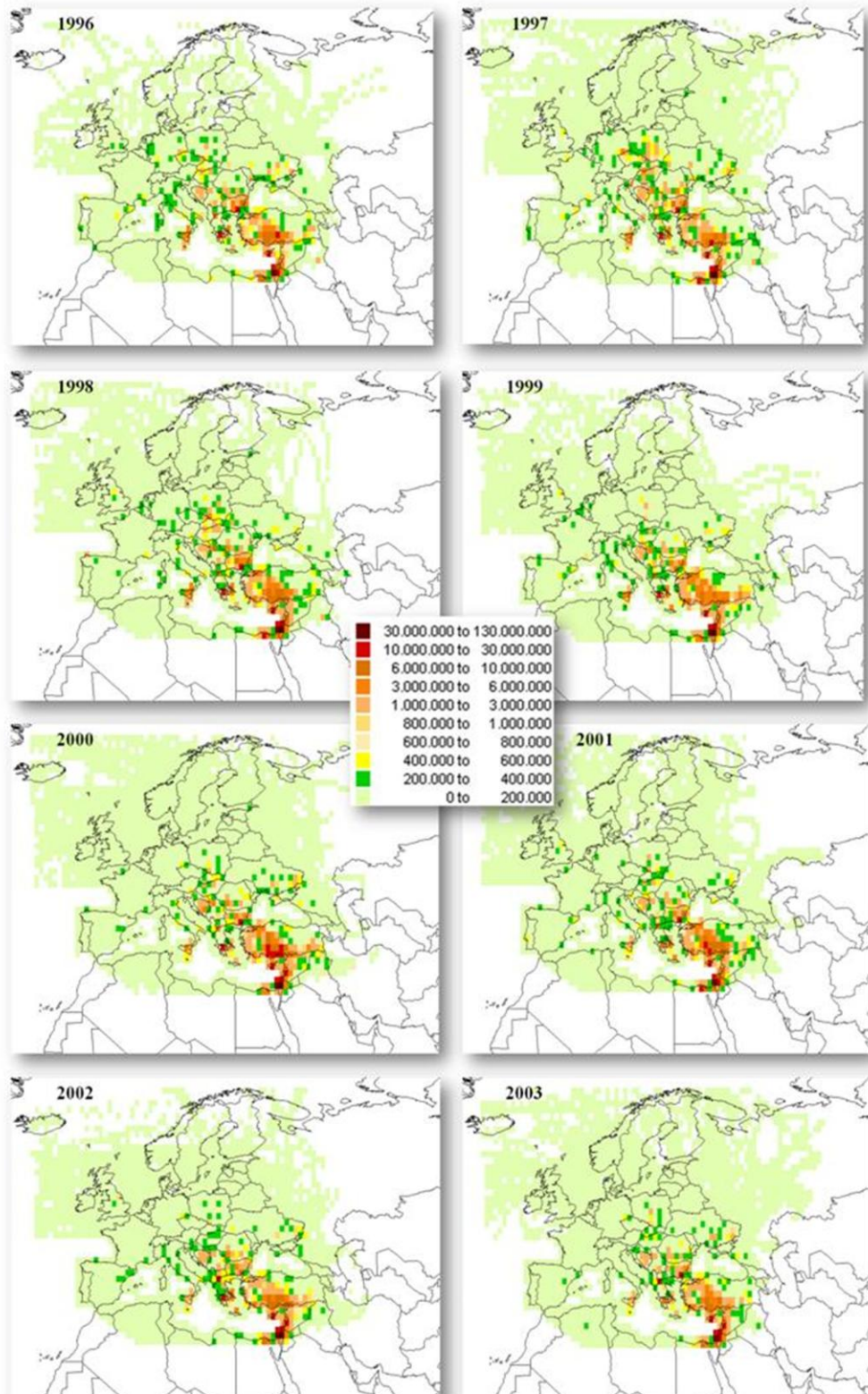


**Figure 4.23 (contd) Yearly change of RoI distribution between 1980 and 2010 calculated for Ashdod Station**

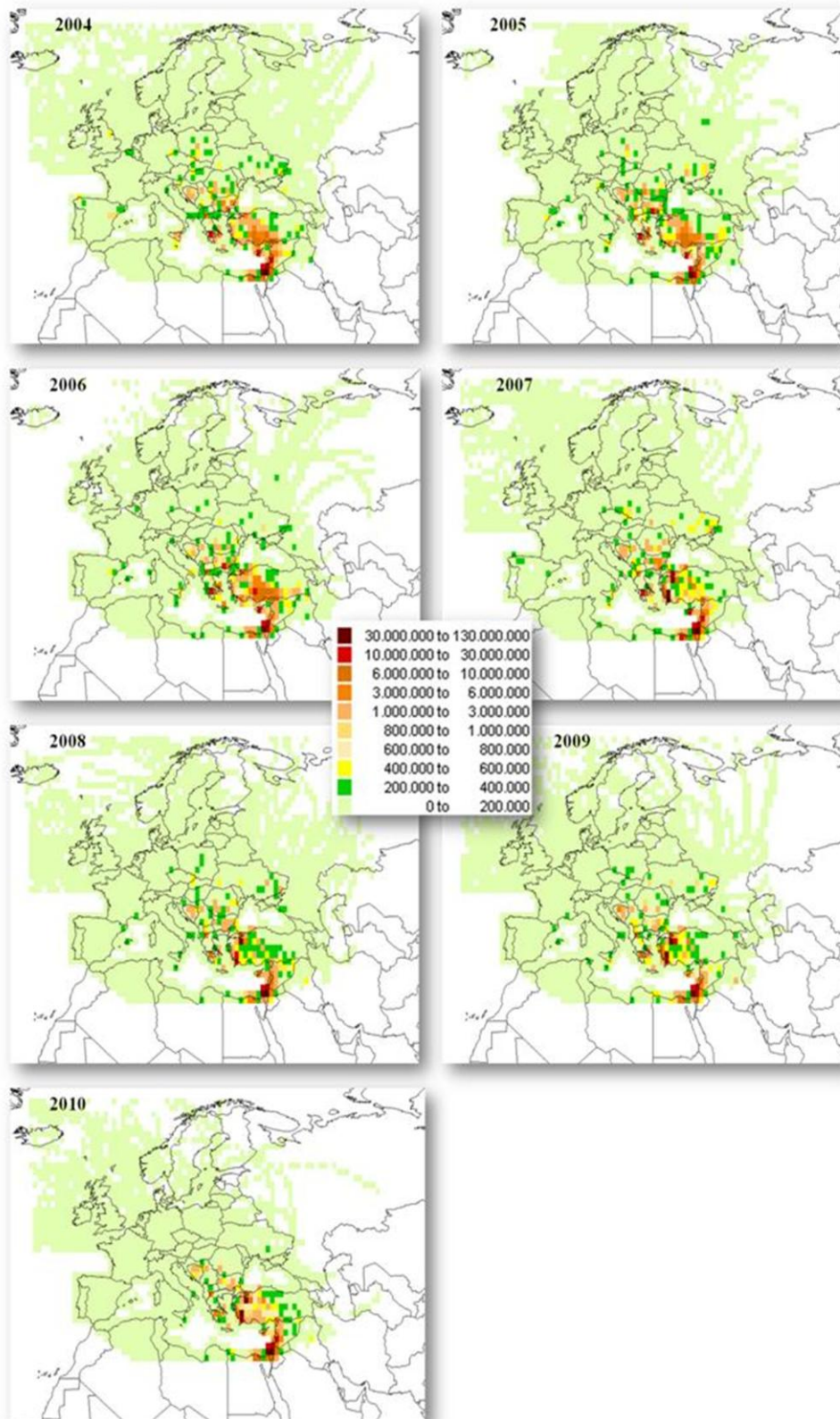


**Figure 4.23 (contd) Yearly change of RoI distribution between 1980 and 2010 calculated for Ashdod Station**

Timing of variation was not so different from that seen in Antalya and Çubuk. After 1995, source regions in Western Europe disappeared. After 2000, west and south of Turkey, Bulgaria, the Balkans, particularly Romania, and east of Ukraine were the basic source regions affecting Israel Coast. It was understood that east of Ukraine substantially affect Eastern Mediterranean region. The distribution of RoI results had not changed until 2010.

Basically, the distribution in 2010 explains why the sulfate concentrations are high in Eastern Mediterranean. Also, it could be understood that why the sulfate concentrations measured in whole Europe rapidly decreased and the concentrations measured in Eastern Mediterranean region did not change.

Because Eastern Mediterranean was not sufficiently affected by source regions in Europe, the reduction of SO<sub>2</sub> emissions in Europe did not have an effective role on SO<sub>4</sub><sup>2-</sup> concentrations measured in stations in Eastern Mediterranean region. Emissions in source regions affecting Eastern Mediterranean, especially in Turkey and the Balkans, reduce slowly compared to emissions in Europe. So, this situation results in that SO<sub>4</sub><sup>2-</sup> concentrations measured in the region have barely started to decrease in recent years.

In Figure 4.24, percent variation of Ashdod RoI values at each grid, relative to 1980 RoI's, between 1985 and 2010 is indicated. For all years, not only decreases in RoI values but also increase of the values were observed. As discussed in Figure 4.23, the emissions of Europe were not so effective on Ashdod, so the percent changes of RoI in Western Europe were not relevant to changes in observed concentrations on the coast of Israel.

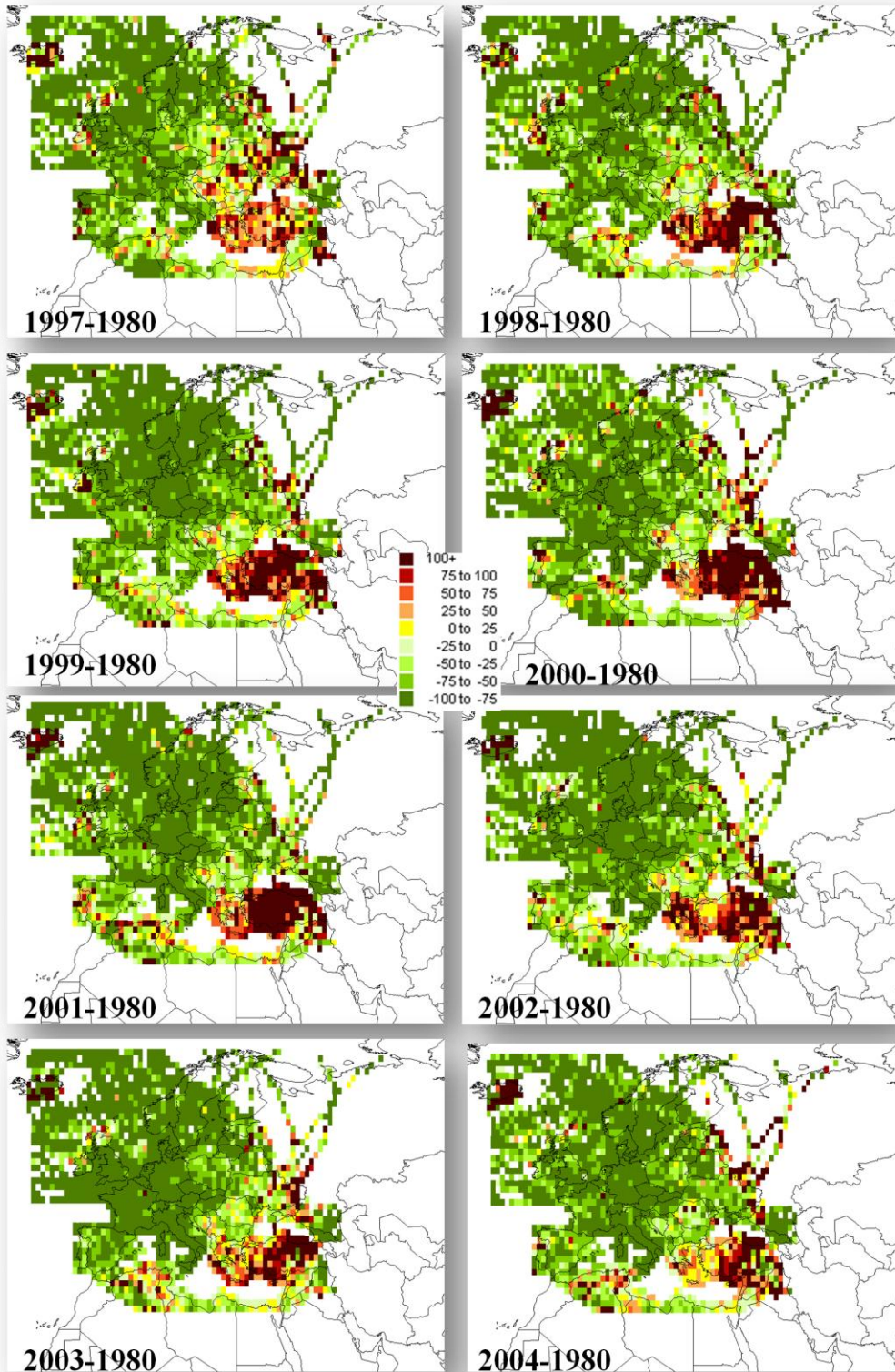


**Figure 4. 24 Percent variation of RoI values calculated for Ashdod, Israel at each grid, relative to 1980 RoI's, between 1985 and 2010**

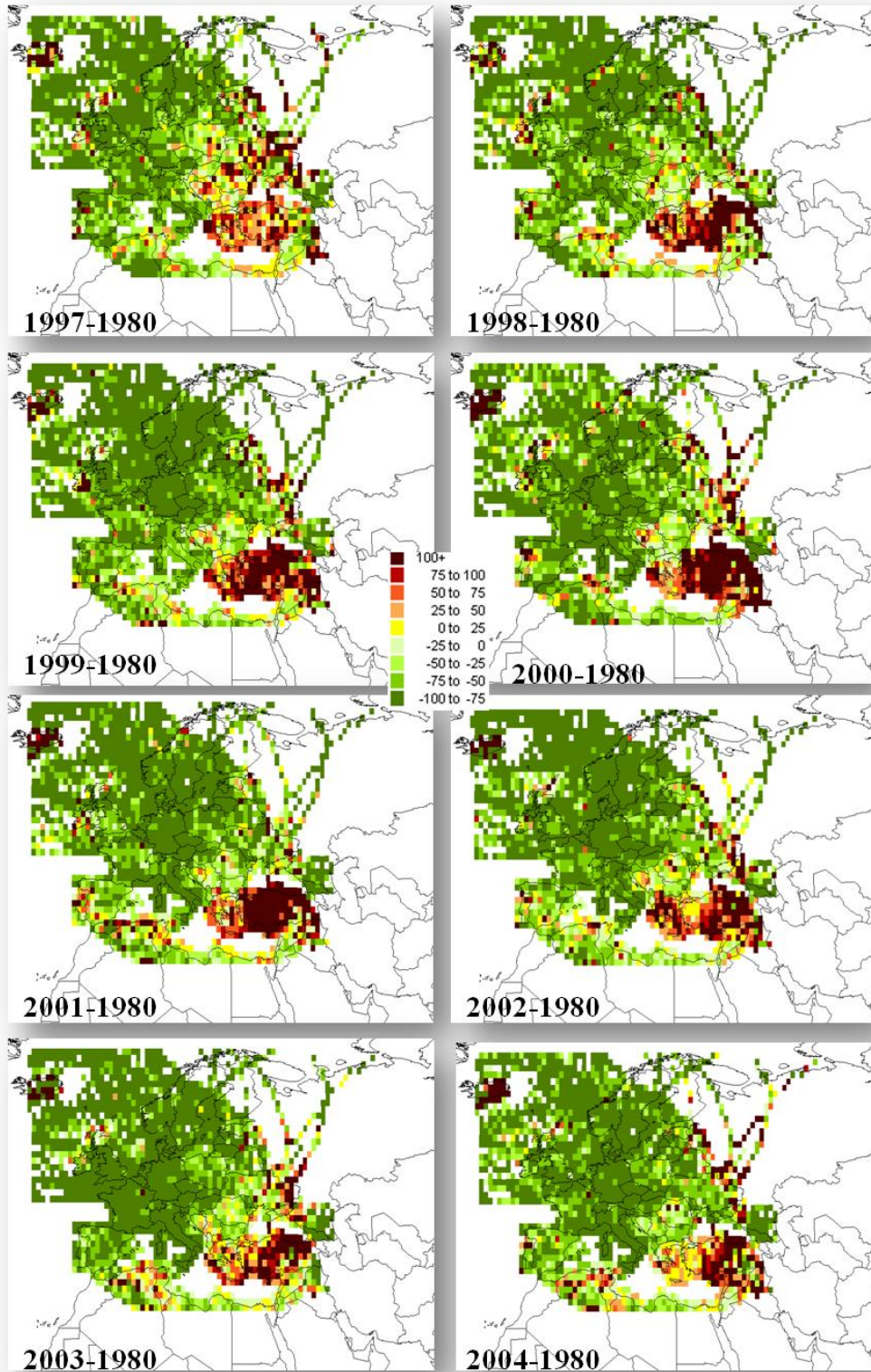


**Figure 4.24 (contd) Percent variation of RoI values calculated for Ashdod, Israel at each grid, relative to 1980 RoI's, between 1985 and 2010**

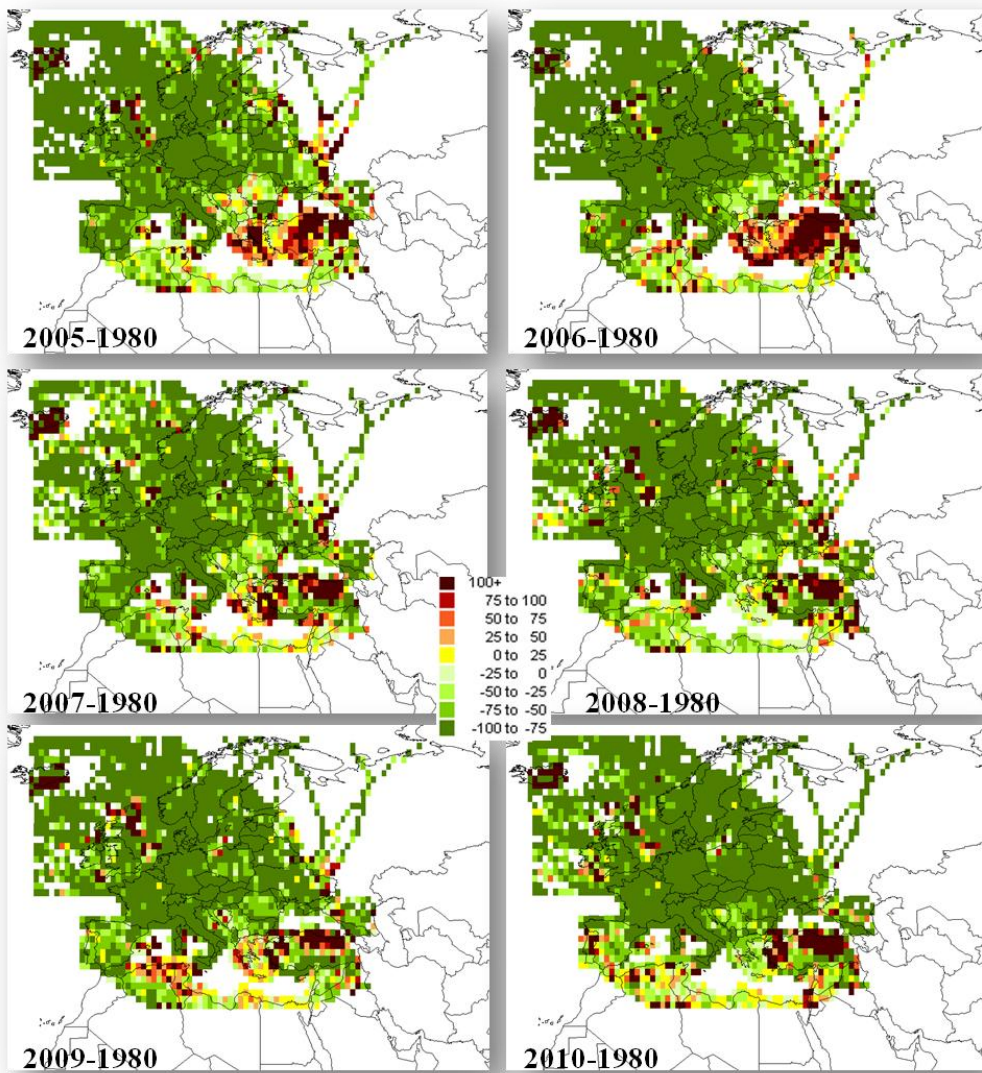


**Figure 4.24 (contd) Percent variation of RoI values calculated for Ashdod, Israel at each grid, relative to 1980 RoI's, between 1985 and 2010**

Until 1995, in Turkey, Russia and Ukraine RoI values increased relative to 1980 values. After 1995, the regions which have higher RoI values than 1980's values were reduced. After 2000, industrial region in Eastern Ukraine and region in Black Sea Coast of Russia and northeast of Turkey and north of Iraq were the only regions with increased RoI values relative to 1980. Finally, in 2010, the dominant regions in terms of increased RoI values were only northeast, west of Turkey and some small parts of Iraq. Therefore, Turkey has been an important source region for Ashdod. Also, there is an interesting result that grids with increased RoI values have decreased in Iceland especially from 2000.

In Figure 4.25, variation of average RoI value at each country, between 1980 and 2010, for Ashdod (Israel) is indicated. In 1980, it was seen that Western Europe slightly affect Ashdod and its effect have disappeared from 1985. From 1990, the most effective countries have identified as Greece, Bulgaria, Turkey, Syria, Jordan and Israel. Especially after 2000, their RoI values have started to reduce. Finally, in 2010, Ashdod station were mostly affected by Israel, it is an expected result, because the station was located there. Furthermore, the secondary important source regions were Greece, Turkey, Syria and Jordan.

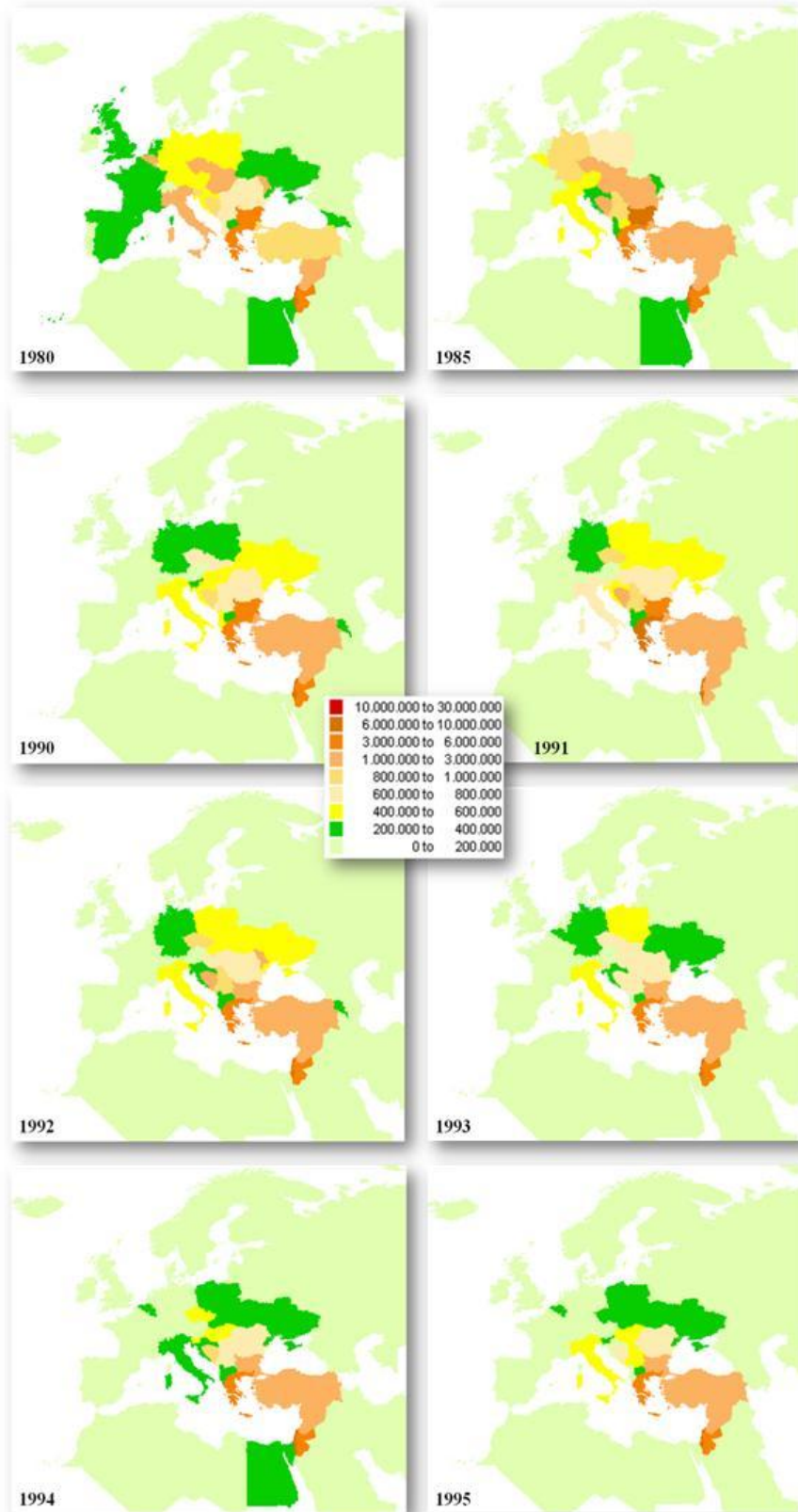


**Figure 4. 25 Variation of average RoI value at each country, between 1980 and 2010, for Ashdod, Israel**

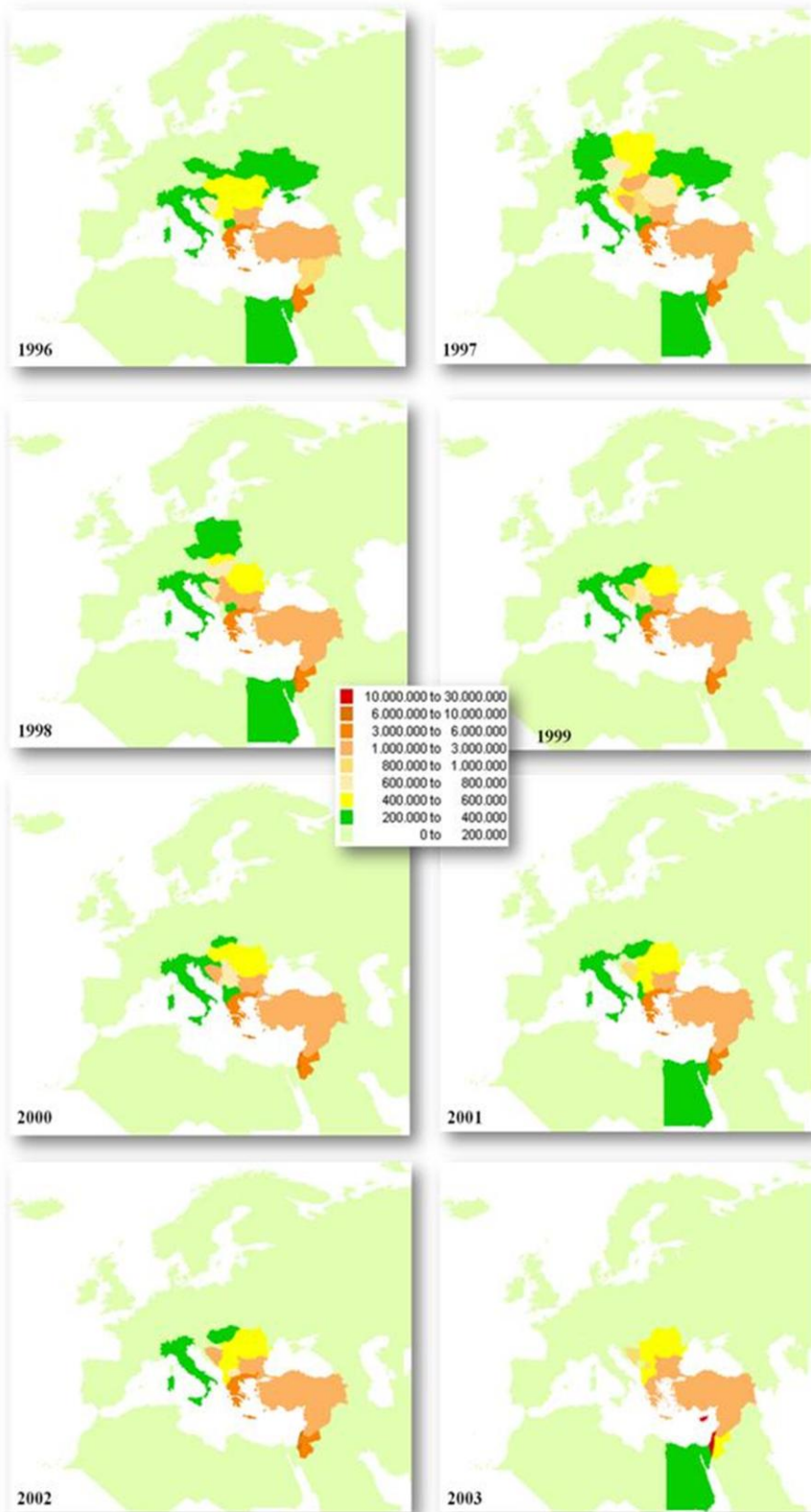


**Figure 4.25 (contd) Variation of average RoI value at each country, between 1980 and 2010, for Ashdod, Israel**

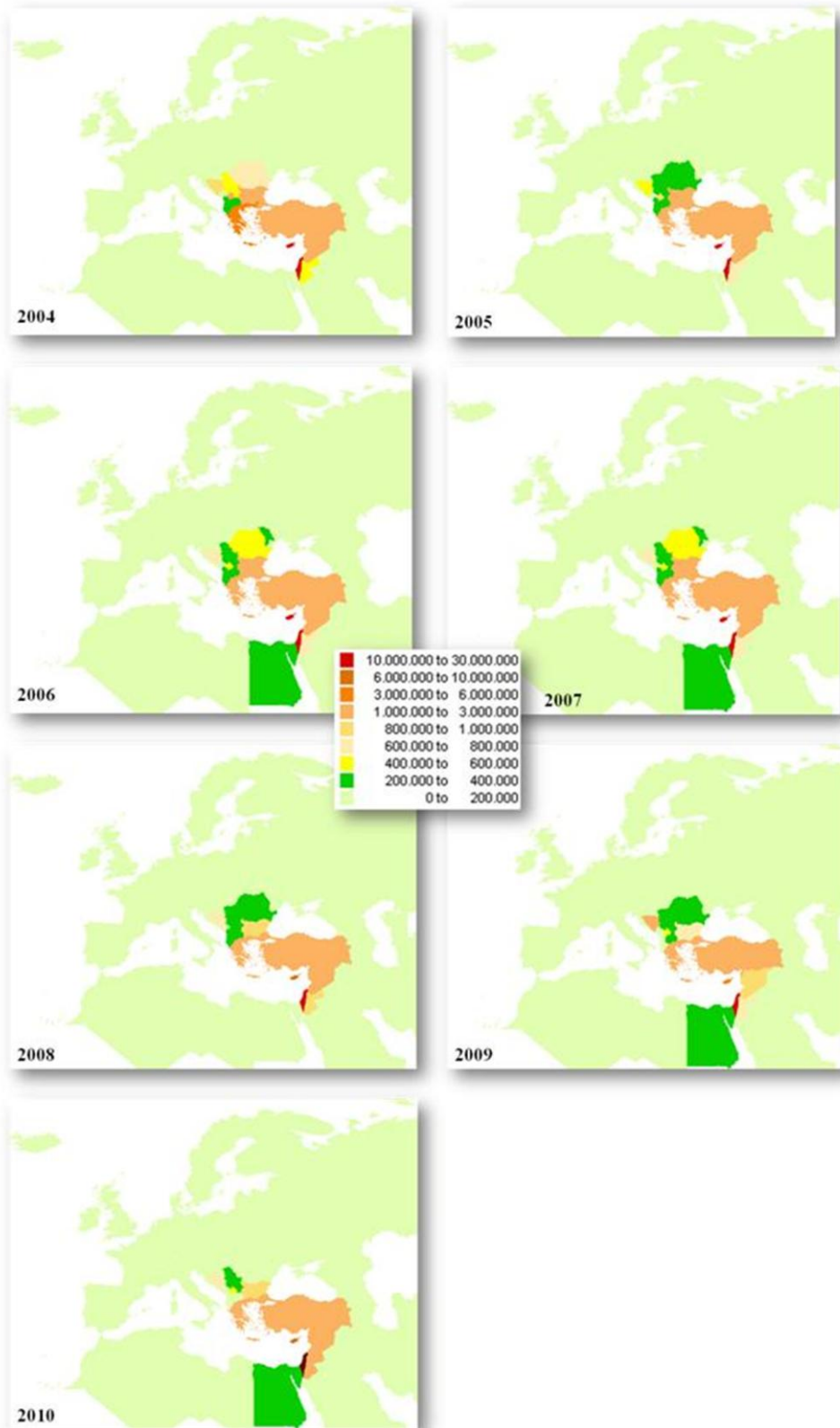


**Figure 4.25 (contd) Variation of average ROI value at each country, between 1980 and 2010, for Ashdod, Israel**

#### 4.3.1.4. At Western Mediterranean (Corsica, France) Station

Yearly change of RoI distribution between 1980 and 2010 for Corsica station is shown in Figure 4.26. The highest level of RoI values were seen in the year 1980 and the high RoI results centered in Western and Central Europe and north of Italy. Moreover, the grids located in southeast (Mediterranean Coast) of France and north of Sicily had high RoI results. The grids with high RoI values in Sicily implied the effect of Etna Volcano on Corsica. The RoI values have decreased from 1990. Although Germany and France were still source regions, their RoI levels reduced. Between 1995 and 2000, the source regions in Western Europe had being disappeared. In 2000, the  $\text{SO}_4^{2-}$  concentrations measured in Corsica were affected by regions close to selected point such as north of Italy, southeast of France. In Europe, some regions of Germany and south of Poland were the more effective regions than the other parts of Europe. The situation had being continued up to 2010. The very interesting point was that the industrial region in between Istanbul and Kocaeli was emerged as an important source region. This result is really terrible in terms of industrial regions of Turkey.

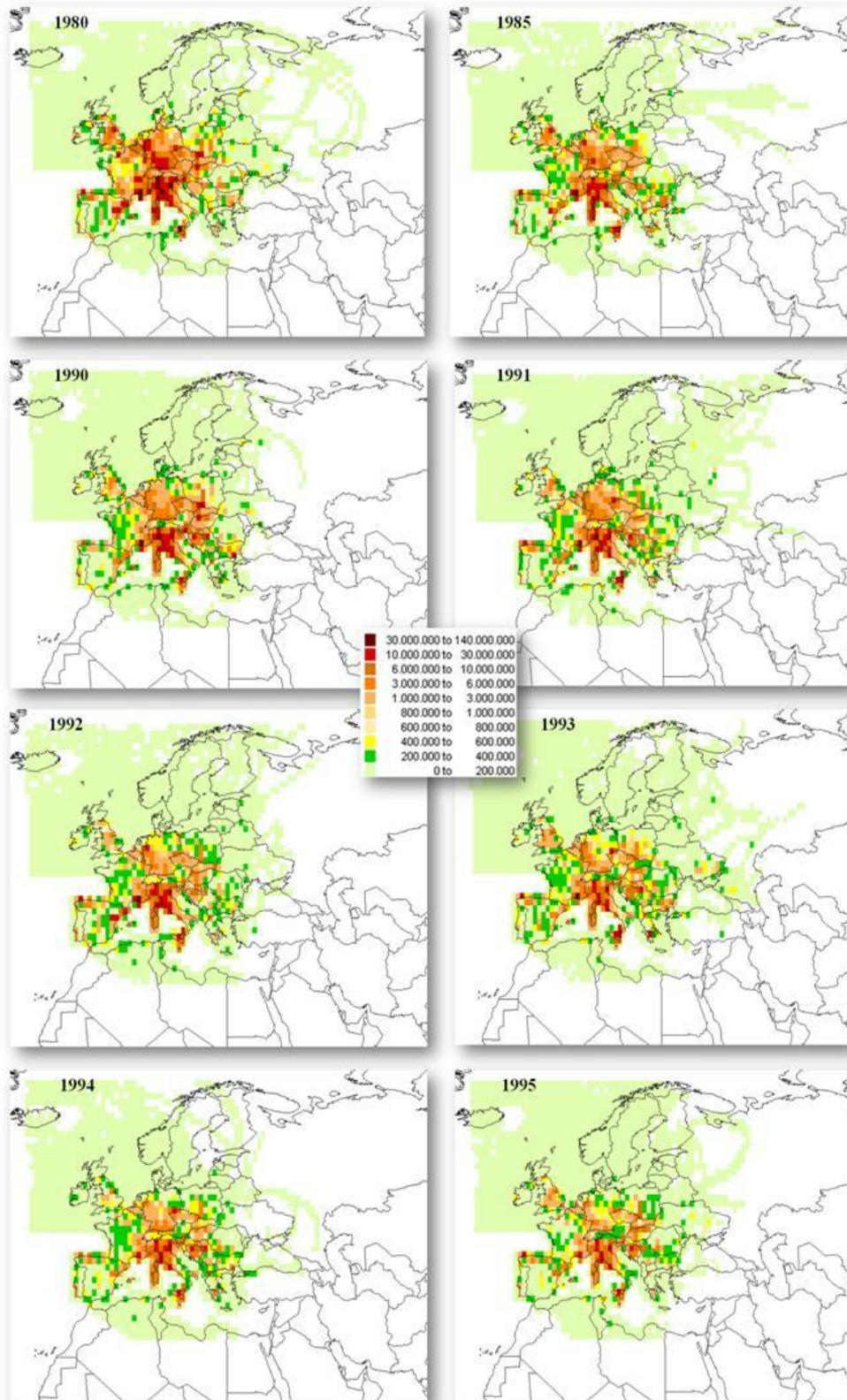


**Figure 4. 26 Yearly Change of RoI distribution between 1980 and 2010 calculated for Corsica Station**

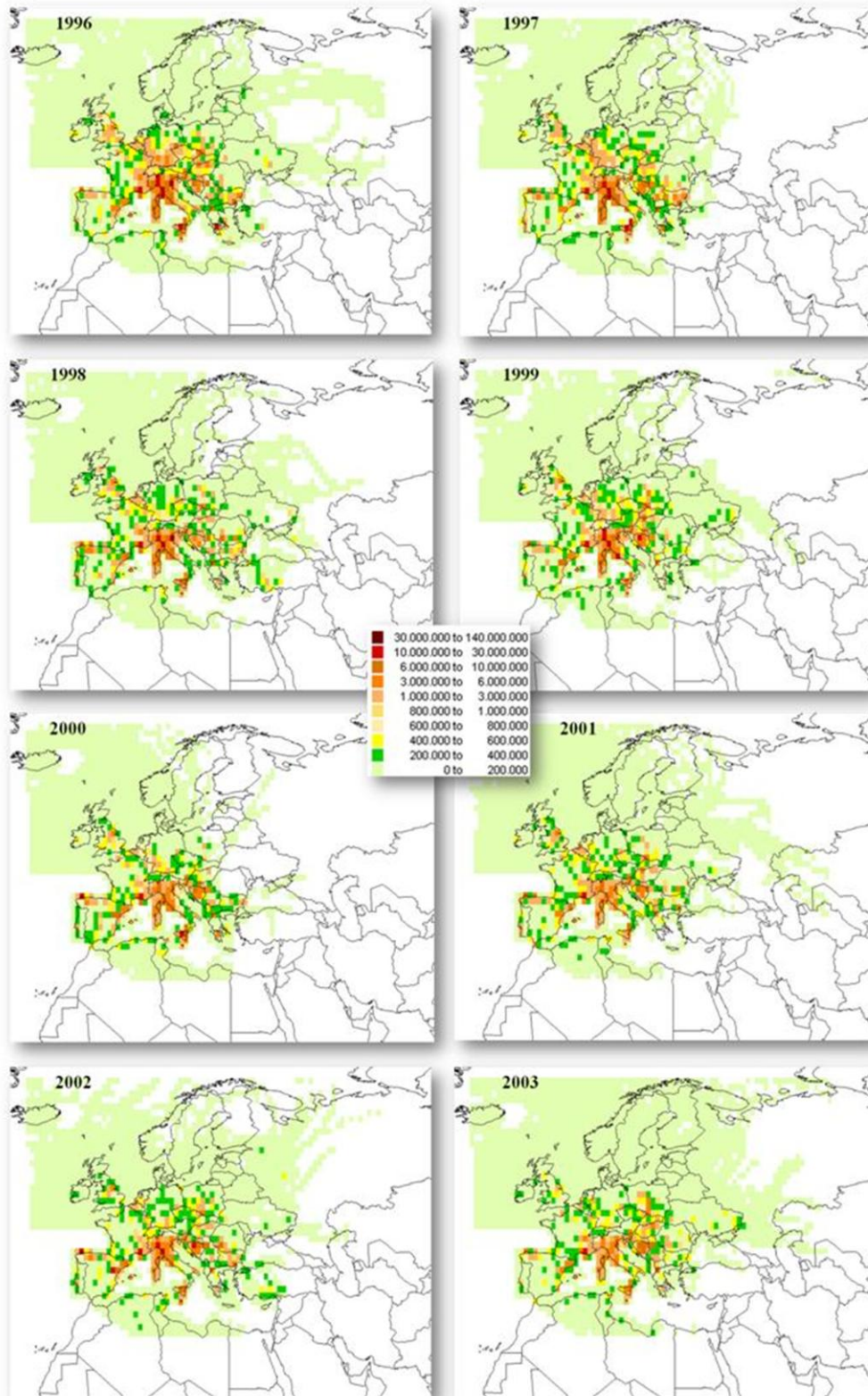


**Figure 4.26 (contd) Yearly Change of RoI distribution between 1980 and 2010 calculated for Corsica Station**

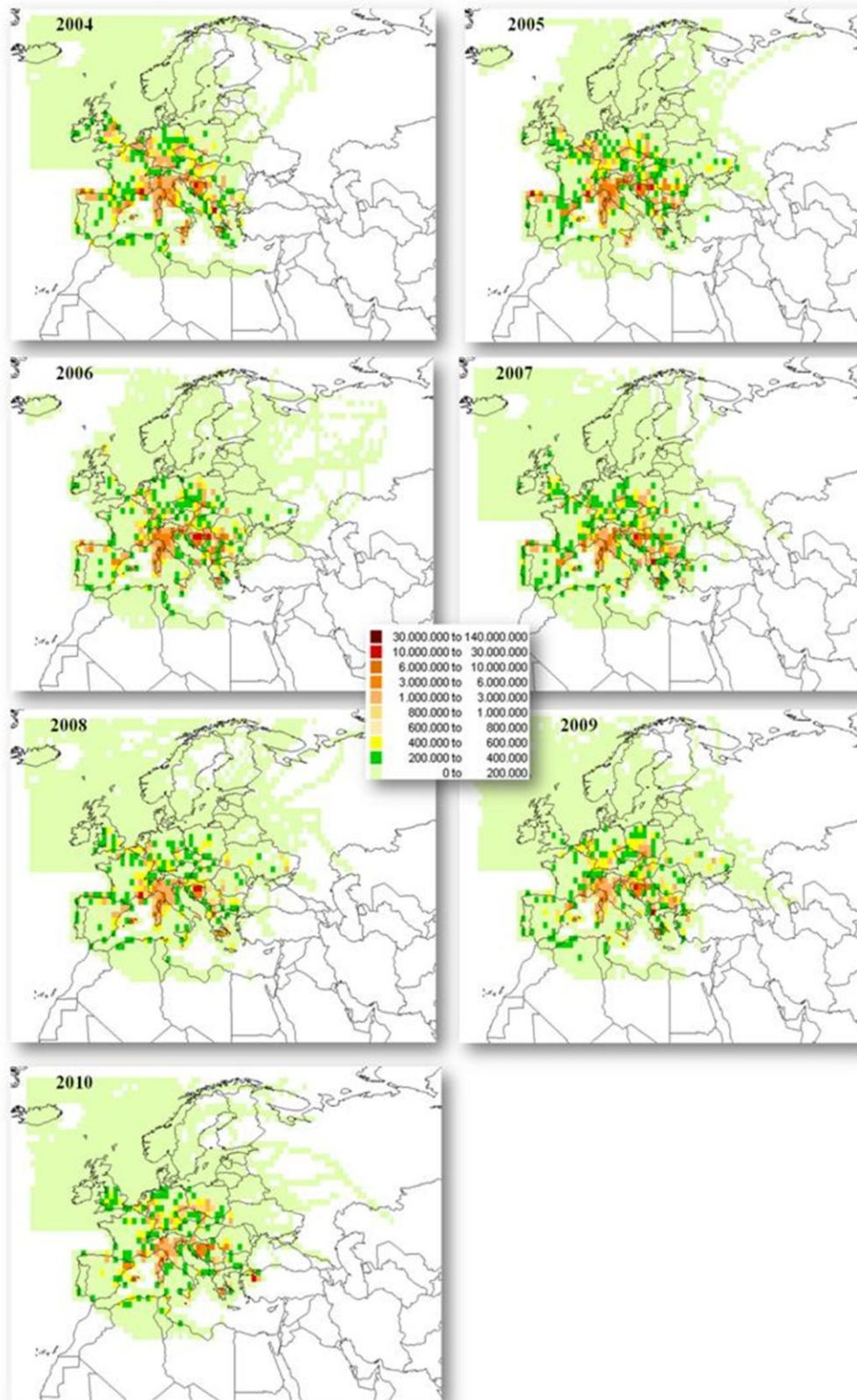


**Figure 4.26 (contd) Yearly Change of RoI distribution between 1980 and 2010 calculated for Corsica Station**

For the years from 1985 to 2010, percent variation of Corsica RoI values at each grid relative to 1980 RoI's is shown in Figure 4.27. The decreased RoI values in Western Europe had been observed from 1985. Figure 4.27 indicated the reduction especially in Germany and France. The dark green regions indicate the lowest RoI values relative to values of 1980, and Central and Western Europe had been observed from especially 1995. In other words, the RoI values in Europe had being decreased, but the distribution of Figure 4.26 did not show a reduction in these regions. Besides, the interesting point which was observed in Figure 4.26 could be seen in Figure 4.27. It was that the regions in west and northwest of Turkey (industrial regions in Istanbul-Kocaeli and İzmir) were observed as regions with higher RoI values relative to 1980. The effects of North Coast of Africa had not being changed significantly until 2010. As for the year 2010, the increased RoI values were identified in northwest of Turkey (Thrace Region), Bulgaria, Greece, Bosnia Herzegovina, and north coasts of Libya, Algeria, and Morocco.

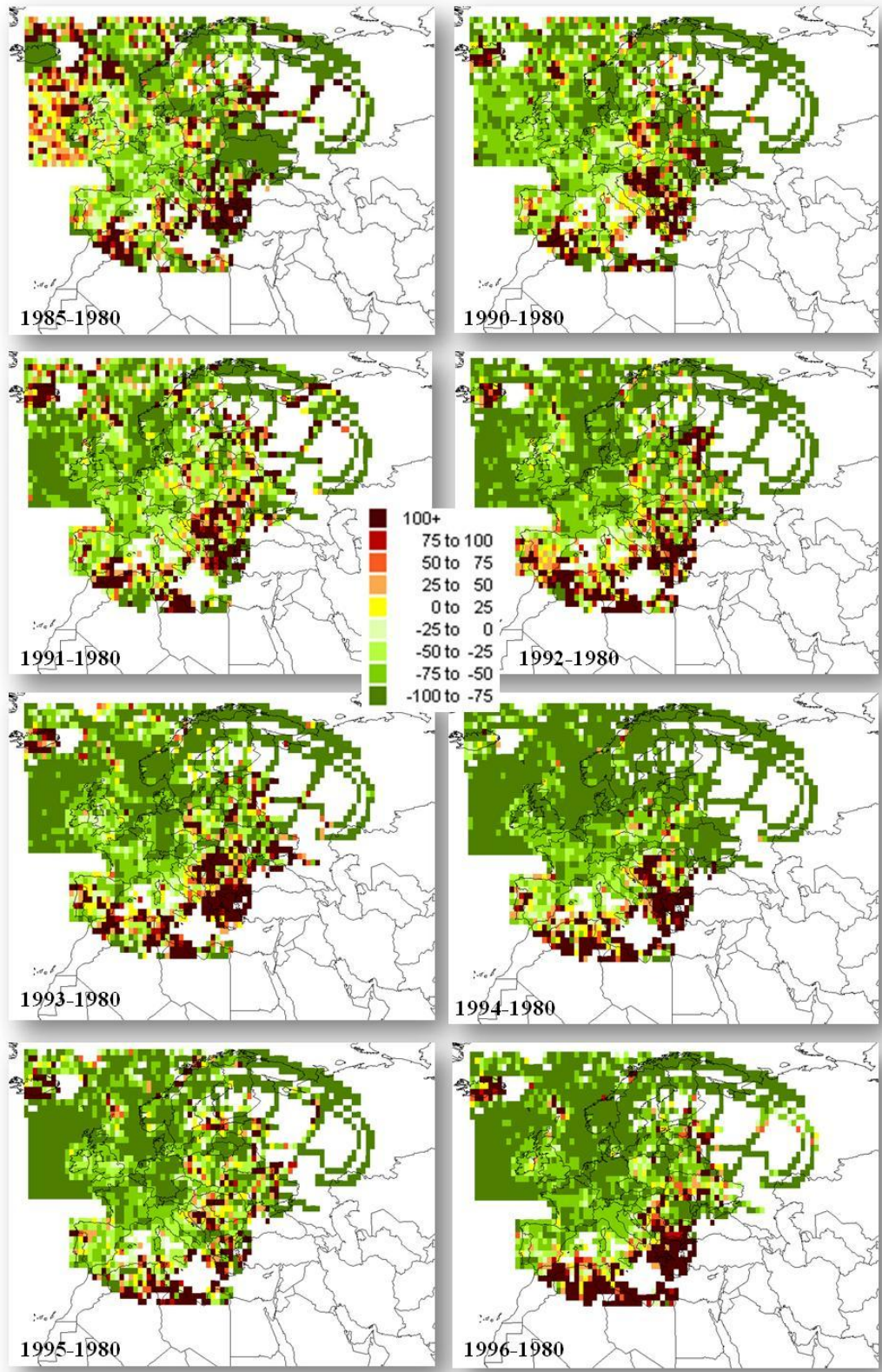


**Figure 4. 27 Percent variation of Corsica RoI values at each grid, relative to 1980 RoI's, between 1985 and 2010**

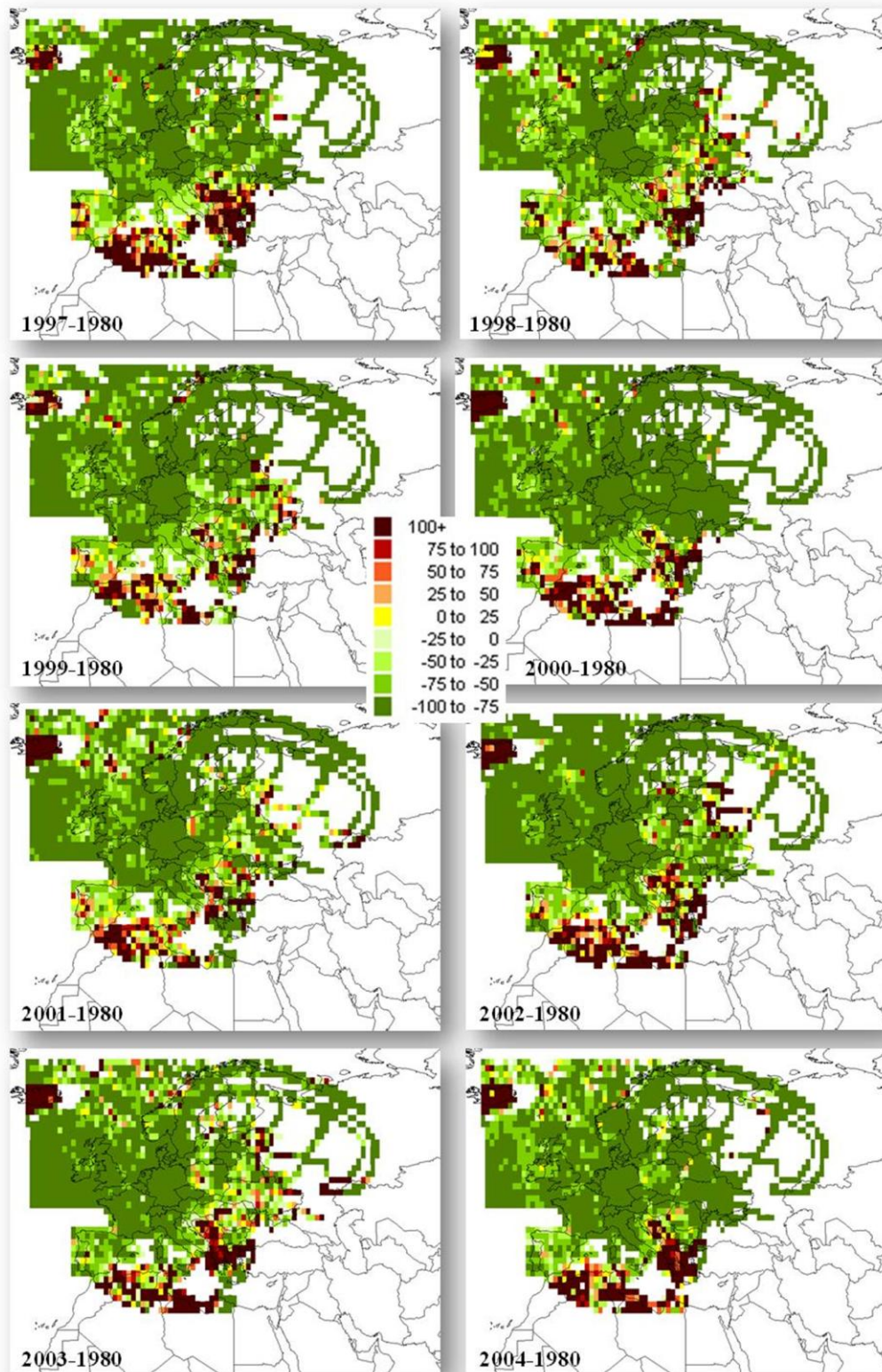
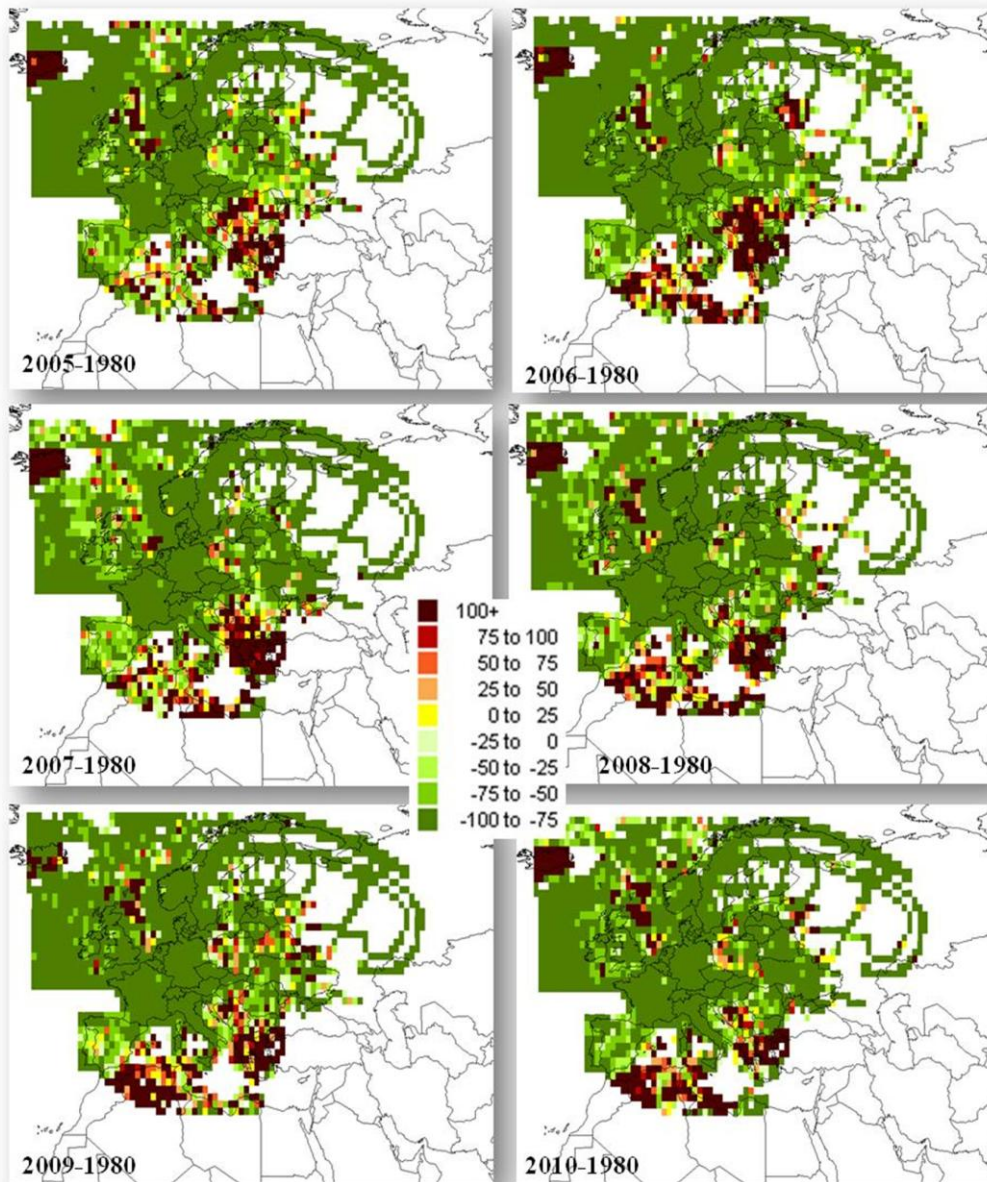
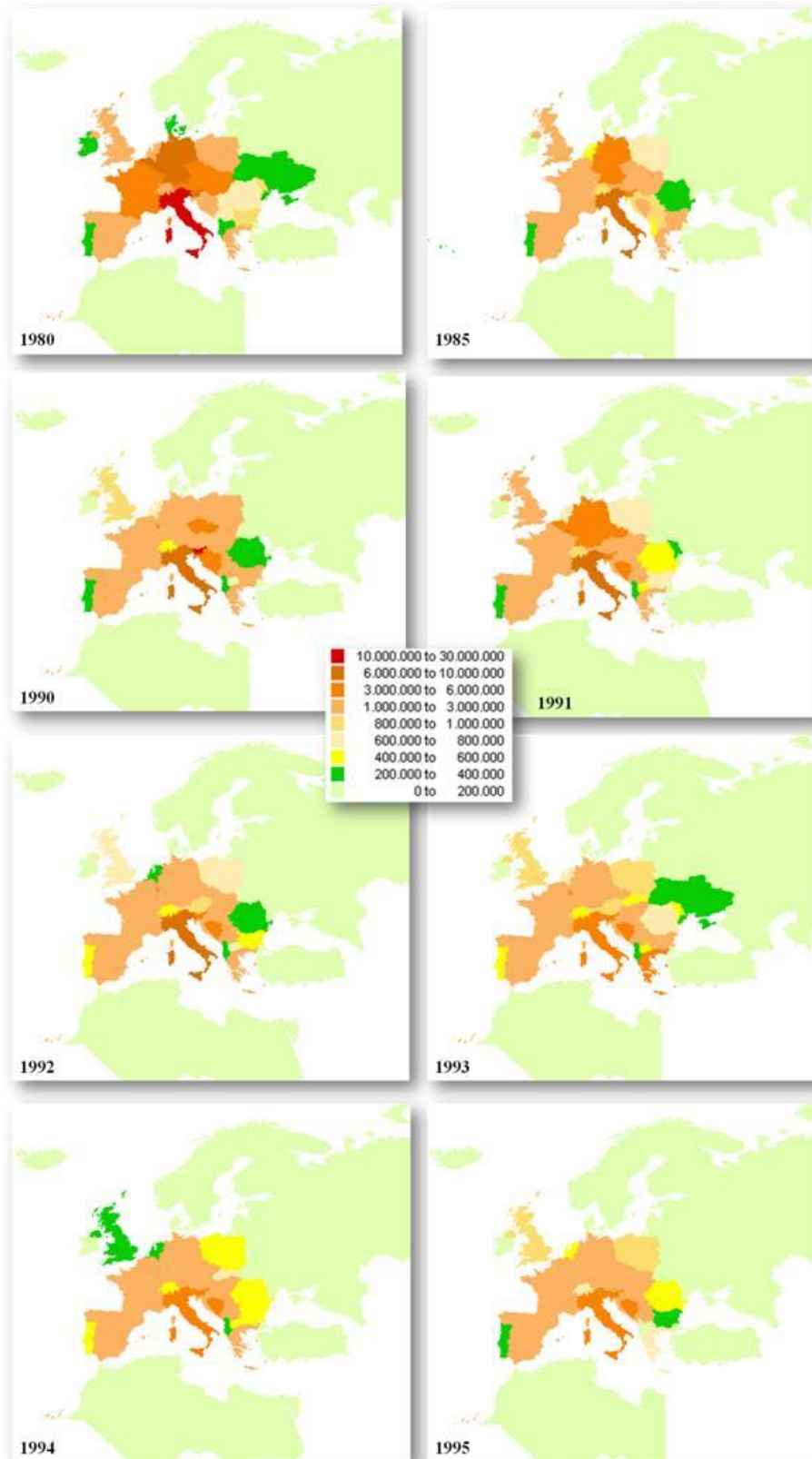


Figure 4.27 (contd) Percent variation of Corsica RoI values at each grid, relative to 1980 RoI's, between 1985 and 2010



**Figure 4.27 (contd) Percent variation of Corsica RoI values at each grid, relative to 1980 RoI's, between 1985 and 2010**

Variation of average RoI value at each country for Corsica station from 1980 to 2010 is shown in Figure 4.28. Fundamentally, change of RoI values of countries was not so different than yearly variation of RoI distribution shown in Figure 4.26.



**Figure 4. 28 Variation of average RoI value at each country, between 1980 and 2010, for Corsica Station**

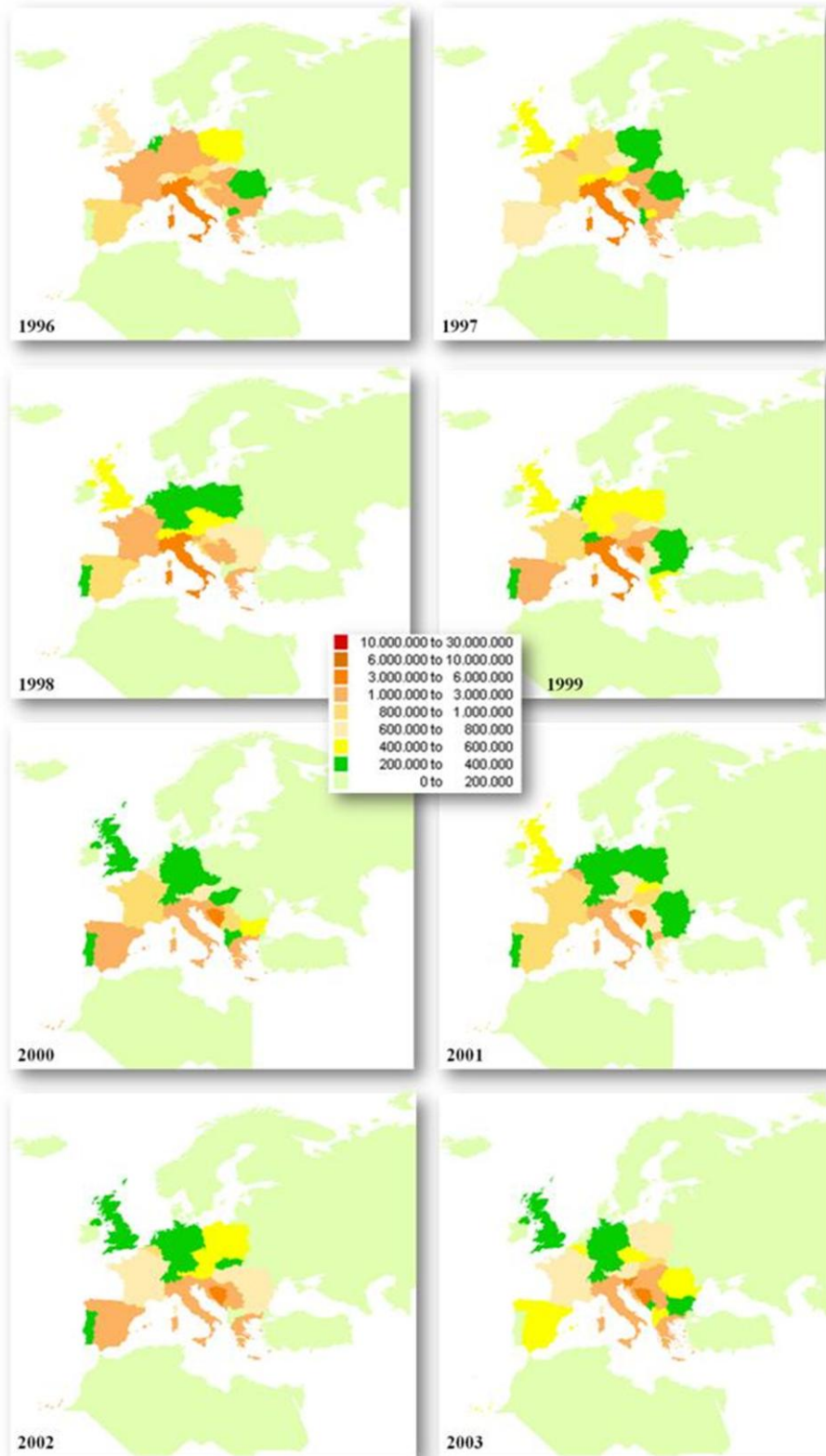


**Figure 4.28 (contd) Variation of average RoI value at each country, between 1980 and 2010, for Corsica Station**

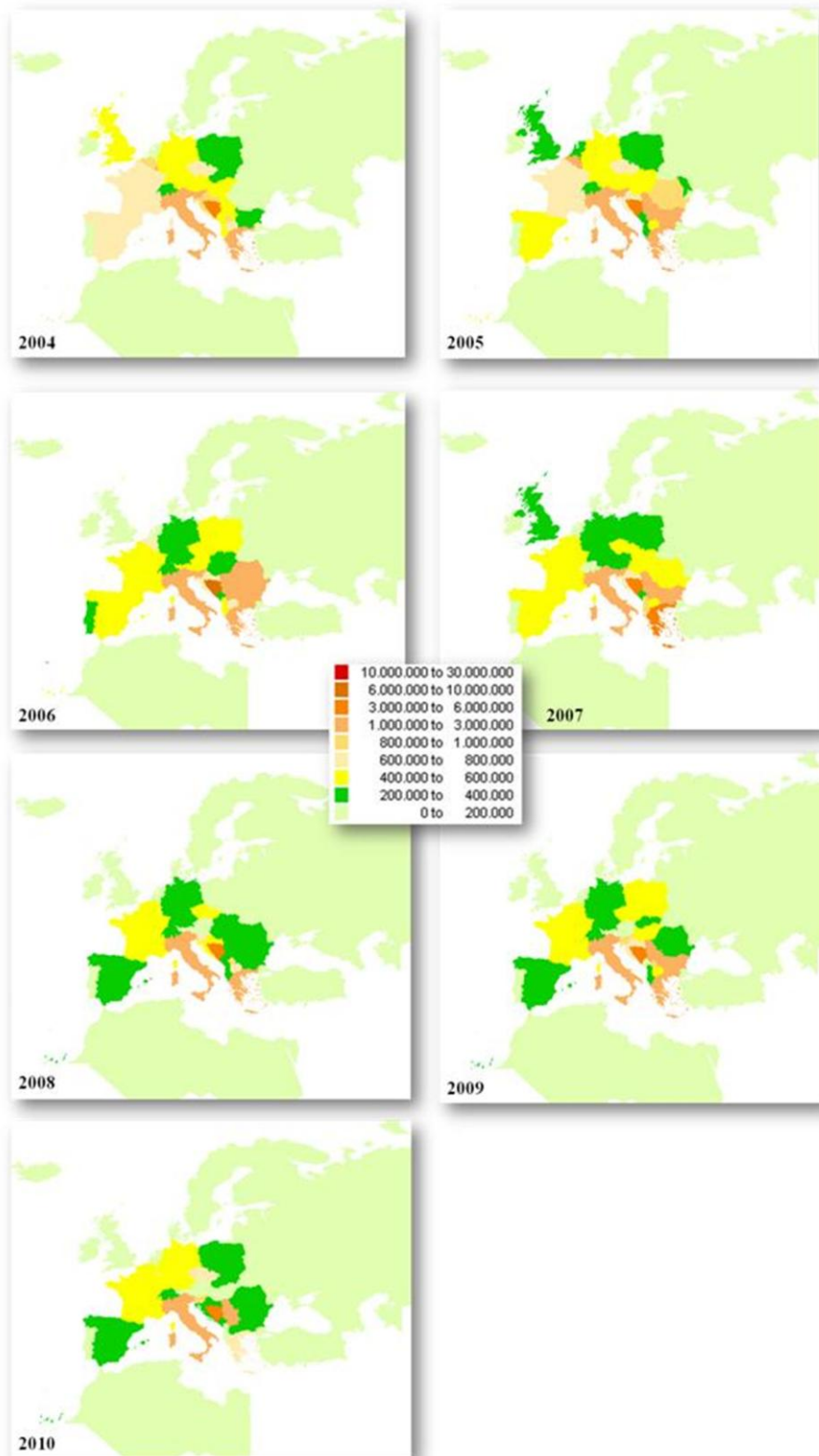


**Figure 4.28 (contd) Variation of average ROI value at each country, between 1980 and 2010, for Corsica Station**

Some of the Central and Western European Countries were the main countries which affect the sulfate concentrations in Corsica. The most effective source region was observed as Italy in 1980, because Corsica station is close to Italy. Probably, most of the trajectories were passing through Italy. The high RoI values of France, Germany, Poland, Czech Republic, Slovakia, Austria, Hungary, and Italy have decreased from 1985. After 1995, the RoI values of Western European Countries (especially England, France and Germany) have reduced over the years. In 2000, the primary countries which affect the sulfate concentration in Corsica station were Spain, Italy, Greece and Bosnia Herzegovina. In 2010, the effect of Central and Western European Countries were minimized and the most effective countries were only Italy and Bosnia Herzegovina. Of course, their RoI values also decreased compared to previous years.

#### **4.4. Comparison of the Results Obtained by PSCF and RoI Approaches**

Both PSCF and RoI approaches generated consistent results in themselves, as discussed in Section 4.2 and 4.3 of this manuscript. However, similarities and differences between the results generated with these two approaches were not compared so far. In this section, results obtained with PSCF and RoI are compared.

For comparison, both PSCF values and RoI values were calculated using Antalya and Çubuk data sets with 2-yr intervals between 1993 and 2000 for Antalya and between 1993 and 2006 at Çubuk. Distributions of PSCF and RoI values in the study domain are given in Figure 4.29 for Antalya and in Figure 4.30 for Çubuk stations. Years covered in the two regions are different due to different data coverage at Antalya and Çubuk stations. Although RoI is independent of data, PSCF does depend on it.

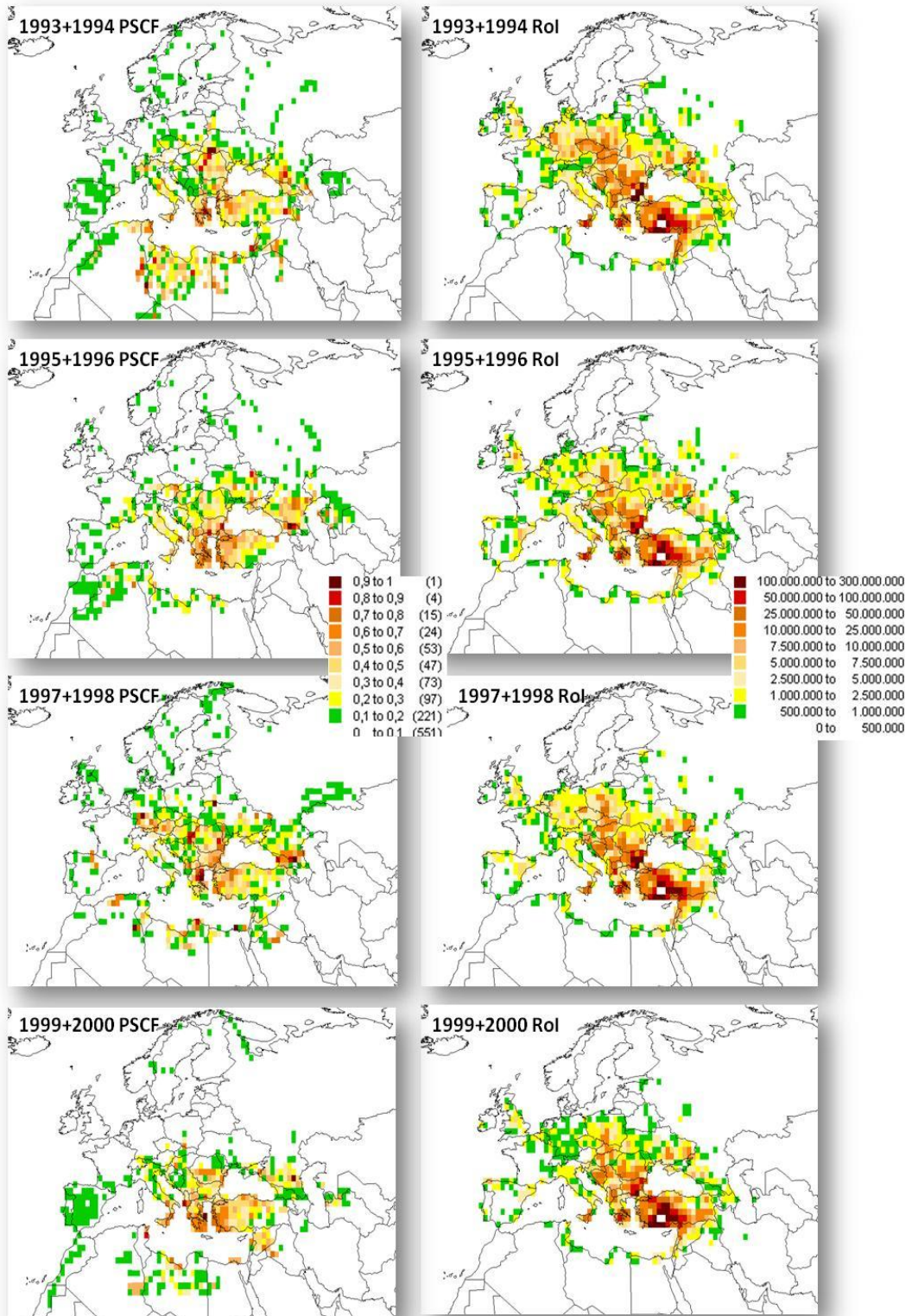


**Figure 4. 29 Comparison of PSCF and RoI results as a two years period from 1993 to 2000 at Antalya Station**

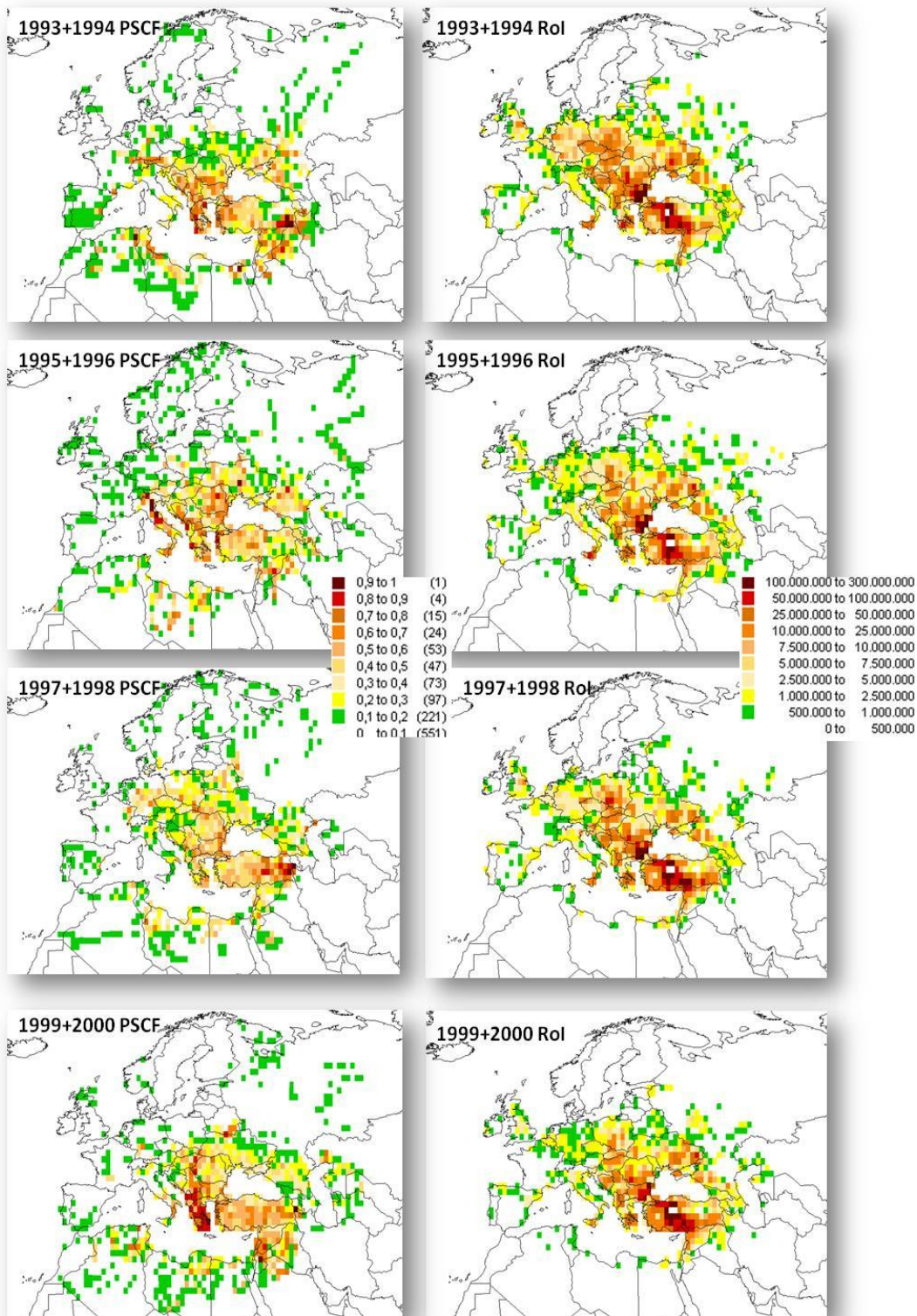


**Figure 4. 30 Comparison of PSCF and RoI results as a two years period from 1993 to 2006 at Çubuk Station**

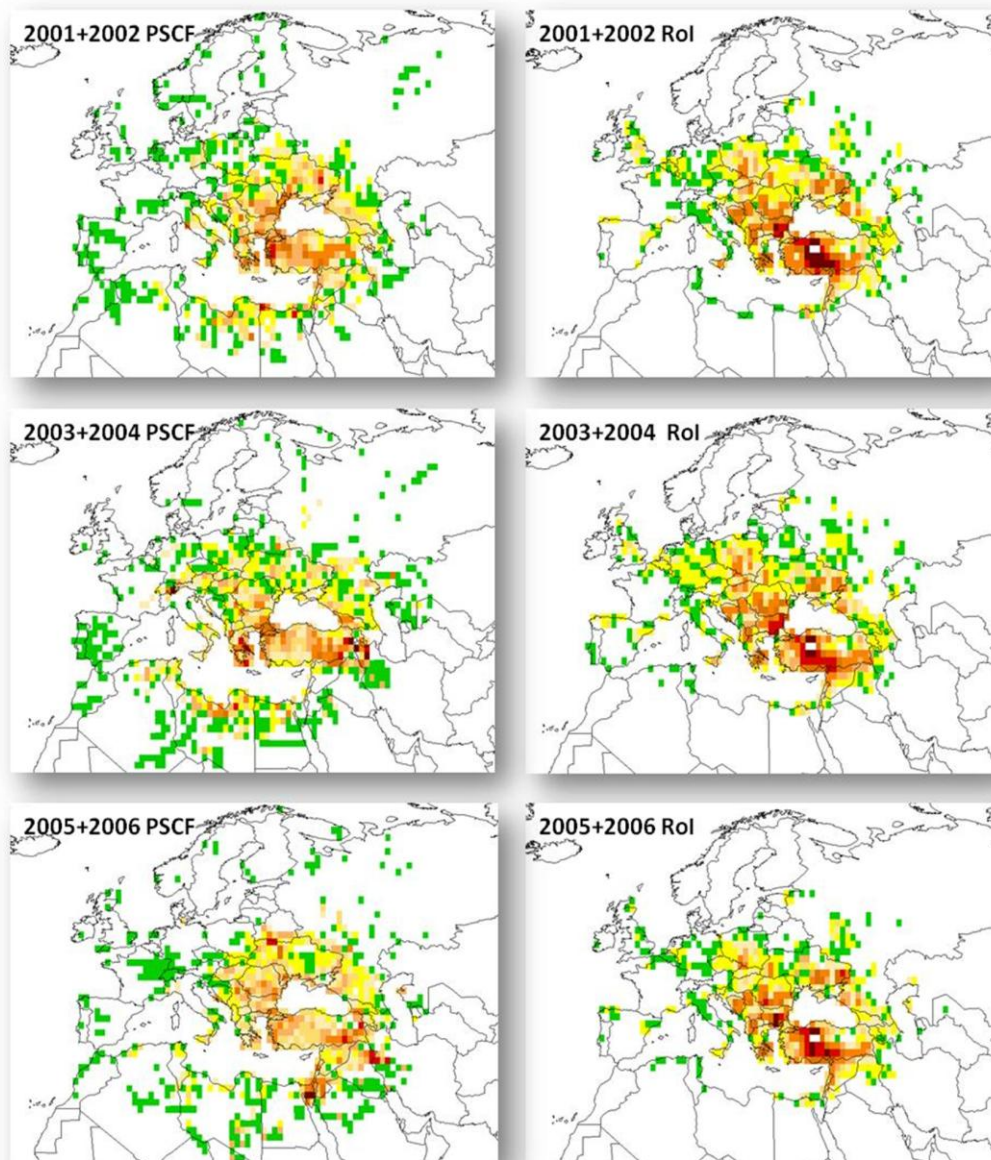


**Figure 4.30 (contd) Comparison of PSCF and RoI results as a two years period from 1993 to 2006 at Çubuk Station**

In Figure 4.29 and 4.30 one may be misled by the coloring. Although we attempted to make coloring similar in PSCF and RoI approaches, different parameters are plotted in the figures and borders between colors may not imply the same thing in PSCF and RoI figures. Consequently, one has to concentrate on the source regions identified by the two methods and how these source regions change in time, instead of comparing colors in PSCF and RoI distributions.

There are similarities and differences in both general appearance of distributions and in specific source regions identified by both methods. In terms of general patterns created by PSCF and RoI calculations, RoI identifies more distant regions, such as Germany, France as weak source regions, whereas these regions were not recognized as potential source areas in PSCF calculations. In more recent years, namely in distribution prepared for years 1999+2000 at Antalya and 2005 and 2006 for Çubuk general appearance of distributions becomes more similar, because emissions in distant source areas like Germany is reduced significantly and these regions ceased to be source regions in RoI distributions as well.

The difference between general appearances of the two distributions can be either due to effect of rain or it can be an artifact in coloring distributions. Rain is one of the parameters that can increase uncertainties in both RoI and PSCF calculations. Rain scavenge particles from atmosphere, consequently once a trajectory goes through rain, it may left the rain event as a clean air mass even if it was coming from a much polluted region. Please note that probability of a trajectory to go through a rain event increase with distance, which means that air masses coming from distant source regions like Germany, UK, France are more likely to be cleaned up by rain scavenging, than air massed that carry pollutants from nearby sources, such as parts of Turkey and Balkan countries.

In the beginning of this thesis one of our objectives was to weight the trajectory segments based on the rain they encounter in each grid, exactly as we did for altitude. Although grid based rain information was available in the output of the trajectory model used in this study, we gave up the idea because we could not figure out how to handle the rain event. For example we found the following questions difficult to answer:

How much of the particles are scavenged out when air mass goes through a rain event. We know it is a large fraction, but what percentage? It may as well be size dependent. What happens if an air mass does not go through a rain event but goes through a cloud, would some of the particles be captured by cloud droplets? Because

of these and other questions like these we abandoned the idea of weighting segments with rainfall they experienced in each grid.

Neither RoI nor PSCF calculations include rain weighting, but PSCF intrinsically include rain weighting in it. Since trajectory segments are counted separately for clean and polluted trajectories separately and since these counts are dictated by  $\text{SO}_4^{2-}$  concentration in the data set, if a trajectory comes from a strong emission grid after passing through rain one or more time,  $\text{SO}_4^{2-}$  concentration in it may be low when it is intercepted at our station. This results in reduced PSCF value in that particular grid. Since trajectories carrying  $\text{SO}_4^{2-}$  from distant sources (in Germany, France, UK etc) are more prone to cleanup by rain that air masses carrying pollutants from more local sources, outskirts of our study domain appears as lighter source areas then they actually are in PSCF calculations. However, rain is by no means included in RoI calculations. This may be one of the reasons of difference in general appearance of the two distributions.

The difference can also be due to coloring the distributions. If we increase the border between white and green and green and yellow to smaller PSCF values some parts of the regions that appear as white low may turn into light yellow. Similarly if increase the limit values that separate white green and light yellow to higher RoI values, some of the distant source areas that are light yellow in the figure would be white.

Source areas identified from PSCF and RoI distributions are also compared to test the consistency of the approaches. Similar source areas are generally identified by both techniques, but there are also source areas specific to one of these methods. Common source areas found by both PSCF and RoI distributions include West and Northwest of Turkey, Balkan countries Bulgaria and Romania, Ukraine Greece and Italy. Israel coast in the Middle East, and south eastern part of Turkey found as potential source region by both techniques.

In addition to these source regions, which were common in both techniques, the RoI approach identified a very strong source area in the central Turkey, which is not seen

in PSCF distributions. This is true for both Antalya and Çubuk studies and observed in every time interval these calculations were performed. We do not exactly know why this region does not appear in PSCF calculations, but one plausible explanation is aggravation of small emissions in the vicinity of receptor site due to very large number of segments in those grids (all trajectories has to pass through those grids before they are intercepted in the station). Exclusion of few grids around the stations or down-weighting RoI values calculated for those grids can be a solution for the observed artifact.

Although Italy did not come out as a strong source region in PSCF and RoI distributions, Sicily appeared as a moderate source area in with both techniques in all time periods. We know that appearance of Sicily as a  $\text{SO}_4^{2-}$  source region in RoI is due to Mt Etna volcano and occasional transport of emissions to our stations. Identification of this specific point source in RoI distributions is not surprising. Identification of that point source in PSCF distributions, on the other hand, increases our confidence in PSCF calculations. Mt Etna appears to be stronger source for Antalya regions then it is for Çubuk. This is probably due to closer proximity of Antalya to Sicily.

One other interesting feature in this comparison is the source regions found in PSCF distributions in North Africa. Transport of pollution from North Africa to Eastern and Western Mediterranean basin had been noted in numerous studies (Kallos et al., 1998; 2007). Most of these based on observed high concentrations of pollution-derived parameters associated with trajectories originating from North Africa. There is no clear explanation for this phenomenon. Some tried to explain it by transport of pollutants from cities in North Africa, some attempts to explain it by recirculation of air masses coming from Europe (Kallos et al., 1998). It was also reported in earlier studies in our group that approximately 30% of trajectories originating from North Africa carried high concentrations of  $\text{SO}_4^{2-}$  and other pollution derived elements to our station on the Mediterranean coast (Öztürk et al., 2012; Doğan et al., 2010). Discussion on reasons for this common observation is beyond the scope of this manuscript. However, PSCF picked up this pollution transport and identified, or

maybe generated, source regions at North Africa affecting both Antalya and Çubuk stations. Likelihood of these source regions to be a transport artifact is high because none of them appeared in RoI distributions.

As a summary we can say that the agreement between general appearances of PSCF and RoI distributions and potential source areas identified by both techniques were remarkably good considering very different natures of the two approaches.



## CHAPTER 5

### CONCLUSION

Sulfate is an important pollutant in the Eastern Mediterranean region, because its concentration measured in this region is among the highest concentration or maybe the highest concentration measured in the world. Although  $\text{SO}_4^{2-}$  concentrations measured in whole Europe decreased as much as 70%, concentrations measured in the Eastern Mediterranean remained more or less the same since early 90's.

In this study, source regions affecting Mediterranean region was investigated using a conventional receptor-oriented trajectory statistics and a new statistical tool which can be described as source oriented trajectory statistics. It is named as "region of influence" (RoI). Both location of  $\text{SO}_4^{2-}$  source regions affecting Mediterranean region and variation of these source regions in time were discussed.

One methodological novelty of this study is the use of altitude weighting in both PSCF and RoI calculations. Since probability of high altitude segments to pick up pollutants from surface sources is smaller than the probability of low lying air masses to pick up pollutants, we weighted contribution of trajectory segments to pollution transport depending on their altitudes from surface. Several weighting scheme was investigated. In the selected weighting scheme in every grid cell number of trajectories that has altitude < 500 m is multiplied by 1.0, segments with altitudes between 500 m and 1000 m were multiplied by 0.3 and number of segments with altitudes < 1000 m were multiplied by 0.1. This weighting scheme was used in both PSCF and RoI calculations.

PSCF was applied to Antalya and Çubuk stations where  $\text{SO}_4^{2-}$  data were available. In Antalya station variation of source regions between 1993 and 2000 and in Çubuk station between 1993 and 2006 were discussed. Time intervals were determined by availability of measurement results.

There are number of common features in both PSCF results. Contribution of Western Europe as source regions affecting Antalya and Çubuk stations were small even in 1980, and their contribution disappeared entirely after 1995. Balkan countries, particularly Greece, Bulgaria and Romania, Western Parts of Turkey, Eastern parts of Ukraine and a region at the Georgia-Russian Federation border are the common regions affecting  $\text{SO}_4^{2-}$  levels at both stations. In addition to these common sources there were also some regions affecting Antalya and Çubuk stations separately.

The distributions of average PSCF results in terms of regions were summarized in Table 5.1. The similar comments can also be seen by looking the values. For example, Turkey and Balkans has higher PSCF results compared to European countries.

**Table 5. 1 Variation of average PSCF results of regions during the study period**

<b>ANTALYA PSCF</b>	<b>1993+1994</b>	<b>1995+1996</b>	<b>1997+1998</b>	<b>1999+2000</b>			
Turkey	0.326	0.278	0.324	0.342			
Balkans	0.268	0.332	0.355	0.356			
Eastern Europe	0.164	0.131	0.255	0.113			
Western Europe	0.092	0.071	0.092	0.066			
Middle East	0.245	0	0.165	0.151			
Russia & Ukraine	0.115	0.133	0.213	0.067			
North Africa	0.090	0.031	0.041	0.037			
<b>ÇUBUK PSCF</b>	<b>1993+1994</b>	<b>1995+1996</b>	<b>1997+1998</b>	<b>1999+2000</b>	<b>2001+2002</b>	<b>2003+2004</b>	<b>2005+2006</b>
Turkey	0.418	0.399	0.513	0.508	0.494	0.496	0.467
Balkans	0.488	0.471	0.364	0.490	0.343	0.329	0.312
Eastern Europe	0.192	0.226	0.273	0.228	0.160	0.270	0.176
Western Europe	0.115	0.112	0.104	0.082	0.088	0.131	0.078
Middle East	0.332	0.203	0.351	0.544	0.296	0.160	0.497
Russia & Ukraine	0.214	0.249	0.214	0.161	0.277	0.234	0.286
North Africa	0.057	0.043	0.053	0.069	0.058	0.081	0.070

Also there is not an effective reduction in Turkey and Balkans as much as in European Countries. Reduction in PSCF values of 1999-2000 for Eastern Europe, Russia and Ukraine may show the positive effect of second S-protocol in 1998. However, it is seen that the reduction did not continue because of insufficient enforcements and reduction control mechanisms on SO<sub>2</sub> emissions. The minimal effect of North Africa can be seen with small PSCF values. Because of almost no industrial activities in this region, most probably the small effect comes from natural sources.

Development of a source oriented trajectory statistical method was necessary, because receptor oriented trajectory statistical methods all rely on the availability of measurement results. Measurement data is not available everywhere in the basin and whenever it is available data sets are not long enough to study variation of source regions in time. The RoI was developed to overcome dependence of source region apportionment on measurement results. The method was used for SO<sub>4</sub><sup>2-</sup> in this study, but it can be used for any pollutant. RoI was applied to four locations in Turkey (Antalya and Çubuk), a site on Israeli coast (Ashdod) and a site at the Western Mediterranean (Corsica). For all these sites RoI calculations were performed between 1980 and 2010. Altitude weighting was performed in all RoI calculations. Any rain weighting factor was not applied in both RoI and PSCF calculations.

RoI calculations revealed interesting points. There is a systematic distribution of source regions affecting Eastern Mediterranean, which is dictated by the upper atmospheric flow patterns of air masses. These source regions were generally located in NW wind sector relative to Turkey. This pattern is valid not only for locations in Turkey, but also for other locations in Eastern Mediterranean, such as Ashdod. The pattern is particularly valid between 1980 and 1995, when SO<sub>2</sub> emissions were high in all countries in Europe. After 1995 emissions decreased in Western Europe but remained high in Eastern European countries. With changes in emissions, dominance of flow pattern in determining source regions is terminated. Also, variation of average RoI results of regions from 1980 to 2010 was given in Table 5.2.

**Table 5. 2 Variation of average RoI results of regions during the study period**

<b>ANTALYA RoI (x1000)Mg</b>	<b>1980</b>	<b>1985</b>	<b>1990</b>	<b>1991+1992</b>	<b>1993+1994</b>	<b>1995+1996</b>	<b>1997+1998</b>	<b>1999+2000</b>	<b>2001+2002</b>	<b>2003+2004</b>	<b>2005+2006</b>	<b>2007+2008</b>	<b>2009+2010</b>
Turkey	2066.6	3682.4	3895.7	3458.3	3541.9	3610.8	4174.8	5397.1	6285.3	3863	3516.8	3348.4	3609.6
Balkans	2363.8	2877.6	2328.8	1768.3	2082	1489.8	1972.7	1507.2	1735.1	1217.4	1106.2	1020	687.1
Eastern Europe	2065.7	1763.5	967.4	1066.5	997.8	462.5	678.8	380.6	376	288.3	193.9	161.7	121.7
Western Europe	629.3	509.8	217.4	215.6	255.8	180.9	171.8	91.1	103.9	70.8	53.4	45.2	34.2
Middle East	624.5	423.8	353.7	377.9	725	310.8	624.4	421.5	526.5	553.2	407.1	291.5	972.8
Russia & Ukraine	494.8	285	595.1	592.1	331.4	262	217.7	128.2	123.6	178.1	193	140.1	119.1
North Africa	16.5	11.6	5.7	7.8	14.7	12.1	13.6	7.5	14.9	14	12.4	12	22.7
<b>ÇUBUK RoI (x1000)Mg</b>	<b>1980</b>	<b>1985</b>	<b>1990</b>	<b>1991+1992</b>	<b>1993+1994</b>	<b>1995+1996</b>	<b>1997+1998</b>	<b>1999+2000</b>	<b>2001+2002</b>	<b>2003+2004</b>	<b>2005+2006</b>	<b>2007+2008</b>	<b>2009+2010</b>
Turkey	2889.5	3966.9	3861.4	4930.6	4050.3	3926.2	5456.4	5729.6	5844.6	3846.7	4289.7	3532.3	4350.2
Balkans	3065.4	2820.6	2350.3	2573.4	2303.2	1613.8	1848.5	1346.1	1361.2	1195.7	1150.7	1137.2	710.1
Eastern Europe	2954.9	2946.3	2096.8	1868.9	1315	624.9	1035.1	479.5	378.8	424.6	233.1	222.3	145.9
Western Europe	656.4	482	488.9	331.8	281.1	170.1	180.6	89.1	74.3	82.5	43.0	54	31
Middle East	422.7	480.9	151.4	369.8	597.3	353.6	563.6	427.8	458.2	496.2	441.2	216.9	890
Russia & Ukraine	1257.4	659.3	1227.2	1332.1	611	439.7	311.3	290.5	223.9	302	314.6	295.7	253.2
North Africa	20.2	22.5	5.1	5.9	7.5	14.2	11.8	6.1	11.7	12.9	8.9	5.3	18.6

**Table 5. 2 (contd) Variation of average RoI results of regions during the study period**

<b>ASHDOD RoI (x1000)Mg</b>	<b>1980</b>	<b>1985</b>	<b>1990</b>	<b>1991+1992</b>	<b>1993+1994</b>	<b>1995+1996</b>	<b>1997+1998</b>	<b>1999+2000</b>	<b>2001+2002</b>	<b>2003+2004</b>	<b>2005+2006</b>	<b>2007+2008</b>	<b>2009+2010</b>
Turkey	843.7	1351.3	1664.4	1692.8	1388.2	1452.2	1539	2277.2	1903.4	1478.2	1633.8	1903.8	1843.3
Balkans	1502.8	1709.3	1421.6	1411.4	1215.9	1004.9	1149.8	993.2	987.1	846.3	878.5	596.2	473.5
Eastern Europe	1059.3	1182.5	498.5	536.4	447.7	284	487.6	185.2	145.1	142	82.8	87.7	51.9
Western Europe	403.6	261.9	141.3	131.9	126.2	93.8	79.1	66.3	57.9	47.5	35.1	28	21.7
Middle East	5128	5442	4088.9	3629.7	5323.3	4295.7	4962.8	5058	4315.1	6103.4	4997.1	6086.5	8409
Russia & Ukraine	285.6	135.3	242.7	242.3	149.1	132.7	93.9	54	23.2	57.2	54.6	67	35
North Africa	76	83.9	47.9	58.9	72.9	64	86.9	51.8	78.4	77.2	64.7	72.8	84.3
<b>CORSICA RoI (x1000)Mg</b>	<b>1980</b>	<b>1985</b>	<b>1990</b>	<b>1991+1992</b>	<b>1993+1994</b>	<b>1995+1996</b>	<b>1997+1998</b>	<b>1999+2000</b>	<b>2001+2002</b>	<b>2003+2004</b>	<b>2005+2006</b>	<b>2007+2008</b>	<b>2009+2010</b>
Turkey	0.944	16.7	2.6	8	22.7	24.1	59.2	11.4	43.9	6.7	8.4	44.6	113.7
Balkans	1682.9	1540	3142.1	1564.5	1970.8	1359.5	1267.6	1110.6	1197.3	1317.7	1671.3	1357	1067.3
Eastern Europe	3160.4	1691.3	2416.7	1590.2	1379.5	1354.8	540.8	592.8	534.6	583.1	475	344.5	369.1
Western Europe	4065.7	2070	1886	1922.4	1497.1	1194.4	915.5	725.3	636.4	531.8	520.7	381.3	332.5
Middle East	0	0	0	0	0	0	0	0	0	0	0	0	0
Russia & Ukraine	289.2	7.4	37.9	90.6	109.1	68.4	40.1	24.9	24.4	37.8	74	40.2	36.1
North Africa	5.7	5.7	6.1	10.1	8	9.7	9	11.3	11.3	11.1	8	9	12.6

When we look at the RoI values of Antalya and Çubuk stations, as it was stated before, their trends are almost same. In Turkey, there is an increasing in RoI values from 1980 to 2010, so it directly shows the weakness in legal enforcements and emission controls. On the other hand, especially in Europe, effective and gradual decrease in SO<sub>2</sub> emissions is seen obviously, because S-protocols were applied properly, and technological developments were noticed. From 1995, RoI values of Balkans started to decrease and after 2000s the reduction was more efficient. The similar increase trend of Turkey is also seen in Ashdod and Corsica stations. It directly indicates increasing and uncontrolled SO<sub>2</sub> emissions. Because of the closeness of Middle East to Ashdod Station and Europe to Corsica Station, the highest RoI results were seen there. Because of inefficient emission control and legal restrictions, RoI values in Middle East increased, environmental exposure of Ashdod did not change so much. On the contrary, significant emission reduction which was obligated by the sulphate protocols was positive effect on sulfate source regions affecting Corsica Station.

Balkan countries, including Greece, Bulgaria and Romania, Turkey, Eastern Parts of Ukraine and Middle East were identified as potential source regions affecting SO<sub>4</sub><sup>2-</sup> concentrations in the Eastern Mediterranean atmosphere. Source regions found for western Mediterranean and their variation different than source regions found for the eastern Mediterranean.

Comparison of results found by PSCF and RoI approaches at Antalya and Çubuk station demonstrated excellent agreement for common source areas affecting both stations. Balkan Countries, Turkey, Eastern Ukraine are found as potential source areas by both techniques.

The very slow decrease in SO<sub>4</sub><sup>2-</sup> concentrations in the eastern Mediterranean atmosphere is successfully explained in this study. Eastern Mediterranean atmosphere is not significantly affected from SO<sub>2</sub> emissions in Western Europe, which decreased rapidly after 1995. Most of the source regions for Eastern Mediterranean are located in Balkan countries, countries located to the north of

Turkey and Turkey itself. Emissions of SO<sub>2</sub> in these regions did not change much in time. That is the main reason why SO<sub>4</sub><sup>2-</sup> levels did not decrease significantly until very recently.

Turkey's increasing significance as source region measured in the Eastern Mediterranean atmosphere came out in a number of occasions in discussions of PSCF and RoI. This is a very serious development. Calculation of country based emissions demonstrated that Turkey is the only country in Europe with SO<sub>2</sub> emissions are not decreasing. In 80's and 90's similar statements were done for Eastern European countries, but now unfortunately this is true for Turkey. This may have significant implications in the near future if we do not take necessary actions to reduce our emissions.

As a conclusion, this study showed the variation of sulfate source regions in the last 30 years, so the increasing effect of Turkey in Eastern Mediterranean atmosphere was seen easily. Within the numerous environmental problems, the impact of human-induced chemical perturbations on the atmosphere has received the majority of attention during the last three decades. In addition to sulfur protocols, many difficult decisions and enforcements will have to be made by policy-makers to deal with atmospheric pollution problems such as acid deposition, increasing greenhouse gas concentrations, stratospheric ozone depletion, increasing tropospheric ozone, direct and indirect climatic response of tropospheric aerosols and anthropogenic sulfate aerosol in particular. Therefore, the study has important results in respect to see the contribution of countries to Eastern Mediterranean atmosphere. Based on the results, the most potential source regions or countries start to take more effective precautions not to be exposed to possible enforcements. On the other perspective, such studies are essential in order to give proper policy decisions.

Similarly, Turkey's significance as potential source region affecting SO<sub>4</sub><sup>2-</sup> levels, in the Eastern Mediterranean increased in time in both PSCF and RoI calculations. In RoI distributions for the year 2010, Turkey appears as the single most important

source region for the  $\text{SO}_4^{2-}$  concentrations in Eastern Mediterranean. As pointed before this is serious development and can have financial consequences in the future.

## CHAPTER 6

### RECOMMENDATIONS FOR FUTURE RESEARCH

In this study, PSCF analyses were performed for only Çubuk and Antalya stations for limited years, because the stations were operated for only the limited years. If the measurements at these stations start again, same analyses can be performed for coming years. In order to define the source regions in more detail, same analyses can be done for other stations that measure concentrations of pollutants.

In order to increase the accuracy of PSCF and RoI approaches, other atmospheric removal mechanisms and chemistry of pollutant transport can be taken into account in future researches. More than three different starting heights can be used in back trajectory calculation to support the locations of trajectories. Also, seasonal differentiation of sulfate source regions will be calculated in future studies to see the seasonal effect on results.

Çubuk Station was the only operational EMEP station in Turkey from 1993 to 2011. After 2011, the station was closed due to the operational problems, so the measured data had been transferred to the EMEP secretariat. If the station was operated again, RoI approach which will be used at coming years will be more realistic.

The  $1^{\circ} \times 1^{\circ}$  grid size was used in both the PSCF and RoI approaches. The smaller grid size can be used at the region which is close to receptors to define the pollutant source regions more specifically.

In order to investigate the location of the sources, the trajectory information as well as pollutant data set was used. Therefore, the uncertainty of the used trajectory model is very important for identification of source regions. Instead of using single layer isobaric back trajectories, 3D trajectories will be particularly useful for the identification of the meteorology associated with pollution transport.

In this study, the analyses were done one by one by using MapInfo program. In following studies, the analyses will be performed faster by using more user friendly application such as MapBasic.

## REFERENCES

Andreae, T.W., Andreae, M.O., Ichoku, C., Maenhaut, W., Cafmeyer, J., Karnieli, A., Orlovsky, L., (2002). Light scattering by dust and anthropogenic aerosol at a remote site in the Negev Desert, Israel. *Journal of Geophysical Research*, 107, 10.

Andreas, E., (1988). Estimating averaging times for point and path-averaged measurements of turbulence spectra. *Journal of Applied Meteorology*, 27(3), 295-304.

Ashbaugh, L.L., Malm, W.C., Sadeh, W.Z., (1985). A residence time probability analysis of sulfur concentrations at Grand Canyon National Park. *Atmospheric Environment*, 19(8), 1263-1270.

Bardouki, H., Liakakou, H., Economou, C., Sciare, J., Smolik, J., Zdimal, V., Eleftheriadis, K., Lazaridis, M., Dye, C., Mihalopoulos, N., (2003). Chemical composition of size-resolved atmospheric aerosols in the eastern Mediterranean during summer and winter. *Atmospheric Environment*, 37(2), 195-208.

Begum, B.A., Kim, E., Jeong, C.H., Lee, D.W., Hopke, P.K., (2005). Evaluation of the potential source contribution function using the 2002 Quebec forest fire episode. *Atmospheric Environment*, 39, 3719-3724.

Bourqui, M.S., (2006). Stratosphere-troposphere exchange from the Lagrangian perspective: A case study and method sensitivities. *Atmospheric Chemistry and Physics*, 6(9), 2651-2670.

Bowman, K.P., (1993). Large-scale isentropic mixing properties of the Antarctic polar vortex from analyzed winds. *Journal of Geophysical Research*, 98(D12), 23013-23027.

Bryant, C., Eleftheriadis, K., Smolik, J., Zdimal, V., Mihalopoulos, N., Colbeck, I., (2006). Optical properties of aerosols over the eastern Mediterranean, *Atmospheric Environment*, 40(32), 6229-6244.

Byers, H.R., (1974). *General Meteorology*, 4th Edn., McGraw-Hill, New York, U.S.A.

Charlson, R.J., Schwartz, S.E., Hales, J.M., Cess, R.D., Coakley, J.A., Hansen, Jr.J.E, Hofmann, D.J., (1992). Climate Forcing by Anthropogenic Aerosols *Science*, 255, 423.

Charlson, R.J., and Wigley, T.M.L., (1994). Sulfate Aerosol and Climatic Change. *Scientific American*, 270(2), 48-57.

Cheng, M.D., Lin, C.J., (2001). Receptor modeling for smoke of 1998 biomass burning in Central America. *Journal of Geophysical Research, Atmospheres*, 106, 22871-22886.

Chester, R., Nimmo, M., Alarcon, M., Saydam, C., Murphy, K.J.T., Sanders, G.S., Corcoran, P., (1993). Defining the chemical character of aerosols from the atmosphere of the Mediterranean Sea and surrounding regions. *Oceanologica Acta*, 16, 231-246.

Colin, J.L., Renard, D., Lescoat, V., Jaffrezo, J.L., Gros, M.J., Strauss, B., (1989). Relationship between rain and snow acidity and air mass trajectory in Eastern France. *Atmospheric Environment*, 23, 1487-1498.

Colette, A., Granier, C., Hodnebrog, Ø., Jakobs, H., Maurizi, A., Nyiri, A., Bessagnet, B., D'Angiola, A., D'Isidoro, M., Gauss, M., Meleux, F., Memmesheimer, M., Mieville, A., Roüil, L., Russo, F., Solberg, S., Stordal, F., Tampieri, F., (2011). Air quality trends in Europe over the past decade: A first multi-model assessment, *Atmospheric Chemistry and Physics*, 11(22), 11657-11678.

Cullis, C.F., and Hirschler, M.M., (1980). Atmospheric sulfur: Natural and man-made sources. *Atmospheric Environment Volume*, 14(11), 1263-1278.

D'Abreton, P.C., and Tyson, P.D., (1996). Three-dimensional kinematic trajectory modelling of water vapour transport over Southern Africa. *Water SA*, 22, 297-306.

Danielsen, E.F., (1961). Trajectories: isobaric, isentropic and actual. *Journal of Meteorology*, 18, 479-486.

Davis, L.S., and Dacre, H.F., (2009). Can dispersion model predictions be improved by increasing the temporal and spatial resolution of the meteorological input data? *Weather*, 64(9), 232-237.

Doğan, G., (2005). Comparison of the rural atmosphere aerosol compositions at different parts of Turkey. M.Sc. Thesis, Department of Environmental Engineering, Middle East Technical University, Ankara, Turkey.

Doğan, G., Güllü, G., Tuncel, G., (2008). Sources and source regions effecting the aerosol composition of the Eastern Mediterranean. *Microchemical Journal*, 88, 142-149.

Doğan, G., Güllü, G., Karakas, D., Tuncel, G., (2010). Comparison of source regions affecting  $\text{SO}_4^{2-}$  and  $\text{NO}_3^-$  concentrations at the Eastern Mediterranean and Black Sea Atmospheres. *Current Analytical Chemistry*, 6(1), 66-71.

Doty, K.G., and Perkey, D.J., (1993). Sensitivity of trajectory calculations to the temporal frequency of wind data. *Monthly Weather Review*, 121, 387-401.

Draxler, R., and Hess, G.D., (1998). An overview of the HYSPLIT 4 modeling system for trajectories, dispersion and deposition. *Australian Meteorological Magazine*, 47, 295-308.

Dutton, J.A., (1986). *The Ceaseless Wind, An Introduction to the Theory of Atmospheric Motion*. Dover, New York, U.S.A.

Dzubay, T.G., Stevens, R.K., Haagenson, P.L., (1984). Composition and origins of aerosol at a forested mountain in Soviet Georgia. *Environmental Science and Technology*, 18(11), 873-883.

Eliassen, A., and Saltbones, J., (1983). Modelling of long-range transport of sulphur over Europe: A two-year model run and some model experiments. *Atmospheric Environment*, 17(8), 1457-1473.

Escudero, M., Stein, A., Draxler, R.R., Querol, X., Alastuey, A., Castillo, S., Avila, A., (2006). Determination of the contribution of northern Africa dust source areas to PM10 concentrations over the central Iberian Peninsula using the Hybrid Single-Particle Lagrangian Integrated Trajectory model (HYSPLIT) model. *Journal of Geophysical Research*, 111, D06210. doi:10.1029/2005JD006395.

Formenti, P., Andreae, M.O., Andreae, T.W., Ichoku, C., Schebeske, G., Kettle, J., Maenhaut, W., Cafmeyer, J., Ptasinaky, J., Karnieli, A., Lelieveld, J., (2001). Physical and chemical characteristics of aerosols over the Negev desert (Israel) during summer 1996. *Journal of Geophysical Research*, 106(D5), 4871-4890.

Forsius, M., Kleemola, S., Vuorenmaa, J., Syri, S., (2001). Fluxes and trends of nitrogen and sulphur compounds at integrated monitoring sites in Europe, *Water, Air, and Soil Pollution*, 130(1-4 III), 1641-1648.

Fuelberg, H.E., Loring R.O., Jr, Watson, M.V., Sinha, M.C., Pickering, K.E., Thompson, A.M., Sachse, G.W., Blake, D.R. Schoeberl, M.R., (1996). TRACE A trajectory intercomparison, 2. Isentropic and kinematic methods. *Journal of Geophysical Research*, 101(23), 927-939.

Ganor, E., Foner, H.A., Bingemer, H.G., Udisti, R., Setter, I., (2000). Biogenic sulphate generation in the Mediterranean Sea and its contribution to the sulphate anomaly in the aerosol over Israel and the Eastern Mediterranean. *Atmospheric Environment*, 34, 3453-3462.

Güllü, G., (1996). Long range transport of aerosols. Ph.D. Thesis, Department of Environmental Engineering, Middle East Technical University, Ankara, Turkey.

Güllü, G.H., Ölmez, I., Aygün, S., Tuncel, G., (1998). Atmospheric trace element concentrations over the eastern Mediterranean Sea: Factors affecting temporal variability. *Journal of Geophysical Research*, 103, 21943-21954.

Güllü, G., Doğan, G., Tuncel, G., (2005). Atmospheric trace element and major ion concentrations over the eastern Mediterranean Sea: Identification of anthropogenic source regions. *Atmospheric Environment*, 39, 6376-6387.

Girish, C.R., (2007). Environmental Pollution. Power point slides presented at the Department of Chemical Engineering, MIT.

Hacısalıhoğlu, G., Eliyakut, F., Balkas T.I., Tuncel, G., (1992). Chemical Composition of Particles in the Black Sea Aerosols. *Atmospheric Environment*, 26A, 3207-3218.

Harris, J.M., and Kahl, J.D.W., (1994). Analysis of 10-day isentropic flow patterns for Barrow, Alaska: 1985-1992. *Journal of Geophysical Research*, 99(25), 845-855.

Haywood, J., and Boucher, O., (2000). Estimates of the direct and indirect radiative forcing due to tropospheric aerosols: a review. *Reviews of Geophysics*, 38, 513-543.

Henderson, R.G., and Weingartner, K., (1982). Trajectory analysis of MAP3S precipitation chemistry data at Ithaca, New York. *Atmospheric Environment*, 16, 1657-1665.

Herut, B., (2001). Levels of aerosol trace metals along the Mediterranean coast of Israel (1996-97). *Fresenius Environmental Bulletin*, 10, 89-93.

Hopke, P.K., Li, C.L., Ciszek, W., Landsberger, S., (1995). The use of bootstrapping to estimate conditional probability fields for source locations of airborne pollutants, *Chemometrics and Intelligent Laboratory Systems*, 30(1), 69-79.

Ichoku, C., Andreae, M.O., Andreae, T.W., Meixner, F.X., Schebeske, G., Formenti, P., Maenhaut, W., Cafmeyer, J., Karnieli, A., Orlovsky, L., (1999). Interrelationships between aerosol characteristics and light scattering in an eastern Mediterranean arid environment. *Journal of Geophysical Research*, 104, 24371-24393.

Im, U., Daskalakis, N., Markakis, K., Vrekoussis, M., Hjorth, J., Myriokefalitakis, S., Gerasopoulos, E., Kouvarakis, G., Richter, A., Burrows, J., Pozzoli, L., Unal, A., Kindap, T., Kanakidou, M., (2014). Simulated air quality and pollutant budgets over Europe in 2008. *Science of the Total Environment*, 470(471), 270-281.

Kahl, J.D., and Samson, P.J., (1986). Uncertainty in trajectory calculations due to low resolution meteorological data. *Journal of Climate and Applied Meteorology*, 25, 1816-1831.

Kalivitis, N., Gerasopoulos, E., Vrekoussis, M., Kouvarakis, G., Kubilay, N., Hatzianastassiou, N., Vardavas, I., Mihalopoulos, N., (2007). Dust transport over the eastern Mediterranean derived from Total Ozone Mapping Spectrometer, Aerosol

Robotic Network, and surface measurements. *Journal of Geophysical Research*, 112, 3202.

Kalivitis, N., Bougiatioti, A., Kouvarakis, G., Mihalopoulos, N., (2011). Long term measurements of atmospheric aerosol optical properties in the Eastern Mediterranean. *Atmospheric Research*, 102(3), 351-357.

Kallos, G., Kotroni, V., Lagouvardos, K., Papadopoulos, A., (1998). On the long-range transport of air pollutants from Europe to Africa. *Geophysical Research Letters*, 25(5), 619-622.

Kallos, G., Astitha, M., Katsafados, P., Spyrou, C., (2007). Long-range transport of anthropogenically and naturally produced particulate matter in the Mediterranean and North Atlantic: Current state of knowledge. *Journal of Applied Meteorology and Climatology*, 46(8), 1230-1251.

Karaca, F., Anil, I., Alagha, O., (2009). Long-range potential source contributions of episodic aerosol events to PM<sub>10</sub> profile of a megacity. *Atmospheric Environment*, 43(36), 5713-5722.

Katsoulis, B.D., and Whelpdale, D.M., (1993). A climatological analysis of four day backtrajectories from Aliartos, Greece, *Theoretical and Applied Climatology*, 47, 93-103.

Koçak, M., Kubilay, N., Mihalopoulos, N., (2004a). Ionic composition of lower tropospheric aerosols at a northeastern Mediterranean site: implications regarding sources and long-range transport. *Atmospheric Environment*, 38(14), 2067-2077.

Koçak, M., Nimmo, M., Kubilay, N., Herut, B., (2004b). Spatiotemporal aerosol trace metal concentrations and sources in the Levantine Basin of the eastern Mediterranean. *Atmospheric Environment*, 38, 2133-2144.

Koçak, M., Theodosi, C., Zarmas, P., Séguret, M.J.M., Herut, B., Kallos, G., Mihalopoulos, N., Kubilay, N., Nimmo, M., (2012). Influence of mineral dust transport on the chemical composition and physical properties of the Eastern Mediterranean aerosol. *Atmospheric Environment*, 57, 266-277.

Koulouri, E., Saarikoski, S., Theodosi, C., Markaki, Z., Gerasopoulos, E., Kouvarakis, G., Mäkelä, T., Hillamo, R., Mihalopoulos, N., (2008). Chemical composition and sources of fine and coarse aerosol particles in the Eastern Mediterranean. *Atmospheric Environment*, 42, 6542-6550.

Kouvarakis, G., Doukelis, Y., Mihalopoulos, N., Rapsomanikis, S., Sciare, J., Blumthaler, M., (2002a). Chemical, physical, and optical characterization of aerosols during PAUR II experiment. *Journal of Geophysical Research*, 107(D18), 8141. doi:10.1029/2000JD000291.

Kouvarakis, G., and Mihalopoulos, N., (2002b). Seasonal variation of dimethylsulfide in the gas phase and of methanesulfonate and non-sea-salt sulfate in the aerosols phase in the Eastern Mediterranean atmosphere. *Atmospheric Environment*, 36, 929-938.

Krijgsman, W., Fortuin, A.R., Hilgenc, F.J., Sierrod, F.J., (2001). Astrochronology for the Messinian Sorbas basin (SE Spain) and orbital (precessional) forcing for evaporate cyclicity. *Sedimentary Geology*, 140, 43. doi:10.1016/S0037-0738(00)00171-8.

Kubilay, N., and Saydam, C., (1995). Trace elements in atmospheric particulates over the Eastern Mediterranean: concentration, sources and temporal variability. *Atmospheric Environment*, 29, 2289-2300.

Kubilay, N., Nickovic, S., Moulin, C., Dulac, F., (2000). An illustration of the transport and deposition of mineral dust onto the Eastern Mediterranean. *Atmospheric Environment*, 34, 1293-1303.

Kuloğlu, E., Tuncel, G., (2005). Size distribution of trace elements and major ions in the Eastern Mediterranean atmosphere. *Water Air Soil Pollution*, 167, 221-241.

Kuo, Y.H., Skumanich, M., Haagenson, P.L. and Chang, J.S., (1985). The accuracy of trajectory models as revealed by the observing system simulation experiments. *Monthly Weather Review*, 113, 1852-1867.

Lajtha, K., and Jones, J., (2013). Trends in cation, nitrogen, sulfate and hydrogen ion concentrations in precipitation in the United States and Europe from 1978 to 2010: A new look at an old problem. *Biogeochemistry*, 116(1-3), 303-334.

Lee, H.N., and Leifer, R., (1993). Backward Air Mass Trajectory Analysis for the First Cloud and Radiation Testbed Site at Lamont, Oklahoma. In *Proceedings of the Third Atmospheric Radiation Measurement (ARM) Science Team Meeting*, Norman, Oklahoma, USA, 357-358.

Lelieveld, J., Berresheim, H., Borrmann, S., Crutzen, P.J., Dentener, F.J., Fischer, H., Feichter, J., Flatau, P.J., Heland, J., Holzinger, R., Korrman, R., Lawrence, M.G., Levin, Z., Markowicz, K.M., Mihalopoulos, N., Minikin, A., Ramanathan, V., de Reus, M., Roelofs, G.J., Scheeren, H.A., Sciare, J., Schlager, H., Schultz, M., Siegmund, P., Steil, B., Stephanou, E.G., Stier, P., Traub, M., Warneke, C., Williams, J., Ziereis, H., (2002). Global air pollution crossroads over the Mediterranean. *Science*, 298, 794-799.

Lucas, D.D., and Akimoto, H., (2007). Contributions of anthropogenic and natural sources of sulfur to SO<sub>2</sub>, H<sub>2</sub>SO<sub>4</sub>(g) and nanoparticle formation. *Atmospheric Chemistry and Physics*, 7, 7679-7721.

Lupu, A., and Meenhaut, W., (2002). Application and comparison of two statistical trajectory techniques for the identification of source regions of atmospheric aerosol species. *Atmospheric Environment*, 36, 5607-5618.

Luria, M., Peleg, M., Sharf, G., Tov-Alper, D.S., Spitz, N., Ami, Y.B., Gawii, Z., Lifschitz, B., Yitzchaki, A., Seter, I., (1996). Atmospheric sulfur over the eastern Mediterranean region. *Journal of Geophysical Research*, 101, 25917-25930.

Mateu, J., Forteza, R., Cerda, V., Colomates, M., (1996a). Particle size distribution and long range transport of metals in atmospheric aerosols from the Alfabia station (Majorca, Spain). *Journal of Environmental Science and Health*, 31, 31-54.

MapInfo Corp, 2003. MapInfo Professional Version 7.5.

Merrill, J.T., Bleck, R., Boudra, D., (1986). Techniques of Lagrangian trajectory analysis in isentropic coordinates. *Monthly Weather Review*, 114, 571-581.

Migon, C., Caccia, J.L., (1990). Separation of anthropogenic and natural emissions of particulate heavy metals in the western Mediterranean atmosphere. *Atmospheric Environment*, 24, 399-405.

Mihalopoulos, N., Stephanou, E., Kanakidou, M., Pilitsidis, S., Bousquet, P., (1997). Tropospheric aerosol ionic composition above the eastern Mediterranean area. *Tellus*, 49B, 314-326.

Miller, J.M., (1981a). A five-year climatology of back trajectories from the Mauna Loa Observatory, Hawaii, *Atmospheric Environment*, 15, 1553-1558.

Miller, J.M., (1981b). A five-year climatology of 5-day back-trajectories from Barrow, Alaska, *Atmospheric Environment*, 15, 1401-1405.

Miller, J.M., and Harris, J.M., (1985). The flow climatology to Bermuda and its implications for long-range transport, *Atmospheric Environment*, 19(3), 409-414.

Miller, J.M., (1987). The use of back air trajectories in interpreting atmospheric chemistry data: A review and bibliography. NOAA Technical Memorandum ERL ARL-155, 28.

Miller, J.M., Moody, J.L., Harris, J.M., Gaudry, A., (1993). A 10-year trajectory flow climatology for Amsterdam Island, 1980-1989. *Atmospheric Environment*, 27A, 1909-1916.

Moulin, C., Lambert, E., Dayan, U., Masson, V., Ramonet, M., Bousquet, P., Legrand, M., Balkanski, Y.J., Guelle, W., Marticorena, B., Bergametti, G., Dulac, F., (1998). Satellite climatology of African dust transport in the Mediterranean atmosphere. *Journal of Geophysical Research*, 103, 13137-13144.

Munzur, B., (2008). Chemical composition of atmospheric particles in the Aegean Region, M.S. Thesis, Department of Environmental Engineering, Middle East Technical University, Ankara.

Nyanganyura, D., Makarau, A., Mathuthu, M., Meixner, F.X., (2008). A five-day back trajectory climatology for Rukomechi research station (northern Zimbabwe) and the impact of large-scale atmospheric flows on concentrations of airborne coarse and fine particulate mass, *South African Journal of Science*, 104, 43-52.

Özsoy, T., Saydam, C., Kubilay, N., Salihoğlu, İ., (2000). Aerosol nitrate and non-sea-salt sulfate over the eastern Mediterranean. *The Global Atmosphere and Ocean System*, 7, 185-228.

Öztürk, F., (2009). Investigation of short and long term trends in the Eastern Mediterranean aerosol composition, Ph.D. Thesis, Department of Environmental Engineering, Middle East Technical University, Ankara.

Öztürk, F., Zararsız, A., Dutkiewicz, V.A., Husain, L., Hopke, P.K., Tuncel, G., (2012). Temporal Variations and Sources of Eastern Mediterranean Aerosols Based on a 9-Year Observation. *Atmospheric Environment*, 61, 463-475.

Pack, D.H., Ferber, G.J., Heffter, J.L., Telegadas, K., Angell, J.K., Hoecker, W.H., Machta, L., (1978). Meteorology of long-range transport. *Atmospheric Environment*, 12, 425-444.

Polissar, A.V., Hopke, P.K., Poirot, R.L., (2001). Atmospheric aerosol over Vermont: chemical composition and sources. *Environmental Science and Technology*, 35, 4604-4621.

Querol, X., Alastuey, A., Rodriguez, S., Viana, M.M., Artinano, B., Salvador, P., Mantilla, E., Garciado Santos, S., Patier, R.F., de Las Rosa, J., Sanchez de la Campa, A., Menendez, M., Gil, J.J., (2004). Levels of particulate matter in rural, urban, and industrial sites in Spain. *Science of the Total Environment*, 334(5), 359-376.

Rodriguez, S., Querol, X., Alastuey, A., Kallos, G., Kakaliagou, O., (2001). Saharan dust contributions to PM10 and TSP levels in Southern and Eastern Spain. *Atmospheric Environment*, 35, 2433-2447.

Rolph, G.D., and Draxler, R.R., (1990). Sensitivity of three dimensional trajectories to the spatial and temporal densities of the wind field. *Journal of Applied Meteorology*, 29, 1043-1054.

Sauliene, I., and Veriankaite, L., (2006). Application of backward air mass trajectory analysis in evaluating airborne pollen dispersion. *Environmental Engineering and Landscape Management*, 14(3), 113-120.

Schoeberl, M.R., Lait, L.R., Newman, P.A., Rosenfield, J.E., (1992). The structure of the polar vortex. *Journal of Geophysical Research*, 97(D8), 7859-7882.

Sciare, J., Bardouki, H., Moulin, C., Mihalopoulos, N., (2003). Aerosol sources and their contribution to the chemical composition of aerosols in the eastern Mediterranean Sea during summertime. *Atmospheric Chemistry and Physics*, 3, 291-302.

Seibert, P., (1993). Convergence and accuracy of numerical methods for trajectory calculations. *Journal of Applied Meteorology*, 32, 558-566.

Seibert, P., Kromp-Kolb, H., Baltensperger, U., Jost, D.T., Schwikowski, M., Kasper, A., Puxbaum, H., (1994). Trajectory analysis of aerosol measurements at high alpine sites. *Transport and Transformation of Pollutants in the Troposphere*, 689-693.

Seinfeld, J.H., and Pandis, S.N., (2006). *Atmospheric Chemistry and Physics, From Air Pollution to climate Change*, Chapter 25- Atmospheric Chemical Transport Models- Trajectories. 2nd Edn., John Willey & Sons, Inc., New Jersey, U.S.A.

Shadbolt, R.P., Waller, E.A., Messina, J.P., Winkler, J.A, (2006). Source regions of lower-tropospheric airflow trajectories for the lower peninsula of Michigan: A 40-year air mass climatology. *Journal of Geophysical Research*, 111(D2), 1117.

Steinacker, R., (1984). Airmass and frontal movement around the Alps. *Rivista di Meteorologia Aeronautica*, 44, 85-93.

Stohl, A., and Wotawa, G., (1995). A method for computing single trajectories representing boundary layer transport. *Atmospheric Environment*, 29(22), 3235-3238.

Stohl, A., (1996). Trajectory statistics - a new method to establish source-receptor relationships of air pollutants and its application to the transport of particulate sulfate in Europe. *Atmospheric Environment*, 30(4), 579-587.

Stohl, A., and Seibert, P., (1998). Accuracy of trajectories as determined from the conservation of meteorological tracers. *Quarterly Journal of Royal Meteorological Society*, 124, 1465-1484.

Stohl, A., (1998). Computation, Accuracy and Applications of Trajectories: A Review and Bibliography. *Atmospheric Environment*, 32(6), 947-966.

Stohl, A., Eckhardt, S., Forster, C., James, P., Spichtinger, N., Seibert, P., (2002). A replacement for simple back trajectory calculations in the interpretation of atmospheric trace substance measurements. *Atmospheric Environment*, 36 4635-4648.

Traub, M., Fischer, H., de Reus, M., Kormann, R., Heland, J., Ziereis, H., Schlager, H., Holzinger, R. Williams, J. Warneke, C. de Gouw, J. and Lelieveld, J., (2003). Chemical characteristics assigned to trajectory clusters during the MINOS campaign. *Atmospheric Chemistry and Physics*, 3, 459-468.

Tov, D.A., Peleg, M., Matveev, V., Mahrer, Y., Ster, I., Luria, M., (1997). Recirculation of polluted air masses over the east Mediterranean coast. *Atmospheric Environment*, 31, 1441-1448.

Walmsley, J.L., and Mailhot, J., (1983). On the numerical accuracy of trajectory models for long-range transport of atmospheric pollutants. *Atmosphere Ocean*, 21, 14-39.

Wang, Y.Q., Zhang, X.Y., Draxler, R., (2009). TrajStat: GIS-based software that uses various trajectory statistical analysis methods to identify potential sources from long-term air pollution measurement data. *Environmental Modelling and Software*, 24, 938-939.

Wehrens, R., Putter, H., Buydens, L.M.C., (2000). The bootstrap: a tutorial. *Chemometrics and Intelligent Laboratory Systems*, 54, 35-52.

Wotawa, G., and Kröger, H., (1999). Testing the ability of trajectory statistics to reproduce emission inventories of air pollutants in cases of negligible measurement and transport errors. *Atmospheric Environment*, 33, 3037-3043.

Xu, X., and Akhtar, U.S., (2009). Identification of potential regional sources of atmospheric total gaseous mercury in Windsor, Ontario, Canada using hybrid receptor modeling. *Atmospheric Chemistry and Physics Discuss*, 9, 24847-24874.

Yıkmaz, R.F., (2010). Development of GIS based trajectory statistical analysis method to identify potential sources of regional air pollution. M.Sc. Thesis, Department of Environmental Engineering, Middle East Technical University, Ankara, Turkey.

Vascancelos, L.A.D., Kahl, J.D.W, Liu, D., Macias, E.S., White, W.H., (1996). A tracer calibration of back trajectory analysis at the Grand Canyon. *Journal of Geophysical Research*, 101, 19329-19335.

Viana, M., Querol, X., Alastuey, A., Cuevas, E., Rodríguez, S., (2002). Influence of African dust on the levels of atmospheric particulates in the Canary Islands air quality network. *Atmospheric Environment*, 36, 5861-5875.

Zeng, Y., Hopke, P.K., (1989). A study of the sources of acid precipitation in Ontario, Canada. *Atmospheric Environment*, 23, 1499-1509.

Zhao, W., Hopke, P.K., (2006). Source investigation for ambient PM 2.5 in Indianapolis, IN. *Aerosol Science and Technology*, 40, 898-909.

URL 1: European Monitoring and Evaluation Programme, EMEP  
<http://www.emep.int> (access Oct. 2013).

URL 2: East Sea Workshop

[http://www.ifremer.fr/lobtln/OTHER/ext\\_abstr\\_East\\_Sea\\_workshop\\_TLM.pdf](http://www.ifremer.fr/lobtln/OTHER/ext_abstr_East_Sea_workshop_TLM.pdf)  
(access May 2013).

URL 3: National Geographic Maps

<http://shop.nationalgeographic.com/ngs/product/maps/wall%20maps/countries-and-region-maps/eastern-mediterranean-political-map> (access May 2013).

URL 4: International Cooperative for the Management of Mediterranean-Climate Ecosystems <http://www.incomme.org/mediterranean-regions/mediterranean-basin-landscape.html> (access May 2013).

URL 5: Air mass trajectories Mt. Kenya <http://lindseynicholson.org/2012/11/air-mass-trajectories-mt-kenya/> (access May 2013).

URL 6: HYSPLIT Airmass Trajectories Help Files

[http://alg.umbc.edu/usaq/archives/HYSPLIT\\_20090921.pdf](http://alg.umbc.edu/usaq/archives/HYSPLIT_20090921.pdf) (access May 2013).

URL 7: Research Experience Placements Scheme ('REP') Climatology of Flow over the Antarctic Peninsula <http://www.see.leeds.ac.uk/admissions-and-study/research-degrees/icas/gadian-smith/> (access June 2013).